ISSN: 2792-0771

Seatific

Volume 4
Number 2
Year 2024

YTU PRESS

seatific.yildiz.edu.tr

Seatific

Volume 4 Number 2 Year 2024

Seatific

Volume 4 Number 2 Year 2024

Journal Contacts

Editor-in-Chief: Ümit Güneş, *Yıldız Technical University, İstanbul, Türkiye*
ugunes@yildiz.edu.tr

Owner on behalf of the Yıldız Technical University: Prof. Dr. Eyüp Debik

Journal Description: Seatific Journal is a double-blind, peer-reviewed, free and open access journal published twice a year by Yildiz Technical University.

Publisher: Yildiz Technical University - YTU Press

Language of Publication: English

Frequency: Biannually

Publication Type: Online e-version

Press Date: December 2024

Seatific

Volume 4 Number 2 Year 2024

Aim & Scope

Seatific Journal aims to present academic data to all stakeholders in the field, taking into account current developments in all types of areas related to shipping and marine sciences such as environmental impacts, energy transition, and artificial intelligence. Seatific Journal strongly aims to only publish innovative and novel studies that will contribute significantly to advancements in the fields of marine engineering, marine science, and technology.

- Aquaculture and Fishing
- Construction
- Coastal Development
- Design
- Electrical Equipment
- Emissions
- Energy
- Hydrodynamics
- Social Aspects
- Logistics
- Machinery and Control
- Marine Engines
- Marine Environment
- Materials
- Navigation
- Noise
- Manoeuvrability
- Off-Shore
- Port Operations
- Propulsion
- Protection of the Environment
- Renewable Energy
- Safety
- Seakeeping
- Ship Resistance
- Shipyards
- Stability
- Structures

Seatific

Volume 4 Number 2 Year 2024

Contents

Research Articles

Reviews

Seatific

Volume 4 Number 2 Year 2024

Author Guidelines

• Seatific Journal is a double-blind, peer-reviewed biannually academic journal publishing articles in both English and Turkish.
• Author(s) should remove all author(s)' names and any personal information that can be used to identify the author(s).
• All articles submitted to Seatific Journal will be uploaded to iThenticate to check the similarity rate of the paper. The Seatific Journal Desk immediately rejects any articles with a similarity rate greater than 10%.
• All submitted articles to Seatific Journal are uploaded to iThenticate to check the similarity ratio of the paper. If the similarity is more than 10%, the article is directly rejected by the Seatific Journal Desk.
• In order to gain acceptance, all articles submitted to Seatific Journal for evaluation are required to have never previously been published.
• Submissions are first reviewed by the editorial board. If an article satisfies the necessary conditions for style and content, reviewers will then proceed to evaluate its suitability for publication.
• Articles under the categories listed below are acceptable for publication:

Research Articles reflecting original experimental and/or theoretical research. A coherent treatment emphasizing new insight is expected rather than a simple accumulation of data.

Review Articles including authoritative reviews of recent advances in the basic and applied sciences with emphasis on the fundamental aspects of the subject. Manuscripts are generally longer than those found in other categories, but contributions dealing in part with original research are not excluded. Contributors who are invited by the editors or who may submit outline proposals directly are offered a small royalty upon the publication of the article.

• All articles undergo evaluation by two anonymous reviewers. If necessary, the article may be sent to a third reviewer for further assessment. The publication of an article depends upon the approval of these reviewers. Author(s) must provide the necessary corrections demanded by the reviewers.
• In general, any submitted work should provide the following formatting conditions.

No page limit or required format is needed for initial submission. A template will be sent to the author(s) of accepted articles. This can also be downloaded from the link below.

Articles should be written in MS Word in Times New Roman script with 12-pt font size, spacing of 1.5 lines, 2.5 cm margins, and left-aligned.

Tables, figures, pictures, and graphs should fit within a journal page (A4). If needed, these may be written with smaller font sizes and single-spaced.

Tables and graphs should be numbered consecutively as they appear in the text. Place footnotes for tables below the table body and indicate them with superscript lowercase letters. Avoid vertical text layout. Be sparing in the use of tables, and ensure that the data presented in tables do not duplicate results described elsewhere in the article.

• Author(s) and article information should be filled out completely on the form in the system. The article should not contain any information about the author(s).
• The study must include an abstract between 150-200 words in length and 5-8 keywords.
• Author(s) should reference and explain every figure, table, and equation used in the article.
• Corresponding author(s) should also fill out the author contributions form.
• Articles should be submitted using the online submission system to initiate the editing process. An automatic confirmation e-mail will be sent after submission. If you do not receive this e-mail, please contact us via e-mail at seatific@yildiz.edu.tr
• Seatific Journal uses APA 7th Edition style formatting for references and citations. The text rules and formats specified by the Publication Manual of the American Psychological Association (APA), Seventh Edition are to be followed both for text citations and the reference list. Here are some reference examples.

Book/eBook

• Reference Section: Bejan, A., Tsatsaronis, G., & Moran, M. J. (1996). Thermal design and optimization. Wiley.
• *In-Text:* (Bejan et al., 1996)

Edited Book

• Reference Section: Torino, G. C., Rivera, D. P., Capodilupo, C. M., Nadal, K. L., & Sue, D. W. (Eds.). (2019). Microaggression theory: Influence and implications. John Wiley & Sons. https://doi.org/10.1002/9781119466642
• *In-Text:* (Torino et al., 2019)

Journal Article

• Reference Section: Bejan, A., Gunes, U., & Sahin, B. (2019). The evolution of air and maritime transport. Applied Physics Reviews, 6(2), 021319. https://doi.org/10.1063/1.5099626
• *In-Text:* (Bejan et al., 2019)

Unpublished Dissertation or Thesis

• Reference Section: Dostal, V. (2004). A supercritical carbon dioxide cycle for next generation nuclear reactors [Unpublished doctoral dissertation]. Massachusetts Institute of Technology.
• *In-Text:* (Dostal, 2004)

Seatific

Volume 4 Number 2 Year 2024

Ethical Principles and Policies

Open Access Policy

Seatific Journal is an open access publication.

All content published in the journal is licensed under the Creative Commons Attribution-NonCommercial (CC BY-NC) 4.0 International License which allows third parties to use the content for non-commercial purposes as long as they give credit to the original work. This license allows for the content to be shared and adapted for non-commercial purposes, promoting the dissemination and use of the research published in the journal.

All published content is available online, free of charge at https://dergipark.org.tr/en/pub/seatific.

Copyright Policy

A Copyright Agreement, which includes an Acknowledgement of Authorship, must be submitted with all manuscripts. Authors, by signing this agreement, consent that if their article is accepted for publication by Seatific Journal, it will be licensed under the Creative Commons Attribution-NonCommercial 4.0 International License (CC BY-NC 4.0). This license permits third parties to share and adapt the content for non-commercial purposes, provided they appropriately credit the original work. Authors must obtain permission from copyright holders to use any previously published material such as figures, tables, or any other content in both print and electronic formats. Authors bear the legal, financial, and criminal liabilities related to copyright infringement. The copyright of their work published in the Seatific Journal remains with the authors.

Authors retain the copyright and commercial rights of their published work in the Seatific Journal.

Self-Archiving Policy

Authors retain the right to self-archive their work on their institutional or personal websites, as well as in open access repositories, after publication. It is expected that authors will appropriately acknowledge the original publication and include the DOI number when sharing their articles. Additionally, authors are requested to provide a link from the deposited version to the URL of the publisher's website. This requirement ensures that the online published version on the publisher's website is recognized as the definitive version of record, maintaining the integrity and authenticity of the scientific record.

Publication Fee Policy

The Seatific Journal is funded by Yıldız Technical University. Authors are not required to pay any fees during the evaluation and publication process.

Peer Review Process

Manuscripts submitted to Seatific Journal will go through a double-anonymized peer review process where both authors and reviewers are anonymous to each other. Each submission will be reviewed by at least two external, independent peer reviewers, who are experts in their fields, in order to ensure an unbiased evaluation process.

Submissions will first go through a technical evaluation process during which the editorial office staff will ensure that the manuscript is prepared and submitted in accordance with the journal's guidelines. Submissions that do not conform to the journal's guidelines will be returned to the authors with requests for technical corrections. Submissions that conform to the journal's guidelines will be assigned to the Editor in Chief, who will assess each submission's suitability to the journal in terms of scope and quality. Submissions that are not suitable for the journal can be rejected at this stage.

For papers that are suitable for the journal, the Editor in Chief will work with Associate Editors, who will recruit reviewers for the manuscript. Once assigned, Associate Editors can decide to reject a manuscript, continue with the peer review process, or request revisions before further peer review.

Associate Editors will submit their recommendations, which are based on reports submitted by the reviewers, to the Editor in Chief. Revised manuscripts will be reassessed by the Associate Editors, who will aim to work with the original reviewers to make a new recommendation.

The Editor in Chief is the final authority in the decision-making process for all submissions.

In the event of delays, authors will be informed of the reason for the delay and given the opportunity to withdraw their manuscript.

Once the peer review process is completed, the authors will receive anonymous peer review reports along with the editorial decision on their manuscript. Peer review reports will not be posted publicly in any medium. The submitted material is considered confidential and must not be used in any way until after its publication. If it is suspected that a reviewer has appropriated an author's ideas or data, the Editorial Board will handle the matter in accordance with the relevant COPE guideline.

Authors can recommend peer reviewers during submission. The handling editor is the sole authority to decide whether or not recommended peer reviewers will be invited to evaluate the manuscript.

Peer reviewers are required to adhere to the principles of COPE's Ethical Guidelines for Peer Reviewers, and these guidelines provide a framework for reviewers to follow in order to ensure the integrity and fairness of the peer review process. The Editorial Board follows COPE's relevant flowchart to minimize peer review manipulation. If there is suspicion of peer review manipulation after publication, the Editorial Board will follow the appropriate flowchart of COPE.

Potential peer reviewers should inform the Editor of any possible conflicts of interest before accepting an invitation to review a manuscript. Informing the editor of any potential conflicts of interest allows them to make an informed decision about whether or not to invite the potential reviewer to participate in the review process. It also helps to ensure the integrity and transparency of the review process.

Seatific

Volume 4 Number 2 Year 2024

Ethical Principles and and Policies

Communications between Editors and peer reviewers contain confidential information that should not be shared with third parties. To ensure an equitable peer review process, Seatific Journal will recruit external editors for manuscripts submitted by the Journal's editorial board members. External editors will be selected based on academic qualifications and peer review experience. We uphold the confidentiality of external editors and reviewers to preserve impartiality. Reviewers and external editors are asked to disclose any potential conflicts of interest, promoting transparency and a reliable evaluation process.

Revisions

Authors of manuscripts requiring either a "minor revision" or a "major revision" will receive a decision letter from the Editor in Chief. This letter will include the suggestions of the reviewers and editors along with a deadline for submitting the revised and updated manuscript.

When submitting a revised version of a paper, authors must include a detailed "Response to the Reviewers" that addresses each issue raised by the reviewers point by point, indicating where in the manuscript the changes have been made (each reviewer's comment is followed by the author's reply and the line numbers where changes have been implemented), as well as an annotated copy of the main document.

Revised manuscripts must be submitted within the timeframe specified in the decision letter. If the revised manuscript is not submitted within this period, the option to revise may be withdrawn. If authors require additional time, they should request an extension before the initial deadline expires.

Publication Ethics

The Seatific Journal is committed to adhering to the guidelines and core practices set forth by several organizations, including the Committee on Publication Ethics (COPE), and the Principles of Transparency and Best Practice in Scholarly Publishing (a joint statement by COPE, DOAJ, OASPA). These guidelines are designed to promote transparency, integrity, and best practices in scholarly publishing. Adherence to these standards ensures that the research published by the journal is of high quality and meets the ethical standards of the scientific community.

Authors are encouraged to use the EASE Ethics Checklist for Authors to ensure their manuscripts comply with ethical standards.

Plagiarism and Ethical Misconduct

All submissions are screened multiple times during the peer-review and/or production processes using similarity detection software (Crossref Similarity Check powered by iThenticate).

When discussing work by others (or your own previous work), ensure that you correctly cite the material in every instance.

Authors are strongly advised to avoid any form of plagiarism and ethical misconduct, which include but are not limited to:

Citation Manipulation: The practice of artificially inflating citation counts through methods such as excessive self-citation, excessive citation of articles from the same journal, or the inclusion of honorary or stacked citations.

Self-Plagiarism (Text-Recycling): The practice of reusing sections or sentences from one's previous publications without proper citation. This is considered plagiarism as it involves using previously published work without proper attribution.

Salami Slicing: The unethical practice of dividing one significant piece of research into several smaller parts and publishing them as separate articles, which can mislead regarding the novelty and significance of the research.

Data Fabrication: Adding data that never occurred in the gathering of data or experiments. This is considered a serious form of research misconduct, presenting false information as real.

Data Manipulation/Falsification: Altering research data to misrepresent the research findings. This includes manipulating images, omitting inconvenient results, changing data points, etc., and is considered a form of research misconduct.

In the event of alleged or suspected research misconduct, such as plagiarism, citation manipulation, or data falsification/fabrication, the Editorial Board will follow the appropriate COPE flowcharts to ensure that the allegations or suspicions are handled in a fair, transparent, and consistent manner.

Authorship

Being an author of a scientific article primarily indicates a person who has made a significant contribution to the article and shares responsibility and accountability for that article. To be recognized as an author of a scientific article, researchers should meet the following criteria:

- Making a significant contribution to the work in one or more of the following phases: research conception or design, acquisition of data, analysis, and interpretation.
- Drafting, writing, or revising the manuscript.
- Agreeing on the final version of the manuscript and the journal to which it will be submitted.
- Taking responsibility and accountability for the content of the article.

Contributions not included in the authorship criteria should be acknowledged in the Acknowledgment section.

In addition to being accountable for the parts of the work they have conducted, authors should also be able to identify which co-authors are responsible for other specific parts of the work. This ensures that all authors' contributions are accurately and appropriately acknowledged. Authors may use the CRediT (Contributor Roles Taxonomy) to provide information about individual contributions at the time of submission. It is expected that all authors agree on their individual contributions as communicated by the corresponding author. The authors' contribution statement will be published with the final article and should accurately reflect contributions to the work.

Seatific

Volume 4 Number 2 Year 2024

Ethical Principles and Policies

Furthermore, authors should have confidence in the integrity of their co-authors' contributions. This means trusting that their co-authors have conducted the research ethically and responsibly, and that the data and results presented in the manuscript are accurate and reliable.

Individuals who do not meet all four of the authorship criteria should not be listed as authors on the manuscript. However, they can be acknowledged on the title page of the manuscript for their contributions to the research. This recognizes the contributions of these individuals and provides transparency about who was involved in the research.

If the editorial board suspects a case of ghost, honorary, or gift authorship, the submission will be suspended, and the relevant COPE flowchart and COPE Policy on authorship and contributorship will be followed.

Change of Authorship

Any requests for changes to authorship, such as the removal or addition of authors, or changes in the order of authors, should be submitted to the editorial office along with a letter stating the reasons for the change. This letter must be signed by all authors, including any who are to be removed.

The journal's Editorial Board will handle all requests for changes to authorship in a consistent and transparent manner, following the relevant COPE flowchart guidelines. These procedures are in place to protect the integrity of the research and the reputation of all involved authors.

Declaration of Interests

Authors must disclose any relationships or interests that could inappropriately influence or bias their work. This disclosure should be made through the online submission system while submitting their manuscript.

The Seatific Journal also requires and encourages individuals involved in the peer review process of submitted manuscripts to disclose any existing or potential competing interests that might lead to potential bias.

The Editorial Board will handle cases of potential competing interests of editors, authors, or reviewers in accordance with the relevant COPE flowcharts.

Financial Disclosure

Seatific Journal requires authors to disclose any financial support they received to conduct their research. This information should be included in the funding statement, which must be provided when the manuscript is submitted to the journal.

The funding statement should include the names of any granting agencies, the grant numbers, and a description of each funder's role in the research. If the funder had no role in the research, this should also be stated in the funding statement. This information is crucial for readers to understand the potential biases and conflicts of interest that may exist in the research.

The Role of Artificial Intelligence (AI) in Manuscript Preparation

Seatific Journal adheres to the guidelines set forth by the Committee on Publication Ethics (COPE) regarding the use of AI and AI-assisted technology in manuscript preparation. Authorship involves tasks that can only be performed by humans. Authors are responsible for ensuring the originality of the article and possessing the necessary qualifications for authorship. While AI can be used for language corrections during the writing process, this usage should be explicitly stated in the article. AI cannot be included as an author because it is crucial to maintain the originality and quality of the article.

Post-Publication Corrections and Ethical Misconduct Handling

All requests for post-publication corrections are subject to editorial review. The editorial board will assess the request to determine whether a correction is necessary and appropriate. The decision to issue a correction will be based on the nature of the error, its potential impact on the article, and the availability of supporting evidence. The editorial board may consult with the authors, reviewers, and other experts as needed to make an informed decision. If a correction request is approved, the article will be corrected in the journal's archive.

The Editorial Board reviews cases in accordance with journal policies and COPE guidelines.

If allegations of misconduct are reported directly by whistleblowers, the Editorial Board will follow the relevant COPE flowchart. The journal will act in accordance with COPE's flowchart on how to respond to whistleblowers when concerns about a published article are raised on a social media site.

In some instances, an ombudsperson may be appointed to resolve claims that cannot be settled internally.

To investigate potential ethical misconduct more efficiently and effectively, the editorial board may share information with other editors-in-chief. If communication with the editor-in-chief is necessary, the editorial board will adhere to the relevant COPE recommendations.

If necessary, the journal may also contact institutions to inform them of suspected misconduct by researchers and provide evidence to support these concerns, following COPE guidelines throughout the process.

In the event of ethical misconduct concerns, the editors will conduct an investigation according to COPE guidelines. Should the investigation confirm the concern, the editors may issue a retraction notice. This notice will be published in the journal, and the article's record will be updated to reflect the retraction. Although retracted, the article will remain in the journal's

Seatific

Volume 4 Number 2 Year 2024

Ethical Principles and and Policies

archives but will be clearly marked as retracted. Additionally, the article's record will be updated in relevant indexes to reflect the retraction.

Appeals and Complaint

The editorial board of the journal is responsible for addressing appeals and complaints in accordance with the guidelines and recommendations of the COPE. If an author has an appeal or complaint, they should contact the editorial office directly to discuss their concerns. The editorial board will review the case and make a decision based on COPE guidelines.

The editor-in-chief has the final authority in the decision-making process for all appeals and complaints. In some cases, an ombudsperson may be assigned to resolve claims that cannot be resolved internally. It is important to note that the journal follows a fair and transparent process for handling appeals and complaints, with the goal of preserving the integrity of the scientific record.

Withdrawal Requests

Withdrawal requests for an article are reviewed by the editorial board of the journal. To request the withdrawal of an article, authors must send a letter signed by all co-authors stating their request and the reasons for withdrawal to the journal editor. The editorial board will then review the request and make a decision based on the reasons provided by the authors. If the request is approved, the article will be withdrawn from the journal, and the authors will be notified of the decision. Authors are advised not to submit their work to another journal for evaluation until the withdrawal request has been approved, to avoid any potential conflicts of interest or duplication of publication.

Preprint Policy

Seatific Journal does not consider preprints as prior publication, allowing authors to present and discuss their findings on a non-commercial preprint server before submitting their work to the journal. However, authors must inform the journal of the preprint server deposition of their article, along with its DOI, during the initial submission process.

If the article is accepted and published in the journal, it is the responsibility of the authors to update the archived preprint and link it to the published version of the article. This ensures that readers can easily access the most up-to-date and accurate information.

Permission Policy

Disclaimer

The statements or opinions expressed in the manuscripts published in the journal reflect the views of the author(s) and not those of the editors, editorial board, or publisher. The editors, editorial board, and publisher are not responsible for the content of the manuscripts and do not necessarily endorse the views expressed within them. It is the responsibility of the authors to ensure that their work is accurate and well-researched. The views expressed are their own. The editors, editorial board, and publisher provide a platform for the authors to share their work with the scientific community.

Price Policy

Seatific Journal does not demand any article processing or submission charges from authors.

Seatific, Vol. 4, Issue. 2, pp. 37–47, December 2024

Seatific Journal
https://seatific.yildiz.edu.tr
DOI: https://doi.org/10.14744/seatific.2024.0006

Research Article

Development of a numerical modeling of the flow in an overtopping device with coupled Savonius turbine

Vinicius HEITMANN AVILA, Rafael Adriano Alves Camargo GONÇALVES, Jaifer Corrêa MARTINS, Emanuel da Silva Diaz ESTRADA, Liércio André ISOLDI, Luiz Alberto Oliveira ROCHA, Elizaldo Domingues DOS SANTOS*

Department of Mechanical Engineering, Federal University of Rio Grande (FURG), Rio, Brasil

ARTICLE INFO

Article history
Received: October 28, 2024
Revised: November 22, 2024
Accepted: November 26, 2024

Key words:
Numerical simulation; overtopping device; savonius turbine; sea wave energy

ABSTRACT

The study of the wave energy conversion (WEC) technologies has been growing, with an emphasis on the overtopping device. Its operation is based on a ramp that directs the wave water into an elevated reservoir. The accumulated water flows through a low-head turbine, generating electricity. This study proposes to develop a complete computational model to simulate a wave channel containing an overtopping device with a Savonius-type turbine inserted in the device's outlet duct. This study deals with the computational modeling of a multiphase (air and water), turbulent, incompressible flow with constant thermo physical properties, generated by the movement of numerical ocean waves. A validation study was conducted to guarantee the reliability of the separated models: i) flow in overtopping device without turbine, ii) flow over a free Savonius turbine. After this step, the two models are coupled and results showed that the coupling was successful, allowing the observation of the flow behavior in the complete model. Despite that, the computational model still needs adjustments to the turbine rotation and outlet channel geometry.

Cite this article as: Heitmann Avila V, Gonçalves RAAC, Martins JC, Estrada ESD, Isoldi LA, Rocha LAO, Dos Santos ED. Development of a numerical modeling of the flow in an overtopping device with coupled Savonius turbine. Seatific 2024;4:2:37–47.

1. INTRODUCTION

The demand for energy is expected to grow by more than 1.0% a year until 2040, which will increase the greenhouse gas emissions and the cost of generating energy with fossil fuels. This scenario brings economic challenges, energy security risks and geopolitical conflicts. In response, the current researches have focused on the development of technologies and the economic impact of renewable sources such as wind, solar, geothermal and wave energy (Jenniches, 2018).

The conversion of ocean energy into electricity is a renewable source with great potential, but which is still little explored globally. In the field of the wave energy, there is no dominant technology. Various devices have been proposed and studied, including point absorbers, attenuators, overtopping, submerged plates and oscillating water columns (Seibt et al., 2019).

The efficiency and durability of the wave energy converters are essential to making them competitive and economically viable. Overtopping and oscillating water column devices stand out for their simplicity and ease of maintenance, offering advantages in this context (Temiz et al., 2021).

Martins et al. (2022) investigated an overtopping device with one and two branches incorporated into a real breakwater, applying the Constructal Design method to analyze the effects of the degrees of freedom on the mean

***Corresponding author.**
*E-mail address: elizaldosantos@furg.br

dimensionless overtopping flow. The study compared different geometric configurations of the device to identify the best hydrodynamic performance, using the Joint North Sea Wave Project (JONSWAP) spectrum and the Volume of Fluid (VOF) model. The equations of mass conservation, momentum and transport of the volume fraction were solved. The results indicated that the two-ramp configuration led to 6.48% more overtopping than the one-ramp configuration, following the theoretical recommendations of Constructal Design for complex configurations. The study was carried out on the São José do Norte breakwater, RS, Brazil.

Santos et al. (2022) developed a computational model to investigate turbulent flows in an oscillating water column (OWC) device, considering a Savonius turbine in the air duct. Incompressible, two-dimensional, unsteady and turbulent flows were analyzed in three configurations: (1) a free turbine in a long channel for verification/validation, (2) a closed domain mimicking an OWC device with constant velocity at the inlet, and (3) the same domain with sinusoidal velocity at the inlet. A dynamic rotational mesh was used in the turbine region. The model, solving the unsteady time-averaged equations of conservation of mass and momentum with the *k-ω* SST (Shear Stress Transport) model, predicted power coefficients (C_p) similar to those in the literature for different tip speed ratios (0.75 ≤TSR ≤2.00). The closed domain increased the C_p compared to the free turbine, and the sinusoidal speed performed as well as the case of constant velocity imposed at the inlet of the domain.

Barros et al. (2023) carried out a numerical study of a full-scale overtopping device coupled to a seabed structure using the Constructal Design for geometric assessment. The aim was to investigate how the design influences the available power of the device, and the influence of the seabed structure in the device performance. The study considered the areas of the overtopping ramp (A_r) and the trapezoidal structure on the seabed (A_t) as constraints, exploiting two degrees of freedom: the ratio between the height and length of the ramp (H_3/L_3), and the ratio between the upper and lower bases of the trapezoidal obstacle (L_1/L_2), while the submergence is kept constant (H_1=3.5 m). The continuity, momentum and volume fraction transport equations were solved using the Finite Volume Method (FVM), and the water-air mixture was treated using the Volume of Fluid (VOF) model. The results indicated that H_3/L_3 had a greater impact on the water accumulated in the reservoir, but the inclusion of the coupled seabed structure increased the performance of the converter by 30% compared to a device without a structure.

Santos et al. (2023) developed a computational model to simulate an Oscillating Water Column (OWC) device coupled with a Savonius turbine. The device was inserted into a wave channel, with a Savonius turbine placed in the converter's inlet/outlet duct. The modeling used a moving rotational mesh, simulating the movement of the turbine under stabilized operating conditions, addressing the two-phase flow of air and water in the channel and the flow of air through the turbine. The model was verified for turbulent flow over a Savonius turbine and for wave flow in the converter without a turbine. The results showed that the model made it possible to calculate both the available power and the mechanical power of the turbine. In addition, for the studied conditions, the turbine did not cause significant changes in the behavior of the wave flow into the OWC chamber in comparison with the case without turbine. Despite that, an increase in the available power is noticed due to the restriction imposed by the turbine in the device. It is also noticed that the power coefficient also increased for similar range of TSR in comparison with the free turbine configuration.

Although there are several studies in the literature on overtopping devices, none have numerically evaluated the insertion of a turbine in these devices. This article seeks to fill this gap by analyzing a full-scale onshore overtopping device with a turbine inserted, an unprecedented investigation in the literature.

2. MATHEMATICAL AND NUMERICAL MODELING

2.1. Governing equations of the turbulent flows

For all simulations, the modeling of the incompressible, two-dimensional, unsteady and turbulent flows for a mixture of air and water is given by the unsteady time-averaged equations (URANS – Unsteady Reynolds-Averaged Navier Stokes) of mass conservation, momentum in the x and y directions, which are given by (Wilcox, 2006):

$$\frac{\partial \rho}{\partial t} + u\frac{\partial \rho}{\partial x} + v\frac{\partial \rho}{\partial y} + \rho\left(\frac{\partial \bar{u}}{\partial x} + \frac{\partial \bar{v}}{\partial y}\right) = 0 \quad (1)$$

$$\rho\left[\frac{\partial \bar{u}}{\partial t} + \bar{u}\frac{\partial \bar{u}}{\partial x} + \bar{v}\frac{\partial \bar{u}}{\partial y}\right] = -\frac{\partial \bar{p}}{\partial x} + (\mu + \mu_t)\left(\frac{\partial^2 \bar{u}}{\partial x^2} + \frac{\partial^2 \bar{u}}{\partial y^2}\right) \quad (2)$$

$$\rho\left[\frac{\partial \bar{v}}{\partial t} + \bar{u}\frac{\partial \bar{v}}{\partial x} + \bar{v}\frac{\partial \bar{v}}{\partial y}\right] = -\frac{\partial \bar{p}}{\partial y} + (\mu + \mu_t)\left(\frac{\partial^2 \bar{v}}{\partial x^2} + \frac{\partial^2 \bar{v}}{\partial y^2}\right) \quad (3)$$

where ρ is the fluid density (kg/m³), t is time (s), x and y are the spatial coordinates (m), u and v are the velocity components in the x and y directions, respectively (m/s), p is the pressure (N/m²), μ is the dynamic viscosity (kg/(m·s)), μ_t is the turbulent viscosity (kg/(m·s)), and the $\bar{u}$ and $\bar{v}$ represents the time-averaged velocities in x and y directions, respectively.

In the simulations of this study, two different phases are considered: air and water. Therefore, the concept of volume fraction (α_q) is used to represent the two phases within a control volume. In this model, the sum of the volume fractions within a control volume must be unitary ($0 \leq \alpha_q \leq 1$). Consequently, if α_{water}=0, the control volume is empty of water and full of air (α_{air}=1). If the fluid has a mixture of air and water, one phase is the complement of the other, i.e. $\alpha_{air} = 1 - \alpha_{water}$. Thus, an additional transport equation for one of the volume fractions is required (Hirt and Nichols, 1981):

$$\frac{\partial \alpha_{water}}{\partial t} + u\frac{\partial \alpha_{water}}{\partial x} + v\frac{\partial \alpha_{water}}{\partial y} + \alpha_{water}\left(\frac{\partial \bar{u}}{\partial x} + \frac{\partial \bar{v}}{\partial y}\right) = 0 \quad (4)$$

As the equations of conservation of mass and momentum are solved for the mixture, it is necessary to obtain the values of the density and viscosity for the mixture, which can be expressed as:

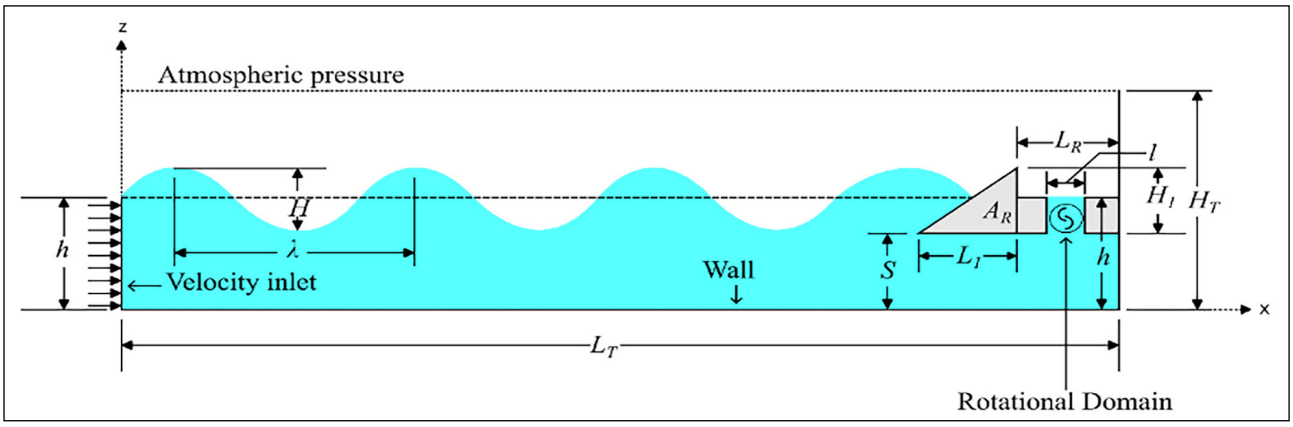

Figure 1. Computational domain of a full-scale overtopping device with an inserted turbine.

$$\rho = \alpha_{água}\rho_{água} + \left(1 - \alpha_{água}\right)\rho_{ar} \quad (5)$$

$$\mu = \alpha_{água}\mu_{água} + \left(1 - \alpha_{água}\right)\mu_{ar} \quad (6)$$

For the k-ω SST closure model, the turbulent viscosity (μ_t) is given by (Menter, Kuntz and Langtry, 2003):

$$\mu_t = \frac{\bar{\rho}\alpha_1 k}{max(\alpha_1\omega, SF_2)} \quad (7)$$

The transport equations for turbulent kinetic energy (k) and its specific dissipation rate (ω) are computed as (Menter, Kuntz and Langtry, 2003):

$$\frac{\partial k}{\partial t} + \frac{\partial(\overline{u_i}k)}{\partial x_i} = \tilde{P}_k - \frac{k^{\frac{2}{3}}}{L_T} + \frac{\partial}{\partial x_i}\left[(\mu + \sigma_k\mu_t)\frac{\partial k}{\partial x_i}\right] \quad (8)$$

$$\frac{\partial \omega}{\partial t} + \frac{\partial(\overline{u_i}\omega)}{\partial x_i} = \frac{\alpha}{\mu_t}\tilde{P}_k - \beta\omega^2 + \frac{\partial}{\partial x_i}\left[(\mu + \sigma_\omega\mu_t)\frac{\partial \omega}{\partial x_i}\right] + 2(1 - F_1)\frac{\sigma_{\omega 2}}{\omega}\frac{\partial k}{\partial x_i}\frac{\partial \omega}{\partial x_i} \quad (9)$$

in which $\tilde{P}_k$ is a function that prevents the generation of turbulence in regions of stagnation, i represents the direction of the fluid flow (i=1 represents the x direction and i=2 represents the y direction), β=0.09, α_1=5/9, β_1=3/40, σ_k=0.85, σ_ω=0.5, σ_2=0.44, β_2=0.0828, σ_{k2}=1 and $\sigma_{\omega 2}$=0.856 are constants used in Menter (1993). The mixing functions F_1 and F_2 are defined by the following equations (Menter, Kuntz and Langtry, 2003):

$$F_1 = \tanh\left\{\left\{min\left[max\left(\frac{k^{\frac{1}{2}}}{\beta^*\omega y}, \frac{500v}{y^2\omega}\right), \frac{4\rho\sigma_{\omega 2}k}{CD_{k\omega}y^2}\right]\right\}^4\right\} \quad (10)$$

$$F_2 = \tanh\left\{\left[max\left(\frac{2k^{\frac{1}{2}}}{\beta^*\omega y}, \frac{500v}{y^2\omega}\right)\right]^2\right\} \quad (11)$$

In equation (10), the term $CD_{k\omega}$ is given by (Menter, Kuntz and Langtry, 2003):

$$CD_{k\omega} = max\left(2\rho\sigma_{\omega 2}\frac{1}{\omega}\frac{\partial k}{\partial x_i}\frac{\partial \omega}{\partial x_i}, 10^{-10}\right) \quad (12)$$

2.2. Description of the case study

The physical problem analyzed here consisted of a two-dimensional overtopping device placed in a wave channel with a Savonius turbine inserted, as shown in Figure 1. The third-dimension y is perpendicular to the plane of the figure. The wave motion was generated by imposing a velocity field on the left surface of the tank. In this study, the ratio between the areas of the ramp and the wave channel were kept fixed (ϕ=A_r/A_T=0,012). Other parameters adopted in this study were: H_T/L_T=0,0612 (ratio between tank height, H_T=20 m, and tank length, L_T=327 m) and H/h=0.1 (ratio between wave height, H=1 m, and water depth, h=10 m). In addition, a reservoir with length of L_R=20 m and a height range for the device of S=6 m were also considered. For this value of S, the ratio H_1/L_1 = 0.14 was simulated.

In the region of the turbine, a constant angular velocity (η) of 0.5 rad/s was imposed in the region called the rotational domain (Fig. 1), simulating the effect of the fluid action on the turbine. A non-slip and impermeable boundary condition was imposed on the walls of the turbine ($u = v =$ 0 m/s) related to the rotational domain. The duct where the turbine is located has a width (l) equal to 2.344 m.

Regarding the other boundary conditions, an atmospheric pressure of P_{abs} = 101.3 kPa was applied to the upper region of the left lateral surface and the upper surface (dashed surfaces in Fig. 1). A no-slip and impermeability conditions ($u = w =$ 0 m/s) were imposed on the lower and right-side surfaces and on the surface of the overtopping device.

The initial conditions are that the fluid is wavy and that the water surface has a free surface with a height of h=10 m. As far as wave generation is concerned, a velocity profile was imposed at the channel entrance (left lateral surface of Fig. 1), simulating the operation of a wave generator (Horko, 2007). The velocity components in the wave propagation (x) and vertical (z) directions for the entrance channel are based on the second-order Stokes theory and are expressed, respectively, by (Chakrabarti, 2005):

$$u = \frac{gH}{2c}\frac{\cosh[k(z+h)]}{\cosh(kh)}\cos(kx - \omega t) + \frac{3}{16}ck^2H^2\frac{\cosh[2k(z+h)]}{\sinh^4(kh)}\cos[2(kx - \omega t)] \quad (13)$$

$$w = \frac{gH}{2c}\frac{\sinh[k(z+h)]}{\cosh(kh)}\sin(kx - \omega t) + \frac{3}{16}ck^2H^2\frac{\sinh[2k(z+h)]}{\sinh^4(kh)}\sin[2(kx - \omega t)] \quad (14)$$

$$\eta = \frac{H}{2}\cos(kx - \omega t) + \frac{kH^2}{16}\frac{\cosh(kh)}{\sinh^3(kh)}[2 + \cosh(2kh)]\cos[2(kx - \omega t)] \quad (15)$$

Table 1. Characteristics of regular waves

Parameter	Symbol	Magnitude
Wave height	H	1.00 m
Wave period	T	7.50 s
Wave length	λ	65.4 m
Channel depth	h	10.00 m

where H is the wave height (m), k is the wave-number given by $k=2\pi/\lambda$ (m^{-1}), h is the water depth (m), T is the wave period (s), $\lambda=2\pi/T$ is the frequency (rad/s), t is the time (s), c is the wave celerity (m/s) and ω is the angular velocity (Hz). Table 1 shows the characteristics adopted for the waves considered in this study.

3. NUMERICAL PROCEDURES

This work used the Finite Volume Method (FVM) (Versteeg and Malalasekera, 2007) for the numerical solution of the equations of conservation of mass, momentum and the volume fraction transport equation. The commercial Computational Fluid Dynamics (CFD) package FLUENT™ was also used. The multiphase Volume of Fluid (VOF) model (Hirt and Nichols, 1981) was applied to the interaction between air, water and the device. The numerical parameters adopted in the ANSYS FLUENT 2022 commercial software are shown in Table 2.

As for the spatial discretization, a stretch mesh was considered, following the recommendations of Gomes et al. (2012) for the wave channel, Martins et al. (2022) for the overtopping device, and Santos et al. (2022) in the Savonius turbine. However, greater refinement was adopted both in the free surface region, where 30 volumes per wave height were used, and horizontally, where 70 volumes per wavelength were considered, as defined by the mesh independence test. The interaction between the wave flow and the ramp of the overtopping device justifies this greater refinement, resulting in approximately 155,000 finite volumes. Figure 2 illustrates the mesh generated by the GMSH software for the computational domain, detailing the region of the overtopping device and the turbine.

Regarding the spatial discretization of the Savonius turbine, triangular and rectangular hybrid finite volumes were used in the computational domain (Santos et al., 2022). Figure 3 illustrates the turbine mesh, Figure 3a, and a detail of the mesh on the blades, Figure 3b, respectively. In detail, it is possible to see a region around the blades with a refined rectangular mesh.

4. RESULTS AND DISCUSSION

Firstly, the validation of the present numerical method for solving of the isolated cases of overtopping (without turbine and exit duct connected to the reservoir) and free Savonius turbine subjected to turbulent air flow is performed.

For the overtopping device, the numerical model used, based on Goulart et al. (2015), was verified, as shown in Figure 4. To do this, a comparison was made between the height of the water accumulated in the reservoir as a function of time obtained in the author's numerical study and the numerical predictions obtained with the current computational method. This comparison is presented in Figure 5.

As can be seen, the numerical results were in close agreement. The numerical results also predicted the onset of overtopping (t~47 s) and the slope of the water accumulation curve in the reservoir. It is therefore possible to state that this computational method is verified.

Table 2. Methods used in numerical simulations

Parameter	Numerical input
Solver	Pressure-based
Pressure-velocity coupling	PISO
Spatial discretization	
Gradient evaluation	Least squares cell based
Pressure	PRESTO
Momentum	First order upwind
Volume fraction	Geo-reconstruct
Temporal differencing scheme	First order implicit
Regime flow	k-ω SST
Under-relaxation factors	
Pressure	0.3
Momentum	0.7
Residual	
Continuity	10^{-6}
Velocity-x	
Velocity-z	
Open channel initialization method	Wavy
Time step (Δt)	2.00×10^{-2} s
Maximum number of iterations per time step	200

PISO: Pressure implicit with split operator; PRESTO: Pressure staggering option; SST: Shear Stress Transport

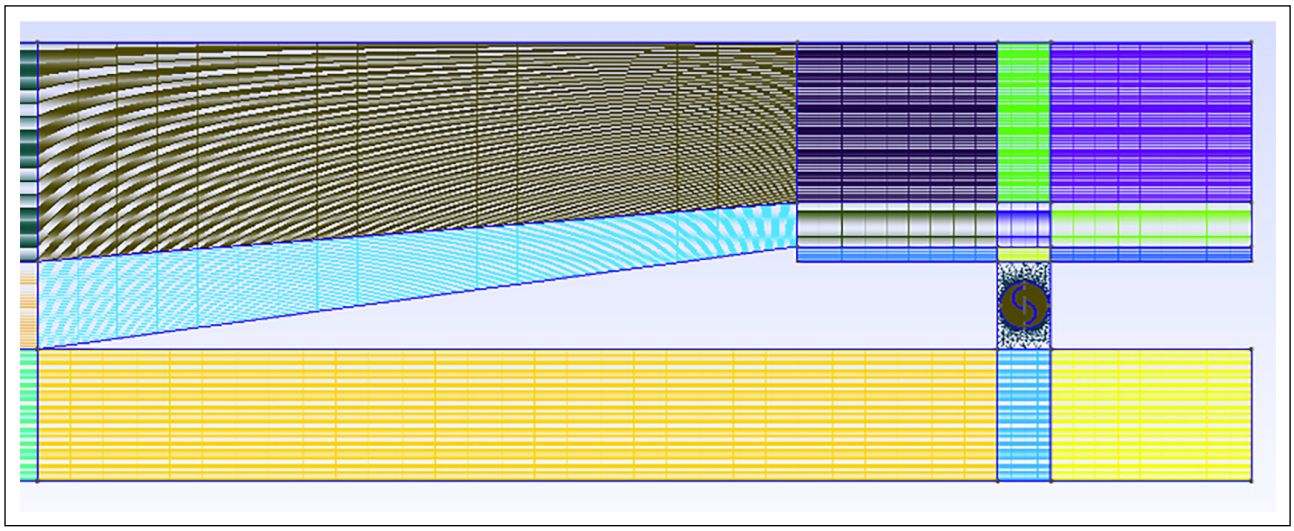

Figure 2. Spatial discretization applied to the full-scale overtopping device with an inserted turbine.

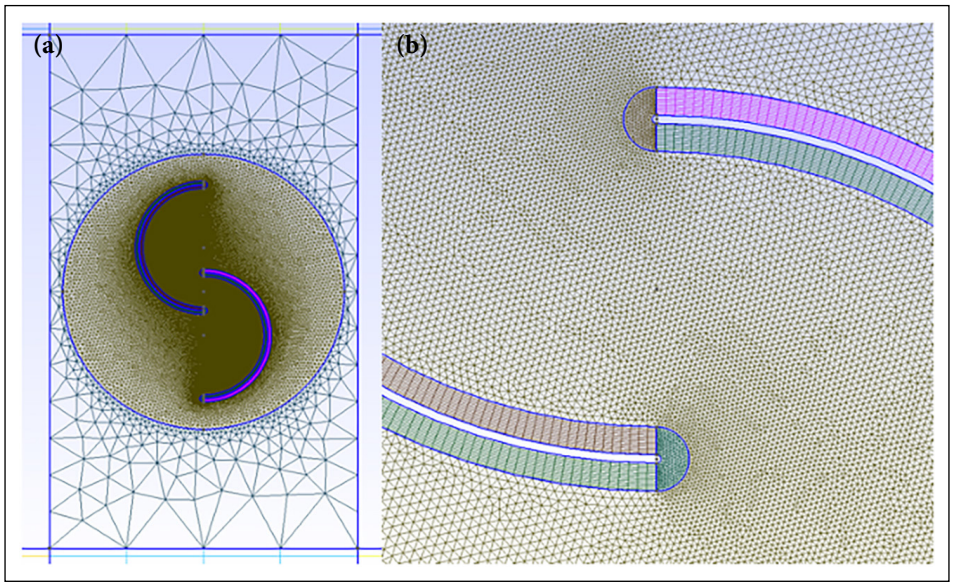

Figure 3. Mesh used in the Savonius turbine region: (a) overview of the entire turbine, (b) mesh refinement detail of the blade surfaces.

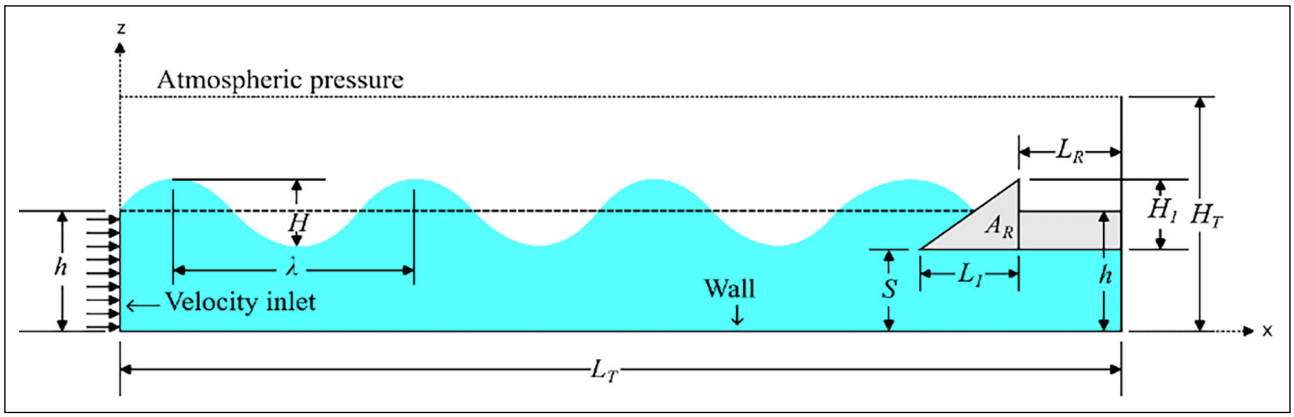

Figure 4. Schematic representation of the domain investigated numerically by Goulart et al. (2015).

For the Savonius turbine, validation of the numerical model was carried out by comparing the results obtained for the power coefficient with the experimental work of Blackwell et al. (1977) and with the numerical works of Akwa et al. (2012) and Santos et al. (2022) for the different tip speed ratios (TSR): 0.75; 1.00; 1.25 and 2.00. Free-flowing air flows with a constant

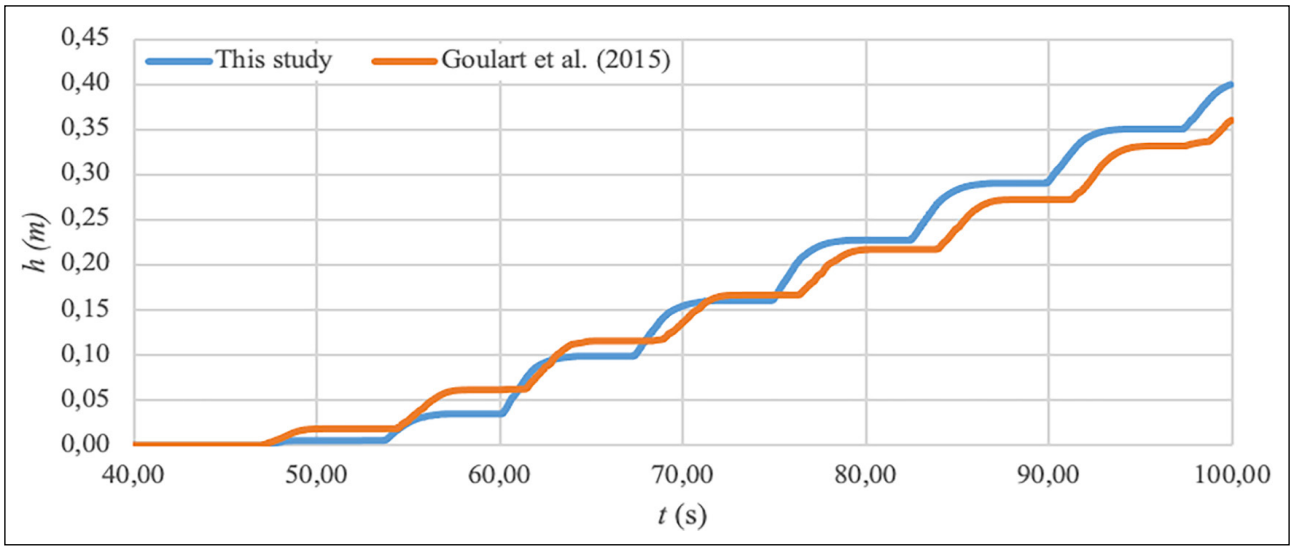

Figure 5. Water accumulated in the reservoir of the overtopping device as a function of time obtained numerically in Goulart et al. (2015) and with the present method.

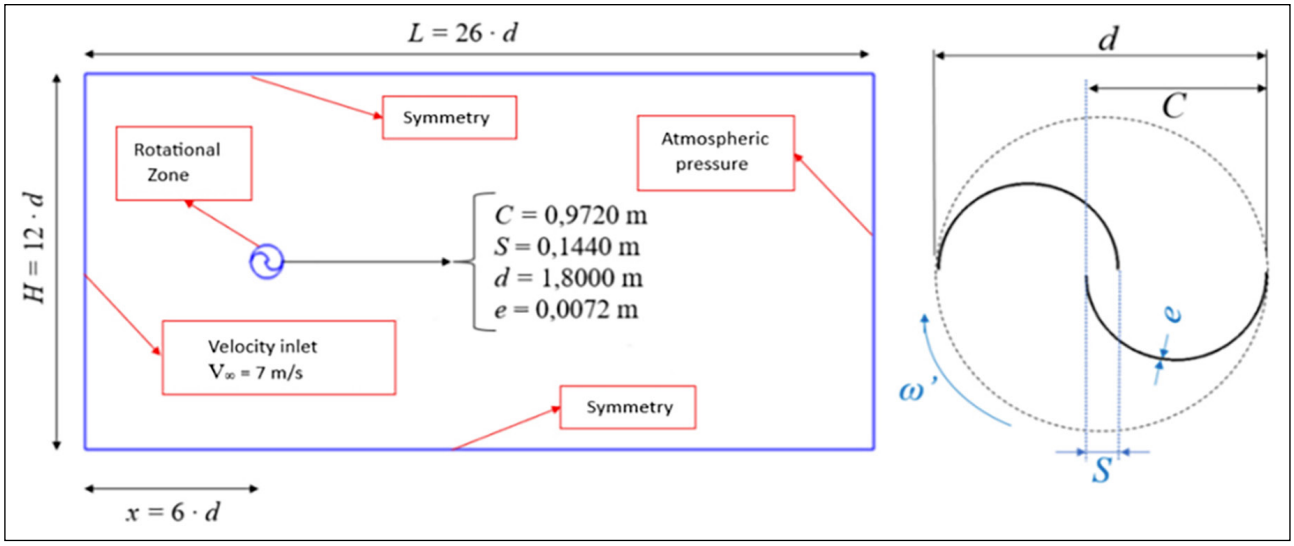

Figure 6. Computational domain of the wind tunnel with a Savonius turbine.

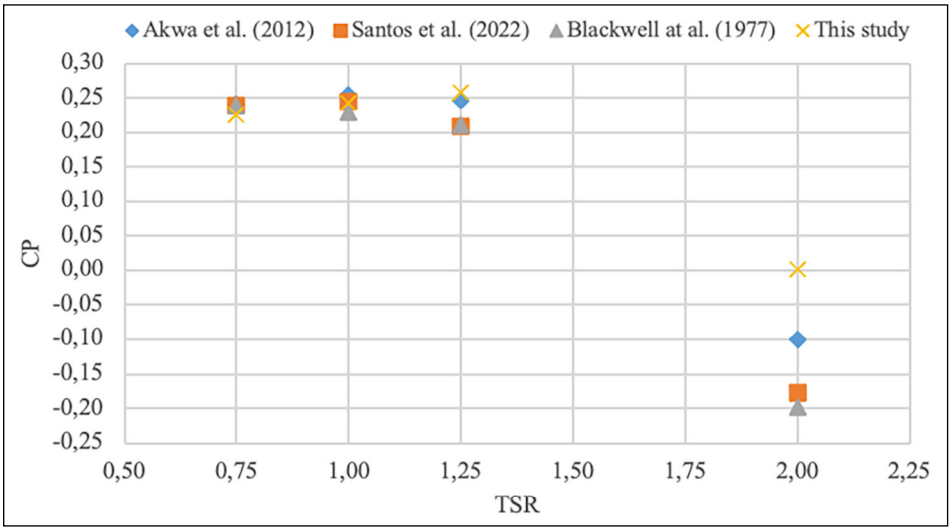

Figure 7. Numerical validation of C_p for Savonius turbine in a wind tunnel.

TSR: Tip speed ratios.

Table 3. Power coefficient for different tip speed ratios

TSR	C_p			
	Akwa et al. (2012)	**Santos et al. (2022)**	**Blackwell et al. (1977)**	**This study**
0.75	0.240	0.238	0.238	0.225
1.00	0.255	0.244	0.230	0.243
1.25	0.247	0.210	0.210	0.257
2.00	-0.100	-0.177	-0.199	0.002

TSR: Tip speed ratios

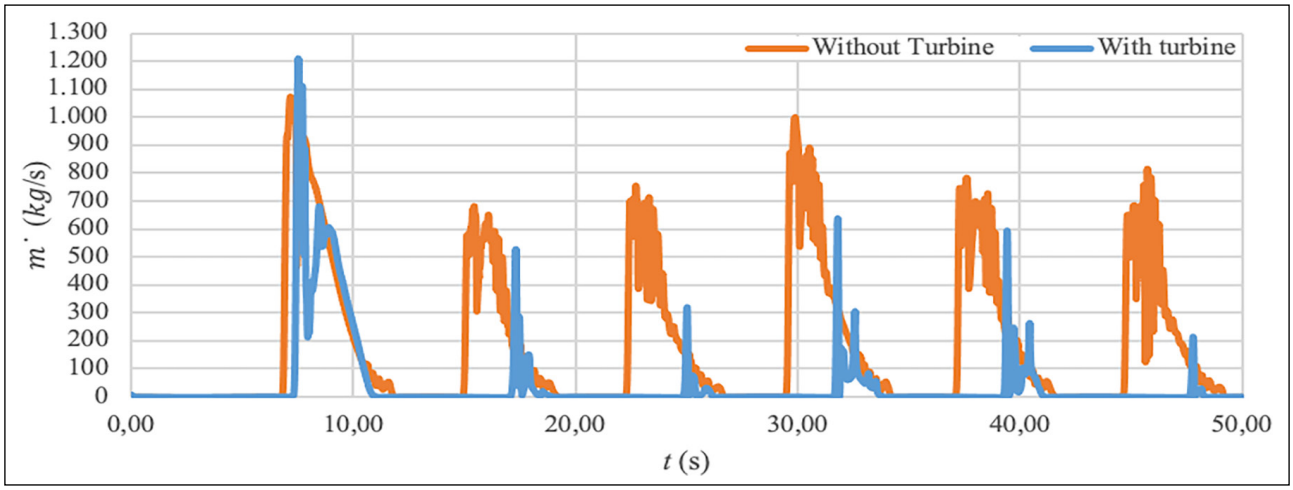

Figure 8. Instantaneous behavior of the water in the overtopping device for the cases without turbine and with turbine inserted over the mass flow.

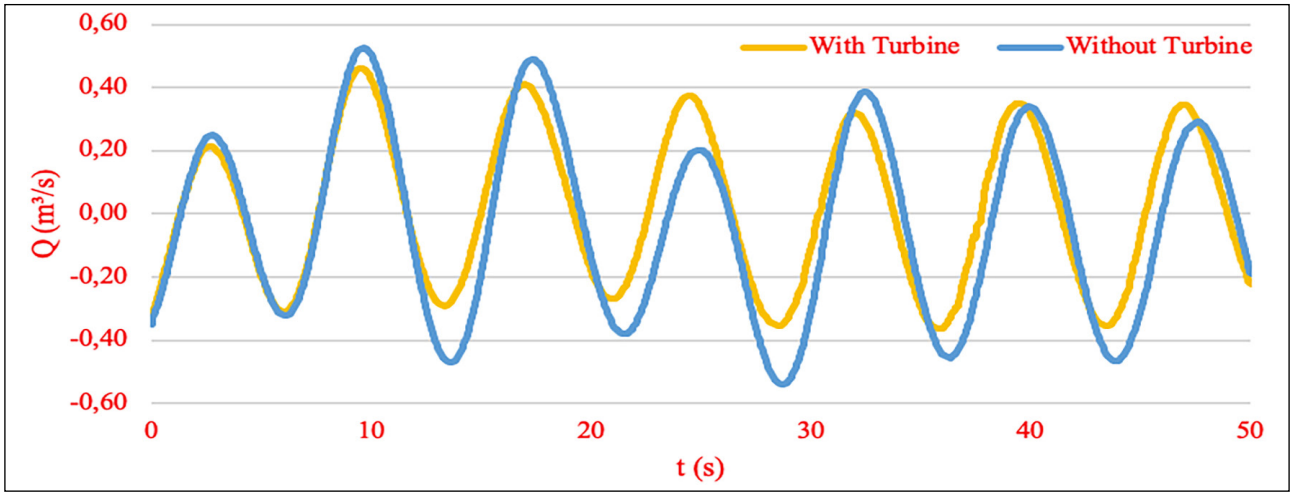

Figure 9. Instantaneous behavior of the water flow over the exit duct in the overtopping device.

velocity of $V_\infty = 7$ m/s and a Reynolds number of $R_{eD} = 867{,}000$ in the rectangular domain impinging a rotational turbine is investigated. The domain analyzed with its dimensions and boundary conditions is shown in Figure 6. The computational mesh for validation was generated in such a way as to be as close as possible to the work of Santos et al. (2022).

The pressure-based solver was used for the simulations of this numerical validation using the ANSYS FLUENT 2022 R2 program. The spatial discretization for the pressure was treated with the second-order formulation, while the second-order upwind is adopted for the equations of the momentum. For the pressure-velocity coupling, the SIMPLE algorithm was employed. For the closure of the turbulence, the k-ω SST turbulence model was implemented.

Figure 7 illustrates and Table 3 presents the comparison of the results of the effect of the blade tip speed ratio on the power coefficient (C_p) of the present work with the experimental and numerical works.

With the results obtained, the numerical validation of the rotating Savonius turbine in a two-dimensional domain simulating a wind tunnel, according to the experimental study by Blackwell et al. (1977) and the numerical study by Akwa et

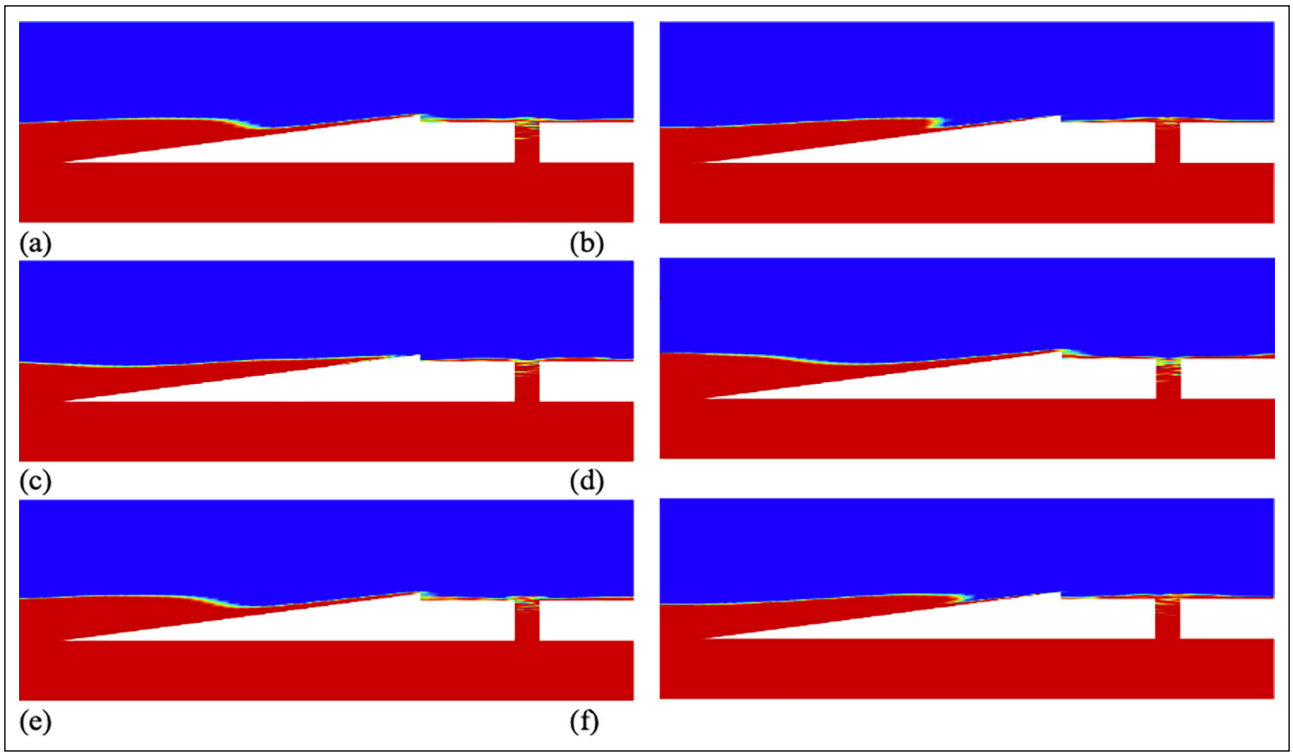

Figure 10. Wave flow as function of time for the cases without turbine: (a) t = 40.0 s, (b) t = 42.0 s, (c) t = 44.0 s, (d) t = 46.0 s, (e) t = 48.0 s and (f) t = 50.0 s.

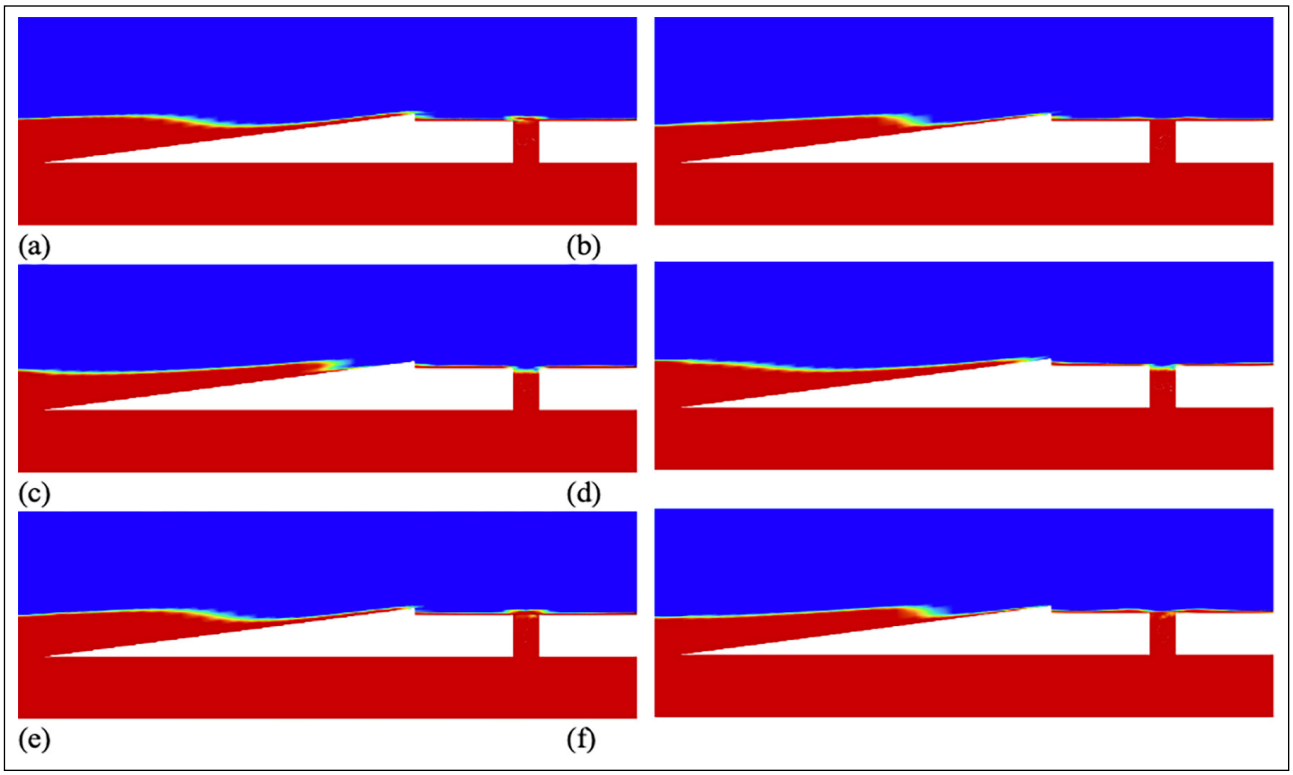

Figure 11. Wave flow as function of time for the cases with turbine: (a) t = 40.0 s, (b) t = 42.0 s, (c) t = 44.0 s, (d) t = 46.0 s, (e) t = 48.0 s and (f) t = 50.0 s.

al. (2012), was considered satisfactory for the continuation of the coupled model proposed in the present study.

Based on the results obtained in the validation studies for each case (overtopping without turbine, and free flow over a Savonius turbine) it is presented here onward the analysis of the overtopping device with the coupled Savonius turbine and some comparison with the overtopping device with the exit duct, but without the turbine mounted in the device.

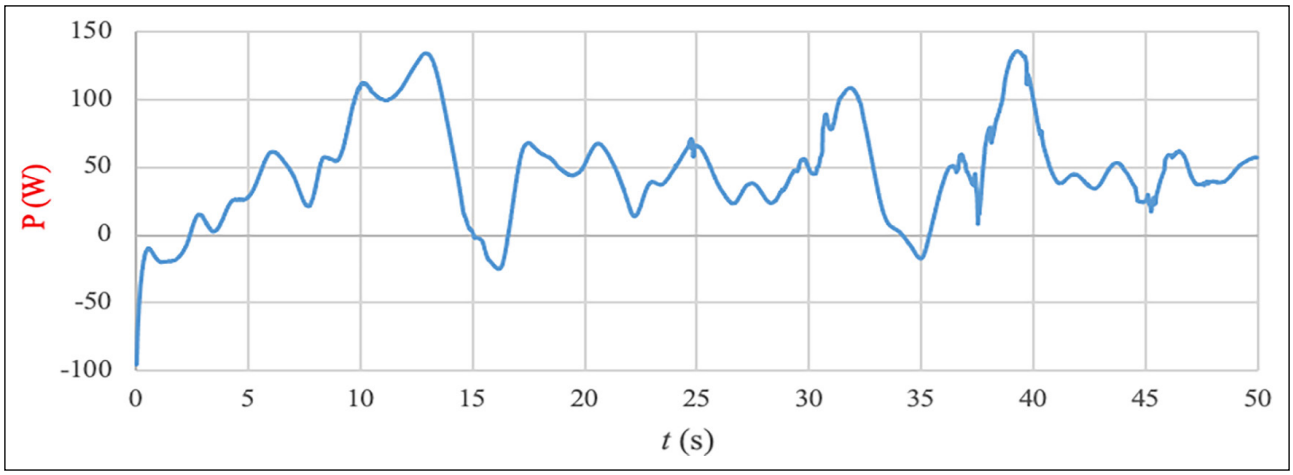

Figure 12. Power extracted from the turbine as a function of time.

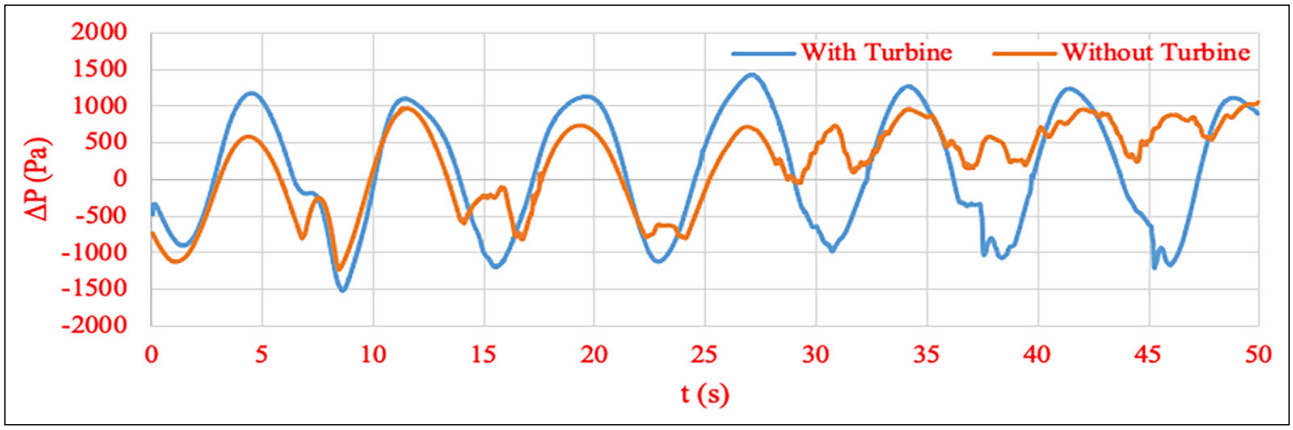

Figure 13. Turbine pressure gradient as a function of time.

Figure 8 shows the instantaneous behavior of the water in the overtopping device on the mass flow rate ($\dot{m}$), for the cases with turbine (Fig. 1) and the same case, but without the turbine insertion. The measure of mass flow rate is recorded by means of a probe placed at the top of the ramp of the device until the end of the reservoir. The results demonstrated that the insertion of the turbine affected the arriving of the wave flow oncoming the ramp, changing the mass flow rate of water overtopping the device, mainly from the second overtopping peak onwards. Figure 8 also shows that, for the two cases analyzed, the mass flow peaks began to occur at a time approximately t~7 s. Both for the situation of the overtopping device without the turbine and with the turbine, the highest magnitudes were observed at t~7 s, being $\dot{m}$=1074.80 kg/s and $\dot{m}$=1212.51 kg/s, respectively. It is important to note that the case of the overtopping device without the turbine inserted obtained a greater accumulation of mass flow compared to those with the turbine inserted, since part of the wave's energy ends up causing a return of the water flow through the duct where the device's turbine is located. Figure 9 shows the instantaneous behavior of the water flow over the exit duct in the overtopping device. In both cases, it can be noticed a pulsating behavior of the flow, which can affect the dynamic of the fluid flow in the frontal region of overtopping device. Figures 10 and 11 show the volume fraction of water in the time interval of 40.0 s ≤ t ≤ 50.0 s for the cases without and with turbine, respectively, considering different instants of time: (a) t = 40.0 s; (b) t = 42.0 s; (c) t = 44.0 s; (d) t = 46.0 s; (e) t = 48.0 s; and (f) t = 50.0 s. The results of the volume fraction illustrate the influence of the flow exiting the power take off region on the wave flow has in the wave flow overtopping the device.

Figures 12 show the power extracted from the turbine and Figure 13 show the pressure gradient in the exit duct for the cases without and with turbine. Based on this data, it was possible to determine the power coefficient C_p and the turbine tip speed, which are equal to 0.12 and 1.85, respectively. The positive magnitude of C_p obtained indicates that the fluid flow provides energy for the device. Despite that, the magnitude of CP for a Savonius turbine can achieve higher magnitudes, showing that the investigation of the imposed rotation and geometric configuration of the exit duct should be analyzed in more detail in future studies. Nevertheless, the developed model is promising for future investigations on the overtopping device in a more realistic approach.

5. CONCLUSION

This study carried out a two-dimensional analysis of an overtopping-type wave energy converter combined with a Savonius rotation turbine in the outlet duct. The simulations

used the Finite Volume Method (FVM) and the Volume of Fluid (VOF) methodology to model the interaction between air and water, with waves generated from the 2nd order Stokes theory. The turbine was included in the model, in a moving mesh with constant angular velocity. The κ-ω SST turbulent model was used to close the equations, and the geometry and meshes were generated in GMSH, while the processing was carried out in ANSYS FLUENT 2022 R2.

Firstly, the present computational model was validated for two isolated cases of overtopping device without turbine and exit duct in the reservoir, and free turbine under turbulent air flow. Later, a comparison of two cases (one with and other without turbine, but with the exit duct) was performed. The results showed that the greatest amount of water entering the reservoir over time was obtained for the case of the overtopping device without the turbine. The insertion of the turbine in the exit duct of the overtopping device conducted to a less amount of water passing through the turbine conduit, affecting the behavior of the wave oncoming the ramp. This difference is reflected in the instantaneous mass flow rate of water entering in the reservoir, mainly from the second occurrence onward.

In general, the developed computational modeling was promising in reproduce the behavior of the device with a coupled turbine, which is a novelty here. However, future studies are required to investigate the rotation (in the present model) that conducts to the highest power coefficient and the design of the exit duct that improves the turbine performance.

ACKNOWLEDGMENTS

The author V. H. Avila thanks CNPq for the master's scholarship (Process: 132159/2023-6) and ANP for the post-doctoral scholarship (Process: 2024/12385-9). The authors L. A. Isoldi, L. A. O. Rocha and E. D. dos Santos thank CNPq for the research productivity grant (Processes: 309648/2021-1, 307791/2019-0, 308396/2021-9). The authors would like to thank CNPq for financial support under CNPq/MCTI Call No. 10/2023 - Universal (Process: 403408/2023-7). L.A.O. Rocha and E.D. dos Santos also thank Fundação para a Ciência e Tecnologia, I.P. (doi.org/10.54499/UIDP/04683/2020 ; doi.org/10.54499/UIDB/04683/2020).

DATA AVAILABILITY STATEMENT

The authors state that the published publication includes all graphics and data collected or developed during the study.

CONFLICT OF INTEREST

The author declared no potential conflicts of interest with respect to the research, authorship, and/or publication of this article.

ETHICS

There are no ethical issues with the publication of this manuscript.

USE OF AI FOR WRITING ASSISTANCE

No AI technologies utilized.

FINANCIAL DISCLOSURE

The work was funded by CNPq and CAPES.

REFERENCES

Akwa, J. V., Silva Júnior, G. A., & Petry, A. P. (2012). Discussion on the verification of the overlap ratio influence on performance coefficients of a Savonius wind rotor using computational fluid dynamics. *Renewable Energy, 38*(1), 141–149. [CrossRef]

ANSYS FLUENT. (2022). *Documentation Manual*. ANSYS FLUENT 2022 R1.

Barros, A. S. de, Fragassa, C., Paiva, M. da S., Rocha, L. A. O., Machado, B. N., Isoldi, L. A., Gomes, M. das N., & Santos, E. D. dos. (2023). Numerical study and geometrical investigation of an onshore overtopping device wave energy converter with a seabed coupled structure. *Journal of Marine Science and Engineering, 11*(2), Article 412.

Blackwell, B. F., Sheldahl, R. E., & Feltz, L. V. (1977). *Wind tunnel performance data for two-and three-buckets savonius rotors (final report SAND76-0131)*. Sandia Laboratories.

Chakrabarti, S. K. (2005). *Handbook of offshore engineering*. Elsevier.

Gomes, M. N., Isoldi, L. A., Santos, E. D., & Rocha, L. A. O. (2012). *Análise de Malhas para Geração Numérica de Ondas em Tanques. In VII Congresso Nacional de Engenharia Mecânica* – CONEM, São Luís, Maranhão, Brasil.

Goulart, M. M., Martins, J. C., Acunha Júnior, I. C., Gomes, M. N., Souza, J. A., Rocha, L. A. O., Isoldi, L. A., & Santos, E. D. (2015). Constructal design of an onshore overtopping device in real scale for two different depths. *Marine Systems & Ocean Technology, 10,* 120–129.

Hirt, C. W., & Nichols, B. D. (1981). Volume of fluid (VOF) method for the dynamics of free boundaries. *Journal of Computational Physics, 39*(1), 201–225. [CrossRef]

Horko, M. (2007). *CFD Optimisation of an oscillating water column energy converter* [Master's thesis]. School of Mechanical Engineering, The University of Western Australia.

Jenniches, S. (2018). Assessing the regional economic impacts of renewable energy sources – a literature review. *Renewable and Sustainable Energy Reviews, 93*, 35–51. [CrossRef]

Martins, J. C., Fragassa, C., Goulart, M. M., Santos, E. D. dos, Isoldi, L. A., Gomes, M. das N., & Rocha, L. A. O. (2022). Constructal design of an overtopping wave energy converter incorporated in a breakwater. *Journal of Marine Science and Engineering, 10*(4), Article 471. [CrossRef]

Menter, F. R. (1993). *Zonal two equation k–ω turbulence models for aerodynamic flows*. In Proceedings of the AIAA 24th Fluid Dynamics Conference, 6–9. Orlando, FL, USA. [CrossRef]

Menter, F. R., Kuntz, M., & Langtry, R. (2003). Ten Years of Industrial Experience with the SST Turbulence Model. In K. Hanjali´c, Y. Nagano, & M. Tummers (Eds.), *Turbulence, Heat and Mass Transfer, 4*, 625–632.

Santos, A. L. G., Fragassa, C., Santos, A. L. G., Vieira, R. S., Rocha, L. A. O., Conde, J. M. P., Isoldi, L. A., & dos Santos, E. D. (2022). Development of a computational model for investigation of an oscillating water column device with a savonius turbine. *Journal of Marine Science and Engineering, 10*(1), Article 79. [CrossRef]

Santos, A. L. G. (2023). *Modelagem numérica e método design construtal para avaliação geométrica de um dispositivo do tipo coluna de água oscilante considerando a inserção de uma turbina Savonius* (Tese de Doutorado). Universidade Federal do Rio Grande, Rio Grande, Brasil.

Santos, A. L. G., Petry, A. P., Isoldi, L. A., Dias, G. C., Souza, J. A., & dos Santos, E. D. (2023). Development of a computational model for the simulation of an oscillating water column wave energy converter considering a savonius turbine. *Defect and Diffusion Forum, 427*, 95–106. [CrossRef]

Seibt, F., De, Camargo, Dos, Santos, Das, Neves, Rocha, L. A. O., Isoldi, L., & Fragassa, C. (2019). Numerical evaluation on the efficiency of the submerged horizontal plate type wave energy converter. *FME Transactions, 47*(3), 543–551. [CrossRef]

Temiz, I., Ekweoba, C., Thomas, S., Kramer, M., & Savin, A. (2021). Wave absorber ballast optimization based on the analytical model for a pitching wave energy converter. *Ocean Engineering, 240*, Article 109906. [CrossRef]

Versteeg, H. K., & Malalasekera, W. (2007). *An Introduction to Computational Fluid Dynamics: The Finite Volume Method* (2nd ed.). Pearson Education.

Wilcox, D. C. (2006). *Turbulence Modeling for CFD* (3rd ed.). DWC Industries.

Seatific, Vol. 4, Issue. 2, pp. 48–56, December 2024

Seatific Journal
https://seatific.yildiz.edu.tr
DOI: https://doi.org/10.14744/seatific.2024.0008

Seatific

Research Article

Correlation of the ship speed and carbon dioxide emissions: A study on a Panamax tanker

Levent BİLGİLİ[1]*, Volkan ŞAHİN[2]

[1]*Department of Naval Architecture and Marine Engineering, Bandırma Onyedi Eylül University Faculty of Maritime, Balıkesir, Türkiye*
[2]*Department of Marine Engineering, Van Yüzüncü Yıl University Faculty of Maritime, Van, Türkiye*

ARTICLE INFO

Article history
Received: October 07, 2024
Revised: November 15, 2024
Accepted: December 02, 2024

Key words:
Fuel consumption; ship emissions; ship speed; regression analysis

ABSTRACT

The amount of energy needed by the maritime industry is increasing depending on the global energy demand and the increase in commercial activities. Larger ships are expected to create greater challenges in the energy demand and environmental performance issues. Therefore, estimating fuel consumption and emissions are important preliminary steps to avoid these problems. In this study, the relationship between speed and CO_2 emissions is reduced to a single equation. It aims to reach fuel consumption and emission amounts by using only speed input. Since emission calculations are mainly based on fuel consumption data, specific fuel oil consumption methodology is utilized and regression analysis is used to reach a single-variable equation. The equation is calculated with a high accurance (R^2 0.9941). Since the speed input includes RPM, weather and sea conditions, cargo quantity and wave course data, the effects of these data on fuel consumption have been obtained indirectly. In this way, fuel consumption and emissions can be predicted depending on the speed through a simple equation, and the solutions on measurements and route optimization would be much easier.

Cite this article as: Bilgili L, Şahin V. Correlation of the ship speed and carbon dioxide emissions: A study on a Panamax tanker. Seatific 2024;4:2:48–56.

1. INTRODUCTION

Energy efficiency and fuel consumption in ships are considered to be crucial issues in the 21st century, due to the environmental awareness has increased with a growing momentum. Increasing population and developing trade lead the world to bigger ships and larger commercial fleets, forming a bigger energy demand. Thus, it is obvious that fuel consumption and consequently ship emissions would be a bigger problem day by day.

According to the International Energy Agency (IEA) report, when world energy consumption amounts are examined, 122 EJ of energy was spent in the transport sector in 2023 and 11 EJ of this energy was used by the shipping sector. This corresponds to approximately 9% of the energy spent in the transport sector. It is predicted that a total of 132 EJ of energy will be spent in the transport sector in 2030 and 12 EJ of this will be used by the shipping sector. When the world CO_2 emission amounts are examined, it is seen that the total CO_2 emission amount in 2023 is 37723 Mt CO_2. While 8213 Mt CO_2 of this emission amount belongs to the transport sector, 856 Mt CO_2 belongs to the shipping sector. The total CO_2 emission amount in 2030 is estimated to be 36170 Mt CO_2. It is estimated that 8537 Mt of this amount will belong to the transport sector and 900 Mt of CO_2 will belong to the shipping sector (IEA, 2024). On the other hand, even in the most optimistic scenario, fuel demand in the maritime sector is projected to increase by 43.5% in 2050 compared to 2002 (Eyring et al., 2005).

***Corresponding author.**
*E-mail address: lbilgili@bandirma.edu.tr

Ship-related emissions emerge as a separate and important environmental problem. Although ships emit a large number and variety of emissions (Kollamthodi et al., 2008) only a few of them are worth examining in terms of environmental damage and quantity. According to the latest report of the International Maritime Organization (IMO), shipping activities are responsible for 2.4%, 13-15% and 12-13% of global carbon dioxide equivalent (CO_{2e}), sulphur oxide (SO_x) and nitrogen oxide (NO_x) production, respectively (Smith et al., 2014). IMO's recent study has shown that greenhouse gas emissions from the shipping sector increased from 977 million tonnes in 2012 to 1,076 million tonnes in 2018, an increase of 9.6% (IMO, 2020a). In addition, it has been determined that 70% of ship emissions occur at 400 km and closer to the shore (Eyring et al., 2010).

Efforts to estimate emissions and increase energy efficiency are essential to guarantee a greener future. For this purpose, in addition to many local, national and regional studies, many international rules and regulations have been developed under the leadership of the IMO. Under the International Convention for the Prevention of Pollution from Ships (MARPOL), IMO has prepared several annexes for the monitoring, reduction and control of various ship-related pollutants. Annex VI is the supplement where ship air pollutants are evaluated and it includes the assessments on ozone-depleting substances (ODSs), particulate matter (PM), and volatile organic compounds (VOCs). Annex VI came into force on 9 May 2005 and is being developed with various updates annually.

Restrictions imposed by the IMO for NO_x and SO_x are presented in Table 1 and Table 2.

Table 1 presents the minimum requirements for ships to meet NOx criteria. Ship main engines must be manufactured according to Tier II standards in the current situation. Ships cruising in the North American and United States Caribbean Sea Areas must be subject to Tier III restrictions. Table 2 presents the SO_x constraints. Accordingly, under the current situation, the fuel used by a ship cruising in global waters may contain up to 0.5% sulphur by mass. If a ship cruises in an Emission Control Area (ECA) (Baltic Sea, North Sea, North American and United States Caribbean Sea Areas), the ratio is set at 0.1%.

In a recent study on the question of whether Annex VI does not include ship-related CO_2 emissions, it is stated that especially developed countries accept CO2 as a greenhouse gas (GHGs) rather than a polluting agent. In addition, there is a concern that possible additions for CO_2 reduction may lead to "tremendous domestic legal obstacles". Therefore, it was concluded that Annex VI should be left as it is and if necessary, a unique regulation should be prepared for CO_2 (Shi, 2016).

The deleterious impacts of ship-related emissions on human health and the environment are well-studied (Corbett et al., 2007; Eyring et al., 2010; Kollamthodi et al., 2008; Moldanová et al., 2009) and detailed inventories of these emissions on a regional and global scale were calculated (Alver et al., 2018; Jalkanen et al., 2016; Johansson et al., 2017). It is clear that emissions from ships have a wide variety of harmful impacts to human health and the environment. Considering the development of the global economy, trade volume and the maritime industry, it is obvious that ship-related emissions and the energy demand of the maritime sector will pose even more serious problems shortly.

The majority of these studies focused on emission estimates based on fuel consumption or engine power. Some of them calculate the emission by estimating the possible fuel consumption considering the dynamic sea conditions. It is crucial to calculate the emissions at an early stage, especially in terms of compliance with the IMO criteria. Another important issue is to calculate the fuel consumption (energy demand) and emission amounts empirically. For this purpose, various studies have been carried out to find the correlation between speed, which is the most important output of dynamic marine conditions, and fuel

Table 1. The limits for NO_x (IMO, 2015a)

Tier	Ship construction date on or after	Total weighted cycle emission limit (g/kWh) n=Engine's rated speed (RPM)		
		n<130	n=130–1999	n≥2000
Tier I	1 January 2000	17.0	$45\times n^{-0.2}$	9.8
Tier II	1 January 2011	14.4	$44\times n^{-0.2}$	7.7
Tier III (ECA)	1 January 2016	3.4	$9\times n^{-0.2}$	2.0

IMO: International Maritime Organization; RPM: Revolutions per minute; ECA: Emission Control Area

Table 2. The limits for SO_x (IMO, 2015b)

Outside an emission control area	Inside an emission control area
4.50% prior to 1 January 2012	1.50% prior to 1 July 2010
3.50% on and after 1 January 2012	1.00% on and after 1 July 2010
0.50% on and after 1 January 2020	0.10% on and after 1 January 2015

IMO: International Maritime Organization

consumption/emission. In addition, there are also studies for fuel consumption and emission calculations depending on the dynamic operating conditions.

(Beşikçi et al., 2016) developed a fuel consumption methodology based on ship speed, revolutions per minute (RPM), mean draft, trim, cargo quantity, wind and sea effects data by using the noon reports. The authors used the artificial neural networks method for this purpose. (Bialystocki & Konovessis, 2016) developed a fuel consumption prediction algorithm based on current fuel consumption, draft, weather and surface roughness data. The main point emphasized in this study is the effect of weather conditions on fuel consumption. Utilizing the Least Absolute Shrinkage and Selection Operator (LASSO) regression algorithm, (Shengzheng Wang et al., 2018) developed a fuel consumption prediction methodology based on historical fuel consumption, length overall, beam, speed, trim angle, air and sea conditions and swell height data. (Gkerekos et al., 2019) They studied on estimating fuel consumption by using distance, draft, RPM, daily fuel consumption, ship speed, propeller angle, sea current, wave direction, sea and weather conditions and wind direction data in different machine learning methods. (Kee et al., 2018) developed a fuel consumption prediction formula based on distance, working hours and deadweight data by utilizing multiple linear regression methods. Although they are not included in the formula, ship speed and wind speed are among the inputs used. (Graf von Westarp, 2020) investigated the correlation between fuel consumption and speed for a container ship. As a result, depending on the e-function, a direct equation between speed and fuel consumption was found to be valid in container ships. (Ayudhia P. Gusti & Semin, 2016) examined the correlation between speed and fuel consumption and emission values for a container ship cruising between two ports in Indonesia. (Ayudhia Pangestu Gusti & Semin, 2018) also compiled studies on the correlations between ship speed and emission.

However, none of these studies found a direct correlation between ship speed and fuel consumption for tankers. An equation, which depends on the ship's speed and without any additional calculation or data, would allow the calculation of fuel consumption and emission amount even when the ship is not cruising. In addition, the simpler the fuel consumption and emission estimation can be achieved, the more useful it will be.

In this study, a correlation was developed between the daily speeds and CO_2 emissions. For this purpose, the average daily engine load of the ship was calculated based on the speed, and then the specific fuel oil consumption (SFOC) in this engine load was determined and the amount of fuel expected to be spent was reached. Emission calculations were realized depending on the amount of fuel consumed. Since the dynamic external conditions (RPM, weather and sea conditions, cargo amount, wave course) to which the ship is exposed directly affect the speed, no further calculations were realized, assuming that these conditions are included in the calculation over speed. Although it is a well-known fact that speed is a decisive dependant for emissions, to the best knowledge of the authors, there is no direct link between these two variables. The novelty of this study is to provide a quick equation to measure the relationship of speed and emission.

This study used data from a Panamax tanker. Panamax tankers have maximum dimensions determined by the Panama Canal Authority due to the size of the canal they pass through. These tankers have dimensions of approximately 275 meters (950 feet) in length, 31 meters (106 feet) in width and 11 meters (39.5 feet) in depth (Autoridad del Canal de Panamá, 2022).

2. MATERIALS AND METHODS

Regression analysis is used in many subjects in the maritime industry. (Lepore et al., 2017) used variable selection methods, penalized regression methods, latent variable methods and tree-based ensemble methods regression techniques to analyze the data collected from the shipping industry scenario and C02 emission estimation in their study. (Öztürk & Başar, 2022) used MLRA (multiple linear regression analysis) method in their studies, and estimated ship fuel consumption with RPM, trim, mean draft, weather condition data. (Uyanık et al., 2020) estimated the fuel consumption of a container ship with data such as main engine rpm, main engine cylinder values, scavenge air, shaft indicators using Multiple Linear Regression, Ridge and LASSO Regression, Support Vector Regression, Tree-Based Algorithms, Boosting Algorithms methods. (Cepowski & Drozd, 2023) used data such as rotational speed, draught, trim, hull fouling time, wind speed, wave height, and seawater temperature of a container ship and examined the hierarchical effects of these parameters on fuel consumption using artificial neural networks and multiple nonlinear regression methods. In this study, Microsoft Excel was used to perform regression analysis.

Design speed of the Panamax tanker used in this study is 14 knots and the base SFOC value is 169 g/kWh. These values are obtained from the booklets published by the ship's main engine manufacturer.

Daily speed values for each day were obtained from the logs and the average daily engine load was calculated first. For this purpose, the following equation, which is called as Propeller Law and presented in was utilized:

$$P_2 = P_1\left(\frac{V_{transient}}{V_{design}}\right)^{\propto} \quad (1)$$

$$LF = \frac{P_2}{P_1} \quad (2)$$

where;

P_2 : Coefficient

P_1 : Engine power (kW)

$V_{transient}$: Daily speed (knots)

V_{design} : Design speed (knots)

α : Constant (Assumed as 2.7)

LF : Engine load (%)

Table 3. Sample set

No	Speed (knots)	P2	LF (%)	$SFOC_{relative}$	SFOC (g/kWh)	Fuel consumption (t)	CO_2 (t)
1	13.7	11224	0.943	1.015	171.6	49.0	152.6
2	13.2	10152	0.853	1.005	169.9	48.5	151.1
3	13.2	10152	0.853	1.005	169.9	48.5	151.1
4	13.0	9742	0.819	1.010	170.7	48.8	155.3
5	13.5	10787	0.906	1.004	169.6	48.4	151.8
…	…	…	…	…	…	…	…

P2: Coefficient; LF: Engine load; SFOC: Specific fuel oil

SFOC values were calculated in accordance with these engine loads after engine loads, which were calculated depending on daily speed. For this, the equation, which is presented below, obtained from the study below (Moreno-Gutiérrez et al., 2015) was utilized:

$$SFOC_{relative}=0.455LF^2-0.71LF+1.28 \quad (3)$$

where;

$SFOC_{relative}$: Relative engine load

LF : Engine load (%)

After that, SFOC value is calculated based on the related engine load with the help of the following equation. The $SFOC_{base}$ value is given by the main engine manufacturer and has been measured as 169 g/kWh for the ships used in this study.

$$SFOC = SFOC_{relative} \times SFOC_{base} \quad (4)$$

Thus, firstly, the engine load depending on the average speed value of that day and then the SFOC value of the ship can be calculated depending on the variable engine load. Then, the total fuel consumption can be calculated.

After calculating the fuel consumption, emission estimates can be estimated. In this study, only CO_2 emissions were evaluated. Emission estimations can be calculated via the following equation (Trozzi, 2010):

$$E_{Trip}=FC \times EF \quad (5)$$

where;

E_{Trip} : Estimated emission amount (t)

FC : Fuel consumption (t)

EF : Emission factor (t/t fuel)

The emission factor for CO_2, which is 3114 g/kg fuel for LSHFO, was taken from (IMO, 2020a).

Thus, based on the fuel consumption data obtained with the help of the equations presented above, the estimation of mentioned emissions can also be realized. These fuel consumption and emission data were processed with the help of regression analysis and formulas were developed to calculate the fuel consumption and emission amounts depending on the speed variable.

Regression analysis is to explain the relationship between two variables with the help of a mathematical formula. For this purpose, first, a dependent variable symbolized by y and an independent variable symbolized by x is determined (Rawlings et al., 1998). The mathematical expression of regression analysis is given by (Ye et al., 2017) as follows:

$$y=\beta_0+\beta_1 x+\beta_2 x^2+\beta_3 x^3+e \quad (6)$$

where;

β_0 : Constant

β_1, β_2, β_3 : Linear, quadratic and cubic coefficients

e : Error

The main purpose of such equations established in the regression analysis is to explain one variable through other variables. Regression analysis is a method developed to find the correlation or relationship between dependent or independent variables by finding the coefficients expressed by β (Bilgili, 2018).

3. RESULTS AND DISCUSSION

3.1. Results

A sample set of data and results used in the study is presented in Table 3. In Table 3, only CO_2 is given as an example of emission to save space and other emissions may also be examined within the scope of the study. The sample set consists of 3080 rows. Only the operational phase is included, thus, manoeuvres, canal transits, and other operational conditions such as berthing or anchoring are excluded, which can be considered a limitation of the study. No split of data was applied as train and test. The minimum and maximum values of the dataset are 153 and 195.9, respectively. Median and mean values are presented as 154.8 and 156.6. The values for 1st and 3rd Quartiles are 154.04 and 156.86, respectively.

The data presented in Table 3 is just a sample and the data of an entire voyage was processed. Figure 1 and Figure 2 show the graphs obtained for fuel consumption and CO_2 emissions, respectively.

Figure 1 and Figure 2 have a slope that is compatible with the SFOC graphics presented by the ship's main engine manufacturer. Accordingly, as speed decreases, fuel consumption and emissions decrease to a certain level. However, although the speed continues to decrease after a certain level, an increase in fuel consumption and emissions

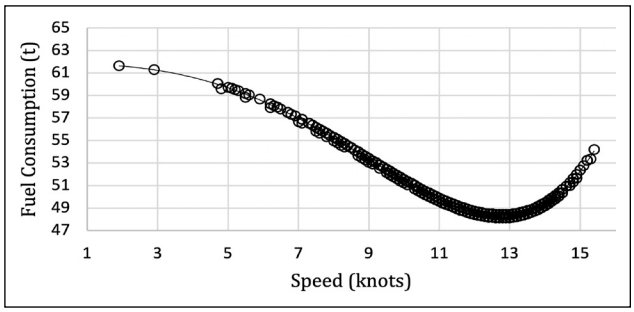

Figure 1. Speed-fuel consumption relationship.

is observed. The reason for this is the engine load-SFOC relationship, as the main engine manufacturer presents. The figures clearly show that the relationship between speed and fuel consumption does not change exponentially or linearly. This relationship has a unique graph type.

In Table 4, the formulas obtained through the regression analysis are presented.

In Table 4, while y value means the dependent variable, the value of x means speed. The R^2 value (not adjusted) of all equations was obtained as 0.9941, which is a very close value to 1. Considering that R^2=1 is the perfect condition, it is seen that the obtained equations express the relationship between speed-fuel consumption/emission quite successfully.

When the speed is replaced with the x value in the equations, results of how much fuel a Panamax tanker will consume at the current speed can be obtained. Besides, the other equation will present the CO_2 emissions produced.

4. DISCUSSION

(Graf von Westarp, 2020) carried out a study on the data of 3 ships, searching for a general speed-fuel consumption formula based on dynamic variable conditions. According to the results of the study, the relationship between speed and fuel consumption was found exponential. Accordingly, the results of the study conducted by the current study and the results of (Graf von Westarp, 2020) are partially compatible. The graphics obtained in the current study (Fisg. 1, 2) are almost exactly compatible with the SFOC curves presented by the ship's main engine manufacturer. The data from the main engine manufacturer shows that SFOC values are decreasing rapidly to a certain level, but then the acceleration reverses and fuel consumption starts to increase although the speed continues to decrease. For this reason, the results obtained in the current study do not change in any way either exponentially or linearly, but as a peculiar graphic. (Moreira et al., 2021) showed that it is possible to predict the ship speed and fuel consumption using only sea conditions data without using variables

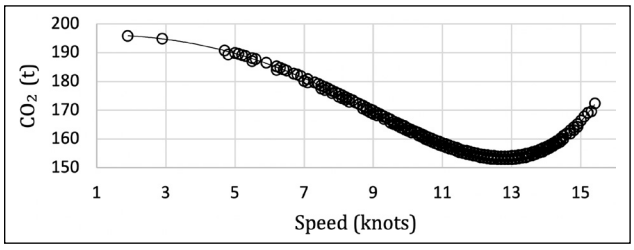

Figure 2. Speed-CO_2 relationship.

such as RPM and torque using an artificial neural network. (Pelić et al., 2023) investigated the effects of slow steam on fuel consumption and CO_2 emissions in their study. They calculated the reduction in fuel consumption between 72.36% and 76.25% at a speed of 12 knots. When compared to a speed of 23 knots, CO_2 emissions were found to be four times less. (Taskar et al., 2023) calculated fuel savings using the speed optimization algorithm for two case ships in different seasons at three different ship speeds. It was observed in the study that fuel savings of up to 6% could be achieved. It was stated that combining slow steaming with speed optimization would support higher fuel savings and emission reductions.

In addition, various studies have been carried out to realize cost estimations, which is the second important issue affected by fuel consumption. These studies generally focus on estimating to perform realistic cost calculations by considering the relationship between speed and fuel consumption. (Notteboom, 2006) assumed that fuel consumption increased with the increase in speed. This increase is exponential and more consistent with the results of (Graf von Westarp, 2020). (Ronen, 1982) conducted a study on the effect of fuel prices on the optimum speed of the ship and examined the effects of optimum speed on fuel cost instead of developing a speed-fuel consumption formula. Similarly, (Corbett et al., 2009; Psaraftis & Kontovas, 2010; Ronen, 2011) studies have also focused on fuel costs and route optimization, mostly through the relationship between speed optimization and fuel consumption.

5. CONCLUSION

Increasing commercial activities and energy demand are accelerating a process that results in the growth of the number and size of ships. Energy demand for ships means more need for fuel. Depending on this energy demand, ship emissions, which are already known to be a major problem, are expected to increase shortly if adequate measures are not taken. Therefore, estimating fuel consumption and emissions and determining whether these values comply with international restrictions have gained great importance.

Table 4. Speed-dependent fuel consumption and emission formulas

Variable dependent	Equation	R^2
Fuel consumption	$y = 7E\text{-}05x^5 - 0.0005x^4 - 0.0078x^3 - 0.0491x^2 + 0.0338x + 61.803$	0.9941
CO_2	$y = 0.0002x^5 - 0.0015x^4 - 0.0247x^3 - 0.1559x^2 + 0.1074x + 196.47$	

In addition, estimating the fuel consumption as simply as possible depending on the dynamic conditions will provide important preliminary data to the relevant subjects such as route and speed optimization by providing accurate and realistic calculations of the fuel costs during the operation. In particular, the relationship between speed and fuel consumption has been studied in several studies, and despite some important progress, it has not been possible to develop a direct and effective correlation. The emission estimation is based on a well-known and frequently applied method, which includes SFOC calculations and utilization of emission factors. The reason for using regression analysis method is to reach a single-variable equation to estimate the target values.

This study aims to calculate fuel consumption on a single variable (speed) that is indirectly linked to other variables (RPM, air and sea conditions, cargo amount, wave course). In addition, emissions from fuel consumption can also be achieved depending on speed (Table 4). The evaluation criteria for the success of this study is to reach a reliable equation to estimate the speed-emission relationship. The equation has a R^2 value as 0.9941, which means the expected success is met. Employing this equation, when the estimated speed of the ship is determined, average fuel consumption and emissions can be calculated. In this way, the speed-fuel consumption relationship, which has not been answered clearly for a long time, has become evident and simple equations, which are ready for use, have been developed. The results are also compatible with the engine load-SFOC curves given by the ship's main engine manufacturer.

DATA AVAILABILITY STATEMENT

The published publication includes all graphics and data collected or developed during the study.

CONFLICT OF INTEREST

The author declared no potential conflicts of interest with respect to the research, authorship, and/or publication of this article.

ETHICS

There are no ethical issues with the publication of this manuscript.

USE OF AI FOR WRITING ASSISTANCE

No AI technologies utilized.

FINANCIAL DISCLOSURE

The authors declared that this study has received no financial support.

REFERENCES

Agrawal, H., Malloy, Q. G. J., Welch, W. A., Wayne Miller, J., & Cocker, D. R. (2008). In-use gaseous and particulate matter emissions from a modern ocean going container vessel. *Atmospheric Environment, 42*(21), 5504–5510. [CrossRef]

Alver, F., Saraç, B. A., & Alver Şahin, Ü. (2018). Estimating of shipping emissions in the Samsun Port from 2010 to 2015. *Atmospheric Pollution Research, 9*(5), 822–828.

Autoridad del Canal de Panamá. (2022). Vessel Requirements. In *OP Notice to Shipping No. N-1-2022* (Vol. 1, Issue 1).

Beşikçi, E. B., Kececi, T., Arslan, O., & Turan, O. (2016). An application of fuzzy-AHP to ship operational energy efficiency measures. *Ocean Engineering, 121*, 392–402. [CrossRef]

Bialystocki, N., & Konovessis, D. (2016). On the estimation of ship's fuel consumption and speed curve: A statistical approach. *Journal of Ocean Engineering and Science, 1*(2), 157–166. [CrossRef]

Bilgili, L. (2018). *Estimation of operation gaseous emissions in ship life cycle with machine learning method* [Doctorial Thesis]. Yildiz Technical University.

Bond, T. C., Streets, D. G., Yarber, K. F., Nelson, S. M., Woo, J. H., & Klimont, Z. (2004). A technology-based global inventory of black and organic carbon emissions from combustion. *Journal of Geophysical Research: Atmospheres, 109*(14), 1–43. [CrossRef]

Burgard, D. A., & Bria, C. R. M. (2016). Bridge-based sensing of NOx and SO2 emissions from ocean-going ships. *Atmospheric Environment, 136*, 54–60. [CrossRef]

Capaldo, K., Corbett, J. J., Kasibhatla, P., Fischbeck, P., & Pandis, S. N. (1999). Effects of ship emission on sulphur cycling and radiative climate forcing over the ocean. *Nature, 400*, 743–746. [CrossRef]

Cepowski, T., & Drozd, A. (2023). Measurement-based relationships between container ship operating parameters and fuel consumption. *Applied Energy, 347*, Article 121315. [CrossRef]

Cooper, D. A. (2003). Exhaust emissions from ships at berth. Atmospheric Environment, 37(27), 3817–3830. Cooper, D. A., & Andreasson, K. (1999). Predictive NO(x) emission monitoring on board a passenger ferry. *Atmospheric Environment, 33*(28), 4637–4650. [CrossRef]

Corbett, J. J., & Koehler, H. W. (2004). Considering alternative input parameters in an activity-based ship fuel consumption and emissions model: Reply to comment by Øyvind Endresen et al. on "Updated emissions from ocean shipping". *Journal of Geophysical Research D: Atmospheres, 109*(23), 1–8. [CrossRef]

Corbett, J. J., Wang, H., & Winebrake, J. J. (2009). The effectiveness and costs of speed reductions on emissions from international shipping. Transportation Research Part D: *Transport and Environment, 14*(8), 593–598. [CrossRef]

Corbett, J. J., Winebrake, J. J., Green, E. H., Kasibhatla, P., Eyring, V., & Lauer, A. (2007). Mortality from ship emissions: A global assessment. *Environmental Science and Technology, 41*(24), 8512–8518. [CrossRef]

De Meyer, P., Maes, F., & Volckaert, A. (2008). Emissions from international shipping in the Belgian part of the North Sea and the Belgian seaports. *Atmospheric Environment, 42*(1), 196–206. [CrossRef]

De Ruyter De Wildt, M., Eskes, H., & Boersma, K. F. (2012). The global economic cycle and satellite-derived NO2 trends over shipping lanes. *Geophysical Research Letters, 39*(1), 2–7. Deniz, C., & Durmuşoğlu, Y. (2008). Estimating shipping emissions in the region of the Sea of Marmara, Turkey. *Science of the Total Environment, 390*(1), 255–261. [CrossRef]

Doney, S. C., Fabry, V. J., Feely, R. A., & Kleypas, J. A. (2009). Ocean acidification: The other CO2 problem. *Annual Review of Marine Science, 1*(1), 169–192. [CrossRef]

Eyring, V., Isaksen, I. S. A., Berntsen, T., Collins, W. J., Corbett, J. J., Endresen, O., Grainger, R. G., Moldanova, J., Schlager, H., & Stevenson, D. S. (2010). Transport impacts on atmosphere and climate: Shipping. *Atmospheric Environment, 44*(37), 4735–4771. [CrossRef]

Eyring, V., Köhler, H. W., Lauer, A., & Lemper, B. (2005). Emissions from international shipping: 2. Impact of future technologies on scenarios until 2050. *Journal of Geophysical Research D: Atmospheres, 110*(17), 183–200. [CrossRef]

Gkerekos, C., Lazakis, I., & Theotokatos, G. (2019). Machine learning models for predicting ship main engine Fuel Oil Consumption: A comparative study. *Ocean Engineering, 188*, Article 106282.

Graf von Westarp, A. (2020). A new model for the calculation of the bunker fuel speed–consumption relation. *Ocean Engineering, 204*, Article 107262. [CrossRef]

Gusti, Ayudhia P., & Semin. (2016). The effect of vessel speed on fuel consumption and exhaust gas emissions. *American Journal of Engineering and Applied Sciences, 9*(4), 1046–1053. [CrossRef]

Gusti, Ayudhia Pangestu, & Semin. (2018). Effect of ship speed on ship emissions. *Asian Journal of Scientific Research, 11*(3), 428–433. [CrossRef]

Henningsen, R., Skjolsvik, K., Andersen, A., Corbett, J., & Skjelvik, J. (2000). *Study of Greenhouse Gas Emissions from Ships Final Report to the International Maritime Organization*. International Maritime Organization

IEA. (2024). *World Energy Outlook*. IEA.

IMO. (2020a). Fourth IMO Greenhouse Gas Study: Executive Summary. In *IMO Greenhouse Gas Study*. IMO.

IMO. (2015b). *Nitrogen Oxides (NOx) – Regulation 13*. https://www.imo.org/en/OurWork/Environment/Pages/Nitrogen-oxides-(NOx)-%E2%80%93-Regulation-13.aspx Accessed on Dec 11, 2024.

IMO. (2015c). *IMO Sulphur Regulation*. https://www.imo.org/en/OurWork/Environment/Pages/Sulphur-oxides-(SOx)-%E2%80%93-Regulation-14.aspx Accessed on Dec 11, 2024

Isakson, J., Persson, T. A., & Selin Lindgren, E. (2001). Identification and assessment of ship emissions and their effects in the harbour of Göteborg, Sweden. *Atmospheric Environment, 35*(21), 3659–3666. [CrossRef]

Jalkanen, J. P., Johansson, L., & Kukkonen, J. (2016). A comprehensive inventory of ship traffic exhaust emissions in the European sea areas in 2011. *Atmospheric Chemistry and Physics, 16*(1), 71–84. [CrossRef]

Johansson, L., Jalkanen, J. P., & Kukkonen, J. (2017). Global assessment of shipping emissions in 2015 on a high spatial and temporal resolution. *Atmospheric Environment, 167*, 403–415. [CrossRef]

Kågeson, P. (1999). Economic instruments for reducing emissions from sea transport. In *Air Pollution and Climate Series* (Vol. 11), European Federation for Transport and Environment.

Kee, K.-K., Lau Simon, B.-Y., & Yong Renco, K.-H. (2018). Prediction of Ship Fuel Consumption and Speed Curve by Using Statistical Method. *Journal of Computer Science & Computational Mathematics, 8*(2), 19–24. [CrossRef]

Kesgin, U., & Vardar, N. (2001). A study on exhaust gas emissions from ships in Turkish Straits. *Atmospheric Environment, 35*(10), 1863–1870. [CrossRef]

Kollamthodi, S., Brannigan, C., Harfoot, M., Skinner, I., Whall, C., Lavric, L., Noden, R., Lee, D., Buhaug, Ø., Martinussen, K., Skejic, R., Valberg, I., Brembo, J. C., Eyring, V., & Faber, J. (2008). Greenhouse gas emissions from shipping: Trends, projections and abatement potential: Final report to the Committee on Climate Change (CCC). In *AEA Technology* (Issue 4).

Lang, J., Zhou, Y., Chen, D., Xing, X., Wei, L., Wang, X., Zhao, N., Zhang, Y., Guo, X., Han, L., & Cheng, S. (2017). Investigating the contribution of shipping emissions to atmospheric PM2.5 using a combined source apportionment approach. *Environmental Pollution, 229*, 557–566. [CrossRef]

Lepore, A., dos Reis, M. S., Palumbo, B., Rendall, R., & Capezza, C. (2017). A comparison of advanced regression techniques for predicting ship CO2 emissions. *Quality and Reliability Engineering International, 33*(6), 1281–1292. [CrossRef]

Matthias, V., Bewersdorff, I., Aulinger, A., & Quante, M. (2010). The contribution of ship emissions to air pollution in the North Sea regions. *Environmental Pollution, 158*(6), 2241–2250. [CrossRef]

Millero, F. J. (1995). Thermodynamics of the carbon dioxide system in the oceans. *Geochimica et Cosmochimica Acta, 59*(4), 661–677. [CrossRef]

Moldanová, J., Fridell, E., Popovicheva, O., Demirdjian, B., Tishkova, V., Faccinetto, A., & Focsa, C. (2009). Characterisation of particulate matter and gaseous emissions from a large ship diesel engine. *Atmospheric Environment, 43*(16), 2632–2641. [CrossRef]

Moreira, L., Vettor, R., & Soares, C. G. (2021). Neural network approach for predicting ship speed and fuel consumption. *Journal of Marine Science and Engineering, 9*(2), 1–14. [CrossRef]

Moreno-Gutiérrez, J., Calderay, F., Saborido, N., Boile, M., Rodríguez Valero, R., & Durán-Grados, V. (2015). Methodologies for estimating shipping emissions and energy consumption: A comparative analysis of current methods. *Energy, 86*, 603–616. [CrossRef]

Notteboom, T. E. (2006). The Time factor in liner shipping services. *Maritime Economics and Logistics, 8*(1), 19–39. [CrossRef]

Öztürk, O. B., & Başar, E. (2022). Multiple linear regression analysis and artificial neural networks based decision support system for energy efficiency in shipping. *Ocean Engineering, 243*, Article 110209. [CrossRef]

Park, R. J., Jacob, D. J., Chin, M., & Martin, R. V. (2003). Sources of carbonaceous aerosols over the United States and implications for natural visibility. *Journal of Geophysical Research Atmospheres, 108*(12), Article 4355. [CrossRef]

Pelić, V., Bukovac, O., Radonja, R., & Degiuli, N. (2023). The impact of slow steaming on fuel consumption and CO2 emissions of a container ship. *Journal of Marine Science and Engineering, 11*(3), Article 675.

Psaraftis, H. N., & Kontovas, C. A. (2010). Balancing the economic and environmental performance of maritime transportation. *Transportation Research Part D: Transport and Environment, 15*(8), 458–462. [CrossRef]

Quinn, P. K., Bates, T. S., Baum, E., Doubleday, N., Fiore, A. M., Flanner, M., Fridlind, A., Garrett, T. J., Koch, D., Menon, S., Shindell, D., Stohl, A., & Warren, S. G. (2008). Short-lived pollutants in the Arctic: Their climate impact and possible mitigation strategies. *Atmospheric Chemistry and Physics, 8*(6), 1723–1735. [CrossRef]

Raven, J., Caldeira, K., Elderfield, H., Hoegh-Guldberg, O., Liss, P., Riebesell, U., Shepherd, J., Turley, C., & Watson, A. (2005). *Ocean acidification due to increasing atmospheric carbon dioxide*. The Royal Society.

Rawlings, J. O., Pantula, S. G., & Dickey, D. A. (1998). Applied Regression Analysis: A Research Tool. In G. Casella, S. Fienberg, & I. Olkin (Eds.), *The American Statistician* (2nd ed.). Springer-Verlag. [CrossRef]

Richter, A., Eyring, V., Burrows, J. P., Bovensmann, H., Lauer, A., Sierk, B., & Crutzen, P. J. (2004). Satellite measurements of NO2 from international shipping emissions. *Geophysical Research Letters, 31*(23), 1–4. [CrossRef]

Ronen, D. (1982). The effect of oil price on the optimal speed of ships. *The Journal of Operational Research Society, 33*(11), 1035–1040. [CrossRef]

Ronen, D. (2011). The effect of oil price on containership speed and fleet size. *Journal of the Operational Research Society, 62*(1), 211–216. [CrossRef]

Saxe, H., & Larsen, T. (2004). Air pollution from ships in three Danish ports. *Atmospheric Environment, 38*(24), 4057–4067. [CrossRef]

Schrooten, L., De Vlieger, I., Int Panis, L., Styns, K., & Torfs, R. (2008). Inventory and forecasting of maritime emissions in the Belgian sea territory, an activity-based emission model. *Atmospheric Environment, 42*(4), 667–676. [CrossRef]

Schrooten, L., De Vlieger, I., Panis, L. I., Chiffi, C., & Pastori, E. (2009). Emissions of maritime transport: A European reference system. *Science of the Total Environment, 408*(2), 318–323. [CrossRef]

Shi, Y. (2016). Are greenhouse gas emissions from international shipping a type of marine pollution? *Marine Pollution Bulletin, 113*(1–2), 187–192. Smith, K. R. (2000). National burden of disease in India from indoor air pollution. *Proceedings of the National Academy of Sciences of the United States of America, 97*(24), 13286–13293.

Smith, T. W. P., Jalkanen, J. P., Anderson, B. A., Corbett, J. J., Faber, J., Hanayama, S., O'Keeffe, E., Parker, S., Johansson, L., Aldous, L., Raucci, C., Traut, M., Ettinger, S., Nelissen, D., Lee, D. S., Ng, S., Agrawal, A., Winebrake, J. J., Hoen, M, … & Pandey, A. (2014). *Third IMO GHG Study 2014*. International Maritime Organization (IMO).

Smith, T. W. P., Jalkanen, J. P., Anderson, B. A., Corbett, J. J., Faber, J., Hanayama, S., O'Keeffe, E., Parker, S., Johansson, L., Aldous, L., Raucci, C., Traut, M., Ettinger, S., Nelissen, D., Lee, D. S., Ng, S., Agrawal, A., Winebrake, J. J., & Hoen, M., A. (2014). *Third IMO Greenhouse Gas Study*. In International Maritime Organization (IMO).

Solomon, S., D., Qin, M., Manning, Z., Chen, M., Marquis, K. B., Averyt, M. T., Miller HL, Solomon, S., Qin, D., Manning, M., Chen, Z., Marquis, M., Averyt, K. B., Tignor, M., & Miller, H. L. (2007). Summary for Policymakers. In: *Climate Change 2007: The Physical Science Basis*. Contribution of Working Group I to the Fourth Assessment Report of the Intergovernmental Panel on Climate Change. In Cambridge University Press..

Streets, D. G., Carmichael, G. R., & Arndt, R. L. (1997). Sulfur dioxide emissions and sulfur deposition from international shipping in Asian waters. *Atmospheric Environment, 31*(10), 1573–1582. [CrossRef]

Streets, D. G., Guttikunda, S. K., & Carmichael, G. R. (2000). The growing contribution of sulfur emissions from ships in Asian waters, 1988-1995. *Atmospheric Environment, 34*(26), 4425–4439. [CrossRef]

Styhre, L., Winnes, H., Black, J., Lee, J., & Le-Griffin, H. (2017). Greenhouse gas emissions from ships in ports – Case studies in four continents. *Transportation Research Part D: Transport and Environment, 54*, 212–224. [CrossRef]

Taskar, B., Sasmal, K., & Yiew, L. J. (2023). A case study for the assessment of fuel savings using speed optimization. *Ocean Engineering, 274*, Article 113990. [CrossRef]

Trozzi, C. (2010). Emission estimate methodology for maritime navigation. *US EPA 19th International Emissions Inventory Conference*. https://www3.epa.gov/ttnchie1/conference/ei19/ Accessed on Dec 05, 2024.

Tyrrell, T. (2008). Calcium carbonate cycling in future oceans and its influence on future climates. *Journal of Plankton Research, 30*(2), 141–156. [CrossRef]

Tzannatos Ernestos, E. (2010). Ship emissions and their externalities for Greece. *Atmospheric Environment, 44*(18), 2194–2202. [CrossRef]

Uyanık, T., Karatuğ, Ç., & Arslanoğlu, Y. (2020). Machine learning approach to ship fuel consumption: A case of container vessel. *Transportation Research Part D: Transport and Environment, 84*, Article 102389. [CrossRef]

Wang, Shengzheng, Ji, B., Zhao, J., Liu, W., & Xu, T. (2018). Predicting ship fuel consumption based on LASSO regression. *Transportation Research Part D: Transport and Environment, 65*, 817–824. [CrossRef]

Williams, E. J., Lerrier, B. M., Murphy, P. C., Herndon, S. C., & Zahniser, M. S. (2009). Emissions of NOx, So2, CO, and HCHO from commercial marine shipping during Texas Air Quality Study (TexAQS) 2006. In *Journal of Geophysical Research Atmospheres, 114*(21), Article D21306. [CrossRef]

Winther, M. (2008). New national emission inventory for navigation in Denmark. *Atmospheric Environment, 42*(19), 4632–4655. [CrossRef]

Ye, X., Kang, Y., Zuo, B., & Zhong, K. (2017). Study of factors affecting warm air spreading distance in impinging jet ventilation rooms using multiple regression analysis. *Building and Environment, 120*, 1–12. [CrossRef]

Seatific, Vol. 4, Issue. 2, pp. 57–76, December 2024

Seatific Journal
https://seatific.yildiz.edu.tr
DOI: https://doi.org/10.14744/seatific.2024.0007

Seatific

Research Article

The effect of various bulbous bow forms on the resistance of a Black Sea type fishing boat

Dursun SARAL*

Department of Naval Architecture and Marine Engineering, Karadeniz Technical University, Trabzon, Türkiye

ARTICLE INFO

Article history
Received: October 07, 2024
Revised: November 19, 2024
Accepted: December 25, 2024

Key words:
Black sea type fishing boat; bulbous bow; computational fluid dynamics (CFD); resistance

ABSTRACT

In this study, resistance analyses of a 35-meter-long Black Sea Type Fishing Boat with various bow forms were conducted using Computational Fluid Dynamics (CFD). The boat's bow shapes included a normal bow without a bulb, a special bulb, a special-elliptical bulb, and an elliptical bulb. To determine the resistance values of these forms, the Realizable k-ε model was chosen as the turbulence model, and the Volume of Fluid (VOF) method was applied. Resistance analyses were performed at five different speeds (5.5, 7.5, 9.5, 11.5, and 13.5 knots), within the Fn range of 0.15 to 0.40. Shear, pressure, and total resistance values were presented in both tables and graphs. The CFD resistance results were compared with those from the Holtrop and Fung resistance estimation methods, and the results were found to be consistent. Performance evaluations of the bulb shapes were made by comparing the friction, pressure, and total resistance coefficients. While the special bulb resulted in the greatest reduction in total resistance, the special-elliptical bulb demonstrated better performance across a wider range of speeds. It was also concluded that the traditional elliptical bulb type is unsuitable for this type of vessel.

Cite this article as: Saral D. The effect of various bulbous bow forms on the resistance of a Black Sea type fishing boat. Seatific 2024;4:2:57–76.

1. INTRODUCTION

Fishing has always been an important occupation in Turkey, a country surrounded by water on three sides. Until the 1980s, fishing boats in Turkey, particularly along the Black Sea coasts, where fishing is intensively practiced, were traditionally built with wood obtained from the region's forests. With advancements in technology and the increased use of sheet metal work, steel fishing boats began to be manufactured in Turkey starting in 1975 (URL-1, 2024; URL-2, 2024). Due to their distinctive features, fishing boats built on the Black Sea coasts have come to be known as Black Sea Type Fishing Boats (Dinçer, 1992; Saral and Köse, 2024). Until the early 2000s, these boats were built without bulbs (Fig. 1), but they are now designed with bulbs (Fig. 2). Since 2002, Black Sea type fishing vessels have begun to be constructed with bulbous bows. Due to a lack of scientific knowledge on bulbous bow applications specific to Black Sea type fishing vessels, the initial applications were implemented according to the preferences of fishing vessel owners and the knowledge and experience of shipyard craftsmen. The primary purpose of these initial applications was to counterbalance the forward trim caused by the positioning of the living quarters and the bridge at the bow by adding extra volume with a bulbous bow. Over time, vessel owners observed that ships equipped with bulbous bows could achieve higher speeds with the same engine power, indicating a reduction in form resistance. Today, bulbous bows on these types of fishing vessels are used both to correct forward trim and to reduce form resistance, thereby increasing speed. However, a comprehensive study on which type of bulbous bow is most efficient for Black Sea type fishing vessels has not yet

***Corresponding author.**
*E-mail address: dursunsaral@ktu.edu.tr

been conducted. In this study, the effect of bulbous bow type on form resistance in such fishing vessels is investigated to provide insights for designers and researchers.

In shipbuilding, the bulbous bow is a crucial hydrodynamic innovation primarily designed to attenuate the wave system generated by the hull, thereby reducing total resistance and improving vessel efficiency. Its operational principle centers on generating a secondary wave system that interacts destructively with the primary wave system created by the hull. This destructive interference reduces the amplitude of the wave system, significantly diminishing wave-making resistance. By effectively dampening these waves, the bulbous bow not only minimizes energy loss to wave formation but also streamlines the water flow along the hull, reducing pressure resistance and enhancing hydrodynamic stability. This design is particularly beneficial at higher Froude numbers and for hull forms with significant wave-making components, leading to measurable improvements in fuel efficiency, reduced emissions, and optimized propulsion performance. As a result, the bulbous bow is a key feature in modern naval architecture, specifically engineered to mitigate wave resistance and maximize vessel performance.

Taylor (1923) was the first researcher to experimentally investigate the effects of bulbous bows on ship hull forms. Subsequently, experimental studies on the delta-type bulbous bow, known as the Taylor bulbous bow, were conducted by Bragg (1930), Inui et al. (1960), Ferguson (1967), and Muntjewerf (1967), systematically varying the bulbous bow parameters. Weinblum (1935), Wigley (1936), Inui (1962), and Yim (1963) conducted detailed theoretical studies on the linearized wave resistance theory. While this theory provides insights into how a bulbous bow functions, it does not offer guidance on how to design a bulbous bow for a specific hull form. Inui (1962) proposed a method for determining the size of a bulbous bow by matching the amplitude functions of the ship's forebody and the bulbous bow in regular waves. Yim (1965) established a relationship between the entrance angle at the bow and the size of the bulbous bow for a given speed. Yim (1974) presented a method consisting of three main considerations for designing spherical bulbous bows. Furthermore, Yim (1980) discussed the sheltering effect of spherical bulbous bows and proposed variations for the optimal bulbous bow position for sinusoidal, cosine, and parabolic hull types. Baba (1969) and Shearer and Steele (1970) noted that bulbous bows could provide additional benefits for ship hull forms, such as reducing wave breaking at the bow and improving flow around the keel line and bilge turn to prevent flow separation. Kracht (1978) developed a statistical method based on data obtained from propulsion model tests. This method, created by compiling data from the Hamburg and Berlin model basins, considers the block coefficient, length-to-beam ratio, and beam-to-draft ratio of the hull form. For the bulbous bow, six parameters were developed to define its size and position: width, length, depth, sectional area, lateral area, and volumetric parameters. The method provides either the power reduction achievable with a selected bulbous bow or the appropriate bulbous bow design for a desired power reduction. The Kracht method is particularly more effective for bulbous bows with nabla (∇) cross-sections. Sharma and Sha (2005) developed a bulbous bow design method that combines two globally recognized theories: the Kracht (1978) and Yim (1980) methods. This approach optimizes bulbous bow parameters for the design speed, reanalyses the sheltering effect using approximate linear theory for resistance prediction, and statistically re-correlates existing model test results from the literature using nonlinear multivariable regression analysis. In recent years, advancements in computer technology and the widespread use of software programs have enabled the application of Computational Fluid Dynamics (CFD) to optimize hull forms with bulbous bows.

As shown in Figure 3, the three basic types of bulbous bow shapes are Delta (Δ), Circular-Elliptic (O), and Nabla (∇) (Kracht, 1978). Theories by Yim (1974) and Kracht (1978)

Figure 1. A fishing boat of the Black Sea type built in 2000 (URL-3, 2024).

Figure 2. A fishing boat of the Black Sea type built in 2019 (URL-4, 2024).

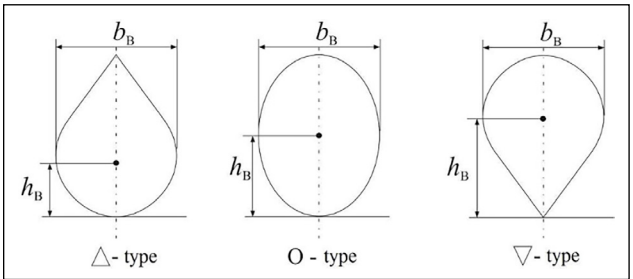

Figure 3. The sections of the bulbs (Saral et al., 2018).

are among the most accepted methods for bulb design. Additionally, specialized bulbous bow designs for specific ship hull forms are being developed.

Academic studies on fishing boats in Turkey began in 1953 with the establishment of the Ata Nutku Ship Model Testing Laboratory at Istanbul Technical University (ITU) (Saral and Köse, 2024). In Turkey, academic research on fishing vessels can be divided into three periods: first-period studies (1955-1970), ITU Fishing Boats Series studies (1979-), and Black Sea Type Fishing Boat studies (1990-) (Saral and Köse, 2024). Kafalı et al. (1979) improved the ITU Fishing Boats Series. The hull forms developed were designated as 148/1, 148/2, 148/3, 148/4, 148/5, 148/6, 148/7, 148/8, and 148/9. Resistance analyses of these generated fishing boat forms were methodically carried out at the Ata Nutku Ship Model Testing Laboratory, and none of these forms featured bulbs. A Delta (Δ) section bulb bow was added to the 148/1 form by Atlar (1977), and resistance tests on the 148/1-Y model were performed. It was determined that at a ship speed of 10.5 knots, total resistance was reduced by approximately 18%. Söylemez (1983) added three types of Delta (Δ) bulb forms, with cross-sectional area ratios of 0.12 (A1), 0.09 (A2), and 0.07 (A3), to the 148/1 model. The Kracht (1978) method was used to design the bulb forms. The resistance tests on the A1, A2, and A3 models produced the following results: The A1 model, which had the largest bulb, provided a 13% increase in effective horsepower at a service speed of 10 knots but had no effect below 9 knots. The A2 model's bulb reduced effective horsepower by 20% at a service speed of 10 knots. However, the A3 model's smaller bulb was found to be ineffective at the loaded waterline.

With the advancement of computer technologies, numerical analyses, whose foundations were first laid in the 1920s, have evolved into commercial software that became easier to use, faster, and more efficient by the 2000s (Saral, 2016). Since the 1990s, flow problems around ships have been more accurately and effectively solved using CFD software, which employs RANS equations and a variety of turbulence models (Özdemir, 2007). CFD software has been used for resistance analyses on warships with military and technical significance, followed by containers, cargo, Ro-Ro, and cargo ships with commercial importance, and most recently, on today's fishing vessels. Below are some academic studies that explore the calculation of resistance using CFD on fishing vessel forms. Setyawan et al. (2010) investigated the multi-hull form using CFD to reduce fuel consumption in fishing vessels. Samuel et al. (2015) used CFD to analyze the resistance of a single-hull fishing boat from Indonesia's Cilacap region, as well as the catamaran created from the same hull. Li et al. (2016) modeled a tuna longline fishing boat and conducted both model resistance experiments and resistance analyses using CFD. Additionally, resistance analyses were performed using CFD by systematically changing the bulb size on the ship. When the total resistance values of the new bulb forms were compared, it was found that the 50% elongated bulb form reduced total resistance by around 5%. Abramowski and Sugalski (2017) examined nine Polish fishing vessels and applied cylindrical (O) and nabla (∇) type bulb forms to two selected designs. CFD was used to perform resistance analyses on these forms. When the total resistance values were compared, it was found that the cylindrical (O) type bulb reduced total resistance by 14%, while the nabla (∇) type bulb reduced total resistance by 16%. Kim et al. (2018) conducted CFD analyses on a traditional catamaran fishing boat from the Cilacap region of Indonesia, applying delta (Δ), nabla (∇), and elliptical (O) type bulbs. The analysis showed that the nabla (∇) type bulb reduced the total resistance of the fishing boat by about 10% at service speed. Bahatmaka and Kim (2019) used CFD to analyze the resistance of two traditional Indonesian fishing boats operating in the north and south of Java Island. The analysis indicated that the fishing boats used in the southern region were more suitable in terms of resistance. Raju et al. (2020) added delta (Δ), nabla (∇), and elliptical (O) bulb forms to a traditional tuna longline vessel. CFD was used to perform resistance analyses on these forms in calm water. The results showed that the elliptical (O) bulb form had 5.35% lower total resistance compared to the form without a bulb. In Tran et al. (2021) study, a new bulbous bow design method that goes beyond traditional Kracht charts is presented. The study optimizes power reduction by resizing the initial design from Kracht charts using a multi-objective function combined with CFD analysis and surrogate models. Applied to the FAO 75 fishing vessel, this method achieved approximately 14% power savings, with results aligning well with theoretical expectations. In Szelangiewicz et al. (2021) study, the impact of adding a simple-shaped bulbous bow as a low-cost retrofit to reduce environmental impact on older fishing vessels is examined. The study's CFD analyses show significant reductions in resistance, fuel consumption, and greenhouse gas emissions in vessels equipped with a bulbous bow. These findings highlight potential environmental and economic benefits, particularly for older fishing vessels modernized at low cost. In Iqbal et al. (2021) study, the use of a foil-shaped center bulb to reduce total resistance in catamaran fishing vessels is examined. The study tested six different bulb configurations using the CFD method and found that Model 6, where the center bulb length was increased by 15% and width and height reduced by 10%, provided the best results. This model achieved a 10.68% reduction in resistance. In Díaz Ojeda et al. (2023) study, the importance of optimizing ship lines to reduce environmental impact and improve operational efficiency is highlighted. The study compares the numerical analysis and towing tank experiments of two fishing vessel hulls, demonstrating a reduction in resistance of over 10% with the addition of a dihedral bulbous bow. This bow structure is noted to reduce pressure resistance by smoothing the flow reaching the bow. In Oyuela et al. (2024) study, the hydrodynamics of a typical Argentinian fishing vessel in calm water were analyzed, with an evaluation of total resistance components at various draft conditions. The study uses experimental data from the University of Buenos Aires towing tank, analyzed with the 1978 ITTC Power Prediction method and validated through numerical studies conducted with OpenFOAM

V10. The resulting numerical model discusses the potential for improving total force prediction by combining EFD results with the CFD form factor. In the study by Díaz Ojeda et al. (2024), the effect of the bulbous bow design, used in naval hydrodynamics to reduce resistance, is examined. The study evaluates a typical Argentinian trawler fishing vessel by comparing configurations with and without the bulbous bow under different load conditions and speeds. Numerical analyses were conducted using OpenFOAM, and the results were validated through towing tank experiments.

CFD studies on Turkish-type fishing vessels are as follows. A CFD application for the ITU Fishing Boats Series was performed by Saral et al. (2018). CFD analyses were conducted on the 148/3, 148/4, 148/8, and 148/9 coded boat forms. Delta (Δ), Nabla (∇), and Elliptical (O) shaped bulbous bows were applied to these forms to evaluate the effectiveness of the bulb shapes. The effectiveness of the bulbs at a service speed of 10 knots was determined to be 10% for boats with a block coefficient of 0.405 and 13% for boats with a block coefficient of 0.495. Saral and Köse (2020) used CFD to analyze the resistance of a Black Sea-type fishing boat in calm water at speeds ranging from 1 to 15 knots (Fn 0.028-0.420). The economic service speed of Black Sea-type fishing boats was determined by CFD analysis to be 11 knots. In Saral (2023) study, a dimensionless offset table was developed to optimize and standardize the "Black Sea Type Fishing Vessel" (KTBG) forms for vessels between 40-60 meters in length. Using StarCCM+ CFD software, resistance values of various KTBG forms were calculated, and the effects of different bow, stern, and skeg designs on resistance were examined. The study indicates that KTBG standard dimensionless offset table forms exhibit improved resistance characteristics.

The objective of this study is to identify the most effective type of bulbous bow in reducing total resistance for Black Sea-type fishing vessels with a length of 35 meters (ranging between 30-40 meters). To achieve this, resistance analyses were conducted under calm water and stationary conditions for the following configurations: the existing fishing vessel form (Form SB), the bulbous bow-less version of this form (Form WB), the elliptical bulbous bow form developed for ITU fishing boats series (Form EB), and a custom elliptical bulbous bow form (Form SBE) that incorporates characteristics of the own bulbous bow and the elliptical bulbous bow. Resistance analyses of the boat forms were conducted using CFD. To evaluate the efficiency of the special bulb, resistance analyses of the form without the bulb were also performed. The elliptical bulb, one of the bulbs used, is based on the optimum elliptical bulb form developed by Saral et al. (2018) for the ITU fishing boats series. The other bulb form is a new special elliptical bulb created by combining the special and elliptical bulb designs. All CFD analyses on the hull forms were performed using the Hull Performance Workflow module of the StarCCM+ software. In these CFD analyses, the Realizable k-ε Model

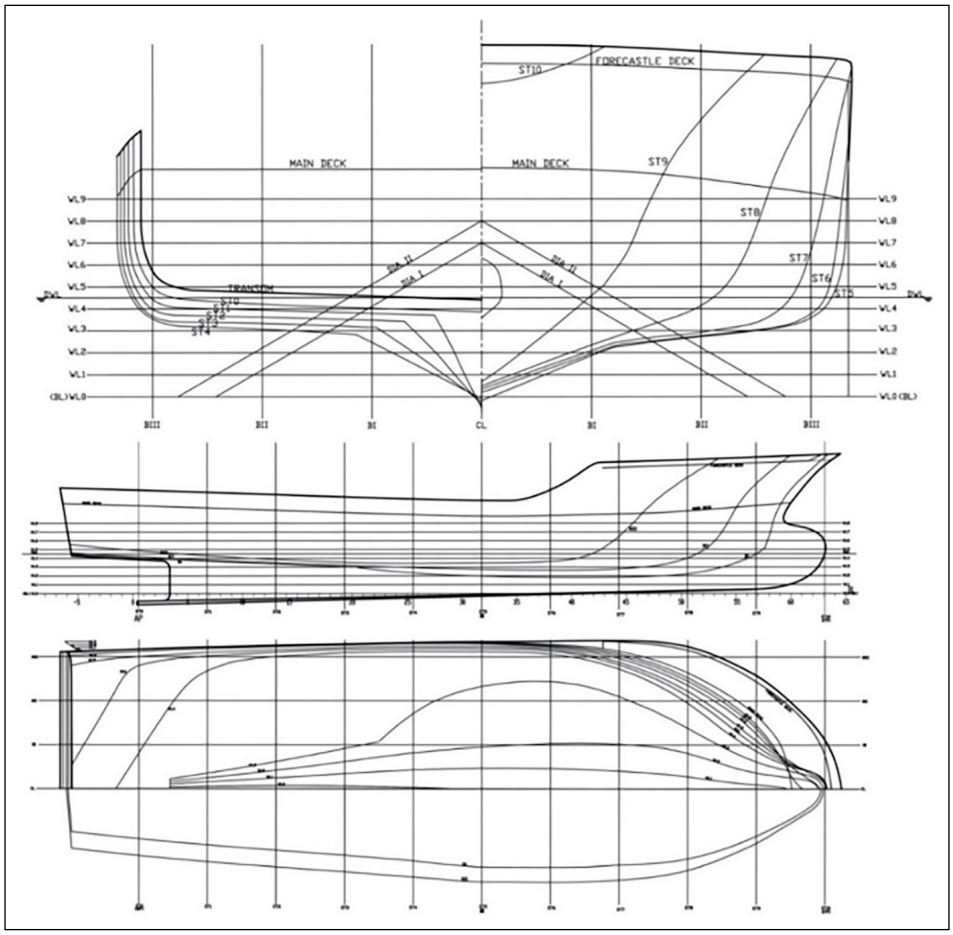

Figure 4. Form SB lines plan (Saral and Köse, 2020).

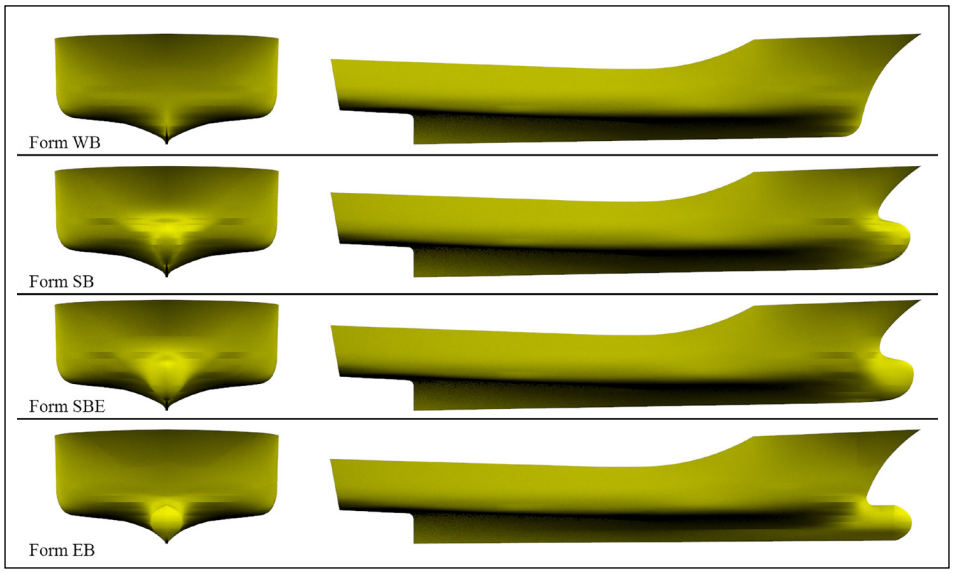

Figure 5. Body and profile views of the three-dimensional forms.

WB: Without Bulb Form; SB: Special Bulb Form; EB: Elliptical Bulb Form

was used as the turbulence model, and the VOF method was applied. Resistance tests were conducted in the Fn 0.15 to Fn 0.40 range at five different speeds (5.5, 7.5, 9.5, 11.5, and 13.5 knots). The total resistance values of the boat forms were compared to determine which head form is most suitable for the Black Sea-type fishing vessels with a length of approximately 35 meters.

2. FISHING BOATS GEOMETRICAL CHARACTERISTICS

In this study, four Black Sea-type fishing vessel forms with an overall length of 35.60 meters and a beam of 13.32 meters (at the main deck) were analyzed. The main form (Fig. 4) used in this study is a typical Black Sea-type fishing vessel constructed at the Yeniay-Çamburnu shipyards (Sürmene-Trabzon), which was previously subjected to resistance analysis using CFD in the speed range of 1-15 knots by Saral and Köse (2020). The other three forms were designed based on this form.

In the article, the forms are named as follows to facilitate tracking of the vessels: Form WB for the bulb-less version, Form SB for the special bulb version, Form SBE for the special elliptical bulb version, and Form EB for the elliptical bulb version.

The body plan of the existing vessel form, Form SB, is provided in Figure 4. The bulbous bow on Form SB was designed based on the preferences of fishing vessel owners and the knowledge and experience of shipyard craftsmen. Academic knowledge was not utilized in determining the dimensions and shape of the bulbous bow. In Black Sea-type fishing vessels, the reason for designing bulbous bows with half of their structure above the design waterline is to balance the forward trim caused by the placement of living quarters and the bridge at the bow.

Form WB is the bulb-less form, developed from Form SB by referencing bulb-less Black Sea-type fishing vessels.

Form EB is the elliptical bulbous bow form. The dimensions and shape of the elliptical bulbous bow were developed using the dimensionless offset values provided by Saral et al. (2018) for the ITU Fishing Vessel series forms. It was selected because it demonstrated the best performance in the ITU Fishing Vessel series.

Form SBE is the special elliptical bulbous bow form. It was created by combining the dimensions of the bulbous bow from Form SB with the dimensionless semi-width offset values of the elliptical bulbous bow from Form EB.

The three-dimensional versions of all forms were created using Rhino software. The body and profile views of the three-dimensional forms are presented in Figure 5.

The frames of the analysed forms between stations 8 and 10 differ depending on the shape of the bulbous bow. The comparison of the changes in bulbous bow shapes in the profile view is presented in Figure 6, while

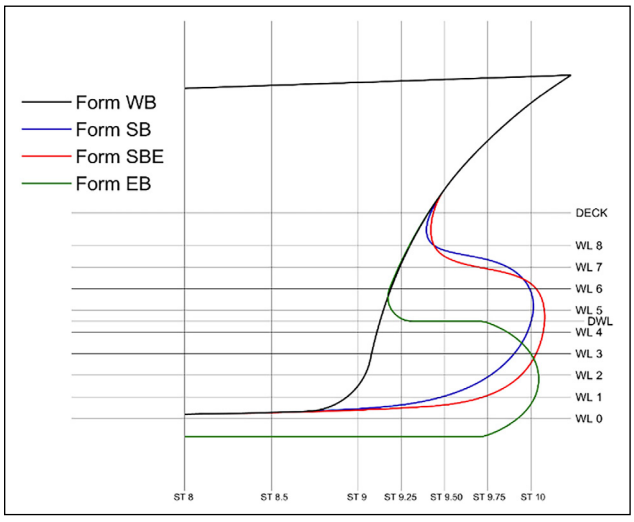

Figure 6. Comparison of the stem profiles of the forms in the profile plan.

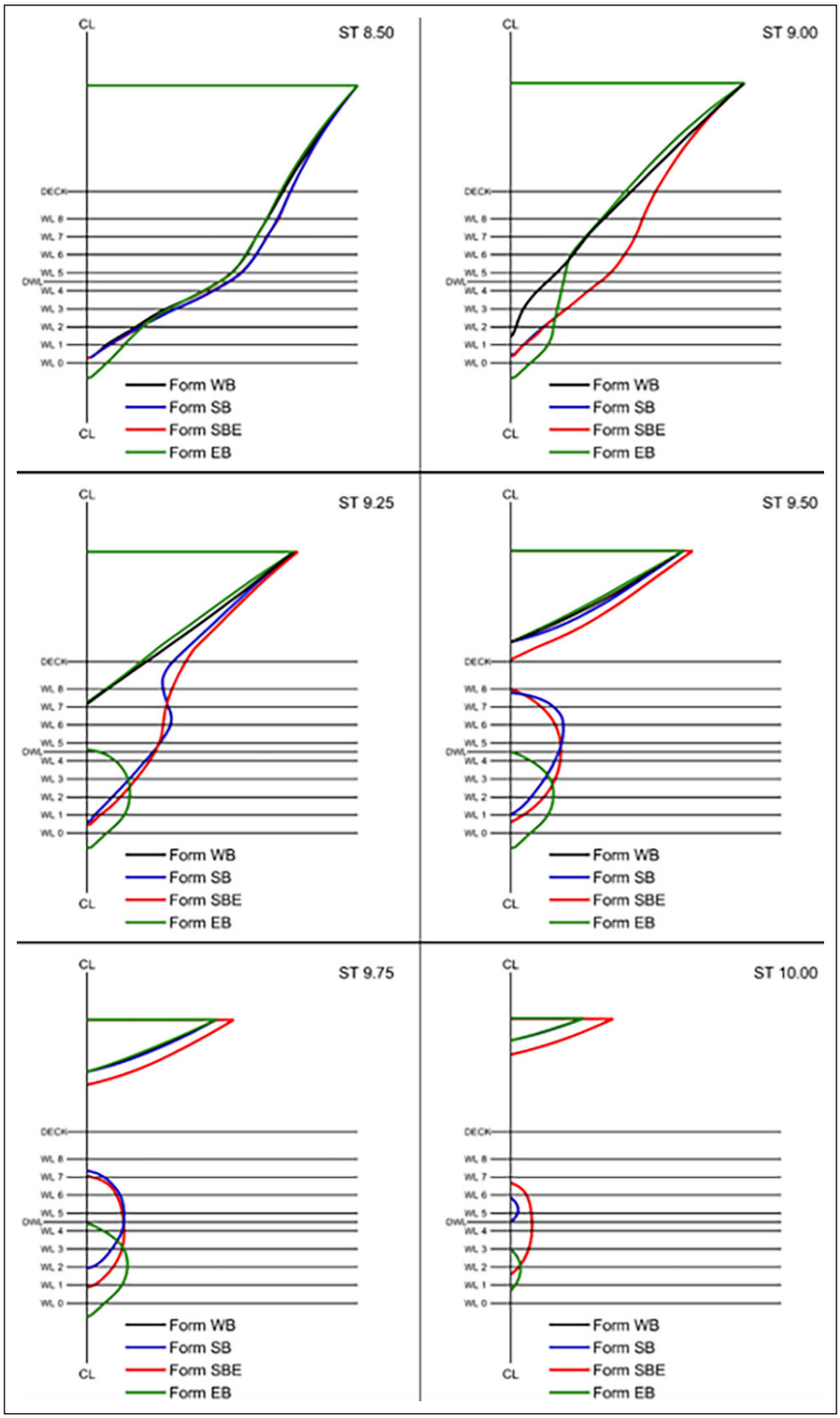

Figure 7. Comparison of the frames of the forms between stations 8 and 10 in the body plans.

the comparison of the changes in the frames between stations 8 and 10 is shown in Figure 7.

In the CFD resistance analyses, it is assumed that the forms have the same displacement value. The fixed displacement value for the forms is 394.313 tons, which corresponds to the displacement of the vessels at their waterline during fishing operations (with full fuel and water tanks, nets on the aft deck, and empty fish holds). The displacement values of the forms were calculated using the weight and volume estimation formulas for Black Sea-type fishing vessels developed by Saral (2023). However, the displacement value of the bulb-less form is approximately

Table 1. Geometric features of boat forms computed using Hull Performance Workflow

Main particular	Symbol	Unit	Form WB	Form SB	Form SBE	Form EB
Length at the waterline	L_{WL}	m	31.808	34.440	34.598	31.863
Length overall	L_{OA}	m	35.580	35.578	35.580	35.569
Beam	B	m	13.125	13.112	13.112	13.098
Draught	T	m	2.542	2.542	2.526	2.586
Displacement (volume)	∇	m^3	380.533	384.494	384.757	384.147
Displacement (mass)	Δ	ton	390.251	394.313	394.583	393.957
Static hull wetted surface	S	m^2	429.610	440.966	442.253	452.013
Block coefficient	C_B	-	0.359	0.335	0.336	0.356
Prismatic coefficient	C_P	-	0.724	0.669	0.664	0.751

WB: Without Bulb Form; SB: Special Bulb Form; SBE: Special Elliptical Bulb Form; EB: Elliptical Bulb Form.

Table 2. The velocity and Fn values at which CFD analyses are performed

Velocities	Velocities tested	Unit	Form WB Fn	Form SB Fn	Form SBE Fn	Form EB Fn
5.5 knots	2.829	m/s	0.160	0.154	0.154	0.160
7.5 knots	3.858	m/s	0.218	0.210	0.209	0.218
9.5 knots	4.887	m/s	0.277	0.266	0.265	0.276
11. 5 knots	5.916	m/s	0.335	0.322	0.321	0.335
13.5 knots	6.944	m/s	0.393	0.378	0.377	0.393

WB: Without Bulb Form; SB: Special Bulb Form; SBE: Special Elliptical Bulb Form; EB: Elliptical Bulb Form.

4 tons less than the other forms, corresponding to the weight of the bulbous bow.

The properties of the forms, as calculated by the Hull Performance Workflow after incorporating the ship forms into the software, are listed in Table 1. Upon examining Table 1, it can be observed that the draft values of the forms vary to maintain the same displacement. The variation in draft values also leads to changes in the waterline length of the forms. This, in turn, causes differences in the Froude numbers (Fn) of the forms at the speed values specified for the resistance analyses. The Froude numbers of the forms at the analyzed speed values are presented in Table 2.

3. NUMERICAL MODELLING

3.1. Theoretical equations

In this study, the theoretical equations governing fluid flow are solved using the Unsteady Reynolds-Averaged Navier-Stokes (URANS) methodology, which is widely employed for analyzing unsteady and turbulent flows. The URANS approach involves time-averaging the Navier-Stokes equations to capture the mean flow behavior while accounting for transient flow phenomena and turbulent fluctuations through appropriate turbulence models. This method is particularly effective for simulating complex flow patterns around ship hulls, including wave formation and flow separation.

The governing equations, which represent the principles of mass and momentum conservation, are solved numerically using the Computational Fluid Dynamics (CFD) software STAR-CCM+.

For incompressible flows, the time-averaged continuity equation and momentum equation are expressed in tensor notation and Cartesian coordinates, as presented in Equations (1) and (2). The continuity equation ensures mass conservation, while the momentum equation accounts for the effects of pressure, viscous forces, and unsteady flow terms. These equations form the mathematical foundation for the simulations, enabling the detailed analysis of hydrodynamic resistance, flow characteristics, and wave patterns around the hull under investigation.

$$\frac{\partial(\rho\bar{u}_i)}{\partial x_i} = 0 \tag{1}$$

$$\frac{\partial(\rho\bar{u}_i)}{\partial t} + \frac{\partial}{\partial x_i}\left(\rho\bar{u}_i\bar{u}_j + \rho\overline{u'_i u'_j}\right) + -\frac{\partial\bar{p}}{\partial x_i} + \frac{\partial\left(\rho\bar{\tau}_{ij}\right)}{\partial x_j} \tag{2}$$

where ρ is density, $\bar{u}_i$ is the averaged Cartesian components of the velocity vector, $\rho\overline{u'_i u'_j}$ is the Reynolds stresses and p is the mean pressure. $\bar{\tau}_{ij}$ is the mean viscous stress tensor components, as shown in equation (3).

$$\bar{\tau}_{ij} = \mu\left(\frac{\partial\bar{u}_i}{\partial x_j} + \frac{\partial\bar{u}_j}{\partial x_i}\right) \tag{3}$$

in which μ is the dynamic viscosity.

3.2. Model of turbulence

The Realizable k–ε model was selected to calculate the resistance of the forms. The Hull Performance Workflow module of the StarCCM+ software specializes in calculating ship resistance using the Realizable k–ε model (Siemens,

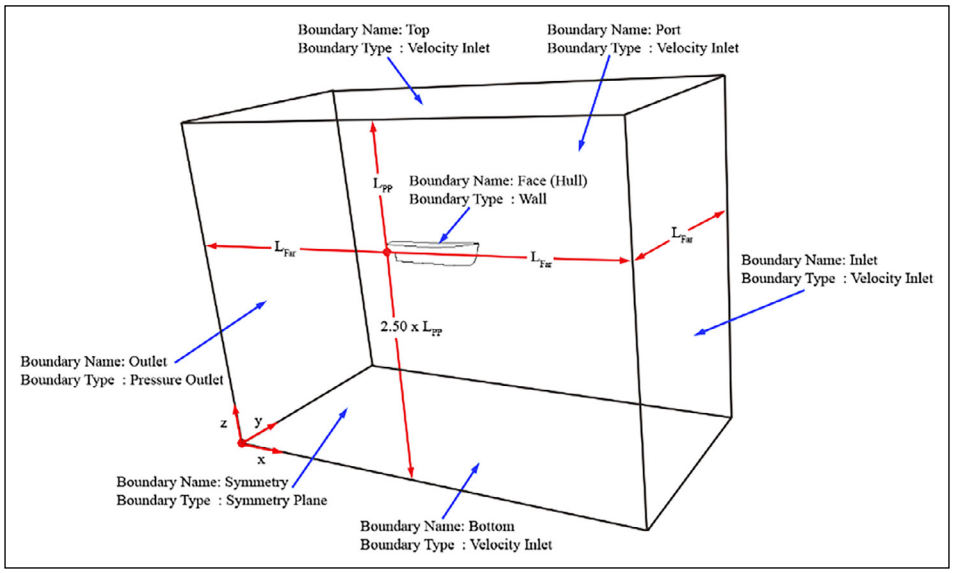

Figure 8. Computational domain dimensions and boundary conditions.

2021). Therefore, this turbulence model was chosen to calculate the resistance of the forms.

The "Realizable k–ε Model," developed by Shih et al. (1995), is the most advanced version of the k–ε model.

There are two basic differences from the standard k–ε model. The first is that the model contains a new transport equation for the turbulence loss rate $\boldsymbol{\varepsilon}$. Second, C_μ, a critical coefficient of the model, is expressed as a function of the mean flow and turbulence properties rather than being fixed as in the standard model. The understanding of an C_μ variable is also compatible with the experimental data in boundary layer.

Shih et al. (1995) developed transport equations (equations (4) and equations (5)) are as follows:

$$\frac{\partial}{\partial t}(\rho k)+\frac{\partial}{\partial x_j}(\rho k u_j)=\frac{\partial}{\partial x_j}\left[\left(\mu+\frac{\mu_t}{\sigma_k}\right)\frac{\partial k}{\partial x_j}\right]+G_k+G_b-\rho\varepsilon-Y_M+S_K \quad (4)$$

$$\frac{\partial}{\partial t}(\rho\varepsilon)+\frac{\partial}{\partial x_i}(\rho\varepsilon u_j)=\frac{\partial}{\partial x_j}\left[\left(\mu+\frac{\mu_t}{\sigma_\varepsilon}\right)\frac{\partial \varepsilon}{\partial x_j}\right]+\rho C_1 S_\varepsilon - \rho C_2\frac{\varepsilon^2}{k+\sqrt{\nu\varepsilon}}+C_{1\varepsilon}\frac{\varepsilon}{k}C_{3\varepsilon}G_b+S_\varepsilon \quad (5)$$

In this equation G_k is the production of turbulent kinetic energy due to average velocity gradients, G_b is the production of turbulence kinetic energy as a result of temperature differences in density, Y_M is constrictive turbulence depicts the effect of turbulence expansion on the entire spread. The terms S_K and S_ε are user-defined source terms.

4. NUMERICAL PROCEDURE

All CFD analyses of the hull forms were conducted using the Hull Performance Workflow (HPW) module in the StarCCM+ software.

The HPW module in StarCCM+ is designed for analyzing displacement hulls without appendages and provides a user-friendly interface for simulations under calm water conditions. It adheres to industry standards, managing critical aspects such as geometric domain definition, mesh refinement, transient simulation settings, and wave damping, ensuring accurate and reliable completion of CFD analyses (Siemens, 2021).

The forms were modeled in three dimensions using the Rhinoceros software and converted to IGS format. Using the HPW module, the IGS-format forms were imported into the Star-CCM+ program, and a computational domain representing a virtual towing tank was created around the boat geometry (Fig. 8).

The names and boundary conditions of the virtual towing tank's boundary surfaces are defined as shown in Figure 8.

The dimensions of the computational domain are determined automatically and are proportional to the length between perpendiculars (L_{PP}) of the hull. Equation (6) defines the L_{Far} parameter as a function of the Froude number and wake wavelengths (Siemens, 2021).

Farfield distance from the hull (LFar):

$$L_{Far} = L_{Dmax} + L_{Bmax} \quad (6)$$

Maximum damping length (L_{Dmax}):

$$L_{Dmax}=4.5e^{-3.75\cdot Fn}\cdot\lambda_{max} \quad (7)$$

Maximum buffer length (L_{Bmax}):

$$L_{Bmax}=0.4925\cdot Fn^{-0.8}\cdot\lambda_{max} \quad (8)$$

Wake wavelength at maximum allowed ship speed (λ_{max}):

$$\lambda_{max}=\frac{2\pi}{g}\cdot V^2_{Smax} \quad (9)$$

Maximum allowed ship speed (V_{Smax}):

$$V_{Smax}=0.4\cdot\sqrt{\cdot gL_{WL}} \quad (10)$$

Froude number (Fn):

$$Fn=\frac{V_S}{\sqrt{g\cdot L_{WL}}} \quad (11)$$

Where L_{WL} is waterline length, V_S is ship speed, g is acceleration due to gravity.

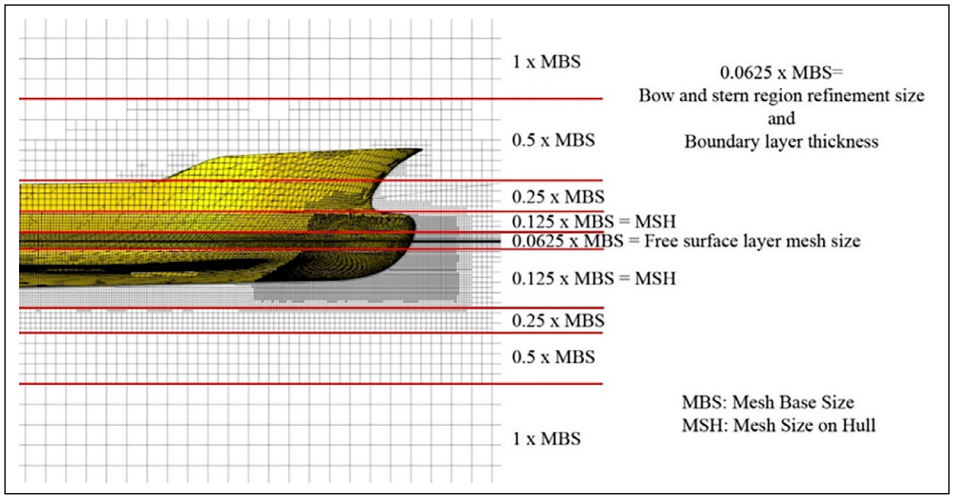

Figure 9. Cell size variation of the volume mesh structure and cell dimensions according to MBS.

MBS: Mesh base size; MSH: Mesh size on the hull.

For each CFD resistance analysis, the HPW automatically generated the volume mesh structure using the surface remesher, trimmed cell mesher, and prism layer mesher tools, resulting in the creation of three-dimensional hexahedral cells. The mesh base size (MBS) was calculated by dividing the LPP values of the forms by a specified denominator, as described in Equation (12). Based on the determined MBS, the mesh size on the hull (MSH) was calculated using Equation (13). Equation (14) was applied to calculate the cell sizes for the free surface layer, boundary layer thickness (BLT), and the refinement size in the bow and stern regions.

Figure 9 illustrates the variation in cell sizes of the volume mesh structure used in CFD resistance analyses, depending on changes in the mesh base size (MBS) and cell dimensions.

$$MBS = \frac{L_{PP}}{Denominator} \quad (12)$$

$$MSH = \frac{12.5}{100} MBS \quad (13)$$

$$BLT = \frac{6.25}{100} MBS \quad (14)$$

The HPW automatically configures the y+ and Δs values based on the specific characteristics of the problem being analyzed. Typically, HPW sets the y+ value to 30; however, variations in the vessel's geometry may cause the y+ value to occasionally deviate above or below this target. These fluctuations have minimal impact on the overall solution accuracy due to the use of a blended wall function. The boundary layer thickness is represented by 6 to 9 cells, depending on the BLT value, with an expansion ratio of 1.5.

The HPW generates a mesh of volumes around the hull and on the free surface using automatic volumetric refinement. The positions and sizes of these refinements are determined according to industry standards to ensure a high degree of accuracy while maintaining a low cell count. There are three volumetric refinements used to resolve the free surface, and these refinements are sized to approximately match the water stagnation height at Fn = 0.15, 0.275, and 0.4 in the vertical direction (Siemens, 2021).

The body, profile, and waterline (free surface) plane views of the volume mesh structure created for the forms are shown in Figure 10.

The mesh properties of the virtual towing tank, generated by HPW based on the selected denominator value, along with the mesh solution times and computer processor specifications, are presented in Table 3. The mesh structures for the forms are shown in Figure 11.

Additionally, the mesh structures in the bow and stern regions of the forms are shown in Figures 12 and 13, respectively, for a closer view.

Once the volume mesh structures were generated, the physical models required for hull resistance analysis in HPW were automatically configured under calm water conditions, as illustrated in Figure 14. For the CFD resistance analyses, the hull forms were treated as fixed, with no adjustments made for trim or sinkage. To optimize computational efficiency, a half-model approach was utilized during the simulations. The CFD resistance analyses were conducted at full scale for the ship's dimensions.

The physical runtime of the simulation is determined automatically. The Hull Performance Workflow monitors the hull's average resistance at each speed. The run terminates if the average resistance fluctuates by less than 0.5 percent over the preceding 500 time steps. If the stopping criterion is not met, the simulation terminates after a maximum of 7500 time steps for the initial hull speed and 3,500 time steps for each subsequent hull speed (Siemens, 2021).

5. MESH DEPENDENCY STUDY

The validation and uncertainty assessment of the CFD resistance analyses was conducted in accordance with the

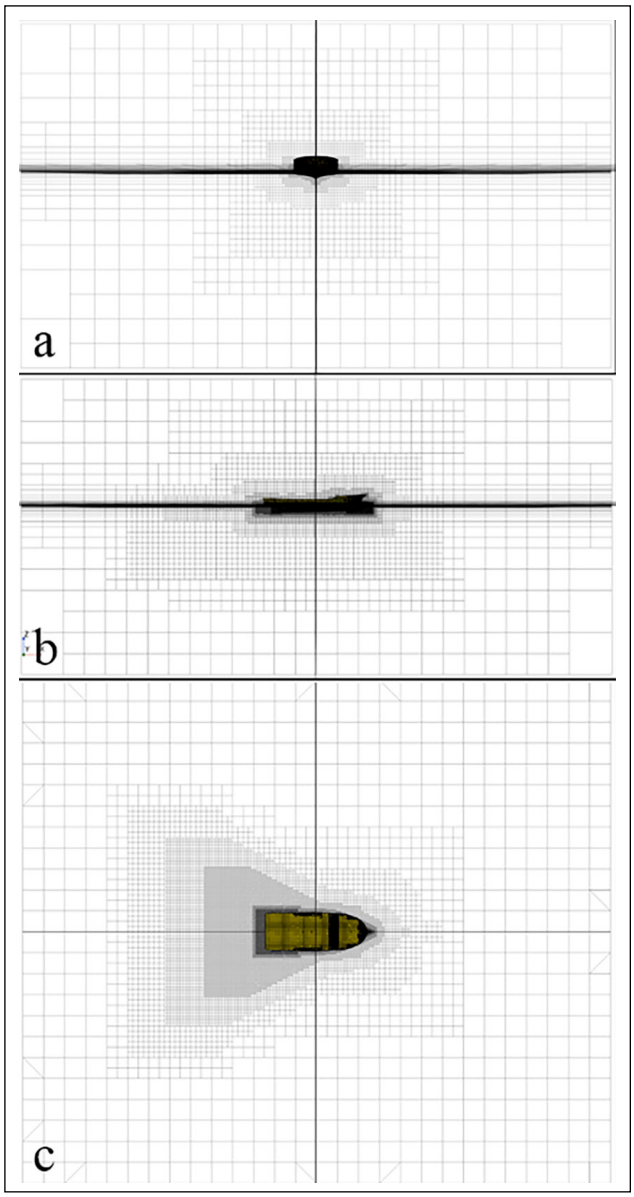

Figure 10. Body (a), profile (b), and waterline (free surface) plane (c) views of the volume mesh.

ITTC (2021) procedure. In the study, a refinement ratio of $\sqrt{2}$ was adopted, and coarse, medium, and fine mesh structures were generated based on the MSH value of Form SB. The properties of the mesh structures created for the analyses and the CFD analysis durations are provided in Table 4, while the total resistance values obtained from the CFD analyses are presented in Table 5.

To assess uncertainty, the Grid Convergence Index (GCI) was utilized, following the proposal by Roache (1994) and in accordance with the ITTC (2021) procedure. The GCI utilizes a grid refinement error estimator based on the generalized Richardson (1927) extrapolation principles. This estimator serves as a robust tool for evaluating the uncertainty associated with grid convergence in an asymptotic setting.

The GCI calculations, based on the total resistance values of Form SB for coarse, medium, and fine grids, are presented in Figure 15. A closer examination of these computations reveals that monotonic convergence is consistently observed across all CFD resistance analyses conducted in this study. This consistent pattern reinforces the reliability and accuracy of the analytical methodology, thereby validating the robustness of the conclusions drawn.

6. RESULTS AND DISCUSSIONS

The results of the CFD resistance analyses conducted on the ship forms are presented in Tables 6, 7, 8, and 9 for Forms WB, SB, SBE, and EB, respectively.

To demonstrate the accuracy of the resistance values derived from the CFD analyses, the forms were modeled using the Maxsurf Modeler program, and the resistance analyses were performed with the Maxsurf Resistance program using the Holtrop and Fung resistance estimation methods. A comparison of the effective power values found by CFD and those estimated by the Holtrop and Fung methods is shown in Figures 16, 17, 18, and 19 for Form WB, Form SB, Form SBE, and Form EB, respectively. The total resistance values found by CFD for each form fall between the total resistance curves estimated by Holtrop and Fung, as seen in Figures 16, 17, 18, and 19. In the Maxsurf Resistance program, when calculating the effective power values, the efficiency for the Fung method was assumed to be 100%. For the Holtrop method, efficiency values of 95%, 80%, 69%, 67%, and 63% were assumed for speeds of 5.5, 7.5, 9.5, 11.5, and 13.5 knots, respectively. These values were derived by subtracting the values obtained from dividing Pressure Resistance by Total Resistance from the values obtained by dividing Shear

Table 3. Mesh properties of the virtual towing tank, mesh solution times, and computer properties

	Unit	Form WB	Form SB	Form SBE	Form EB
LBP	m	28.767	31.393	31.559	28.792
Denominator		35	35	35	35
Mesh base size	m	0.822	0.897	0.902	0.823
Mesh size on hull	m	0.103	0.112	0.113	0.103
Mesh cell count	m	1,556,187	1,423,762	1,413,366	1,557,309
Total runtime	s	86449	78709	84600	84500
# of Processors		2×Intel Xeon E5 2667 (16×3.30 GHz)			

WB: Without Bulb Form; SB: Special Bulb Form; SBE: Special Elliptical Bulb Form; EB: Elliptical Bulb Form; LBP: Length Between Perpendiculars.

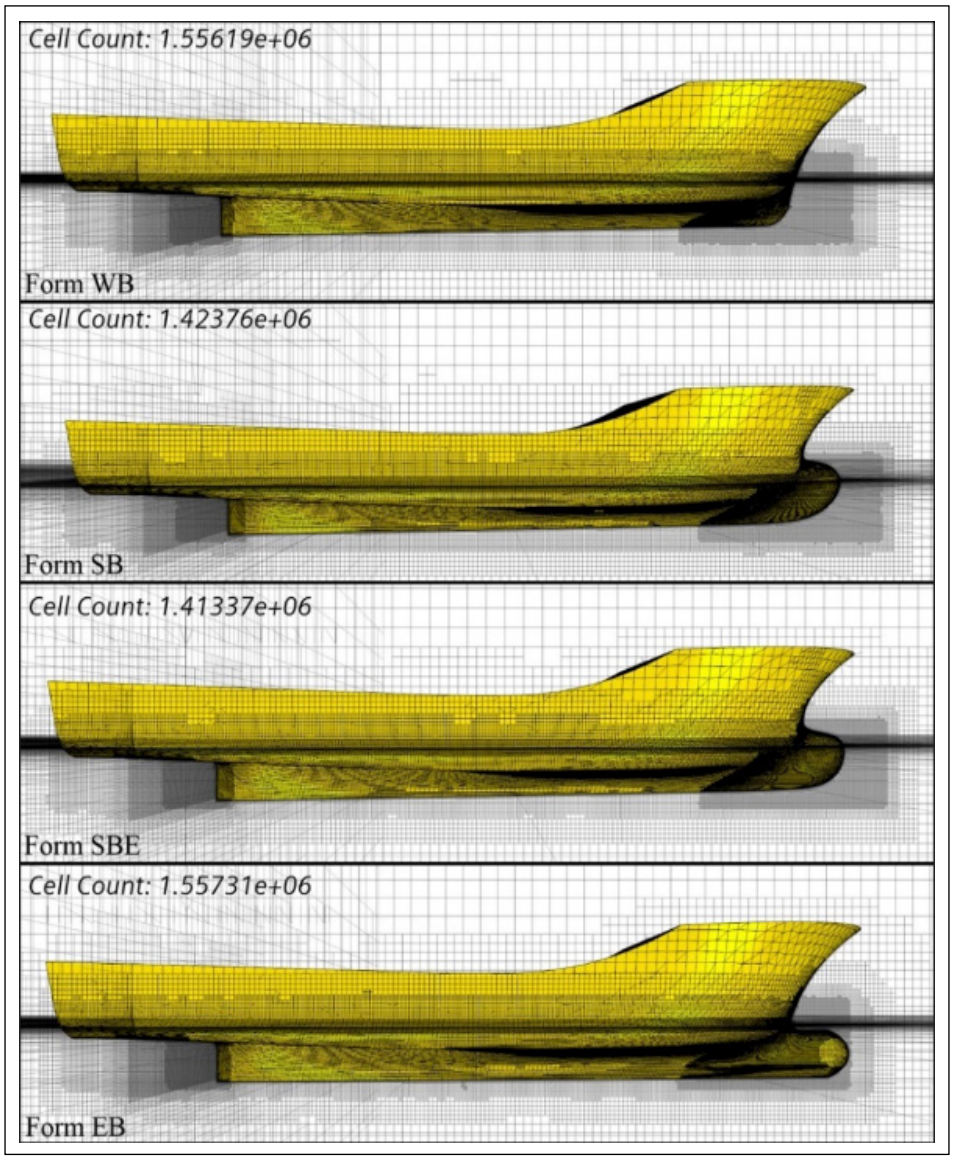

Figure 11. The mesh structures for the forms.

WB: Without Bulb Form; SB: Special Bulb Form; SBE: Special Elliptical Bulb Form; EB: Elliptical Bulb Form.

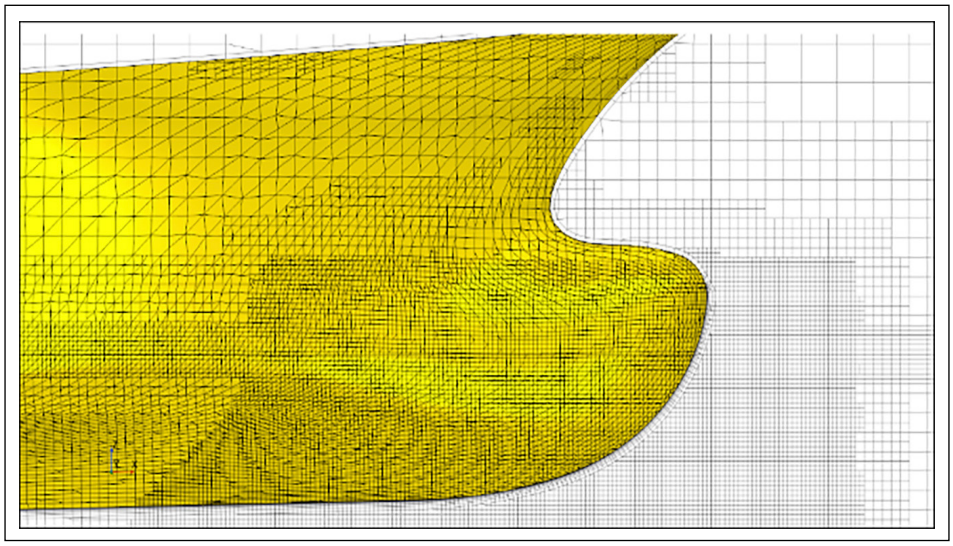

Figure 12. The view of the mesh structure on the bow form of the vessel in the profile plane.

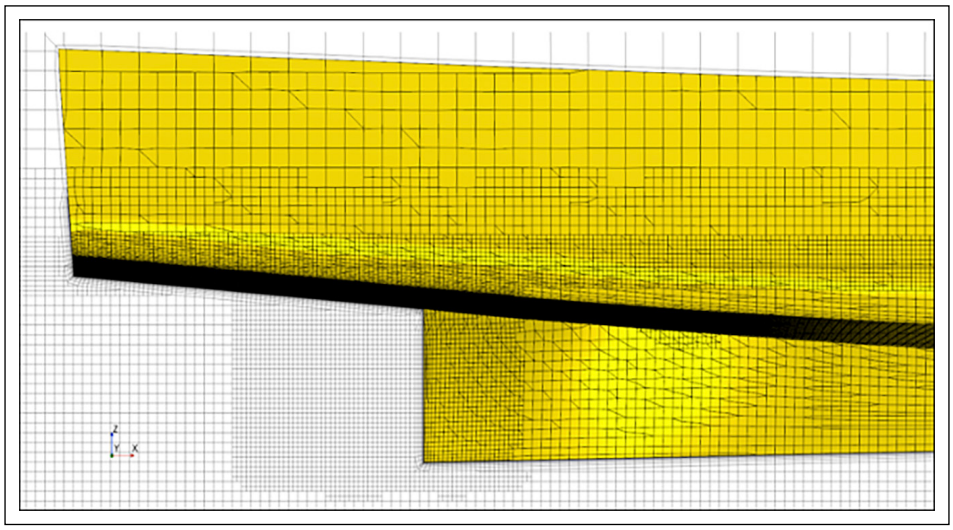

Figure 13. The view of the mesh structure on the stern form of the vessel in the profile plane.

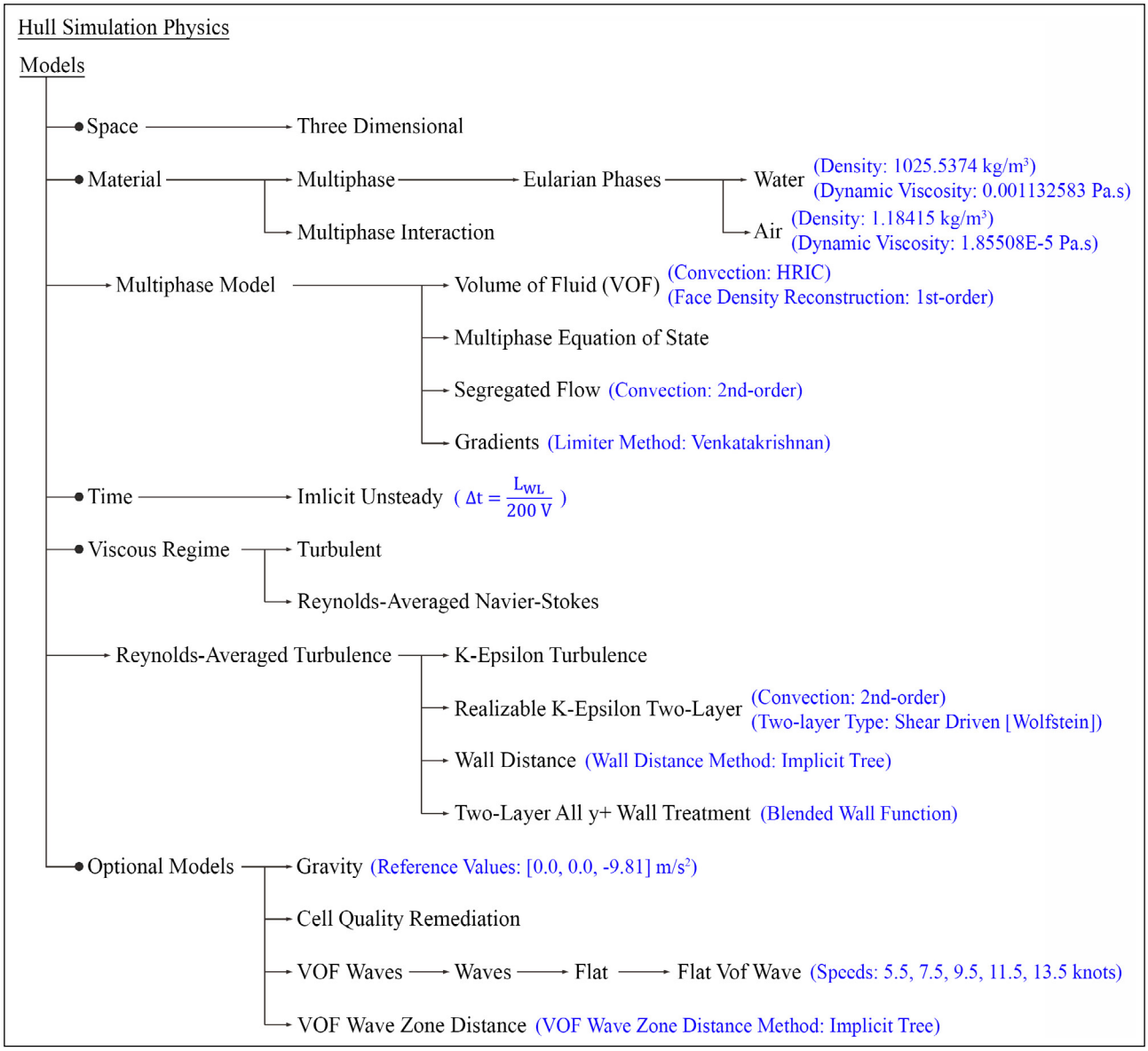

Figure 14. Models automatically selected by HPW for CFD resistance analyses.

HPW: Hull Performance Workflow; CFD: Computational Fluid Dynamics; VOF: Volume of Fluid.

Table 4. Properties of computational domains created according to denominators for the Form SB and solution times of CFD analyses

Ship code	L_{OA} (m)	L_{PP} (m)	Denominator	MBS (m)	MSH (m)	Mesh cell count	Total runtime	
							(sec)	(hour)
Form SB-coarse grid	35.578	31.393	24.8	1.269	0.158	661,907	36591	10.16
Form SB-medium grid	35.578	31.393	35.0	0.897	0.112	1,423,762	78709	21.86
Form SB-fine grid	35.578	31.393	49.6	0.634	0.079	3,181,538	175883	48.85

SB: Special Bulb Form; CFD: Computational Fluid Dynamics; L_{OA}: Length Overall; L_{PP}: Length Between Perpendiculars; MBS: Mesh base size; MSH: Mesh size on the hull.

Table 5. Total resistance values obtained from CFD resistance analysis of Form SB for mesh independence

Velocity		Fn	Form SB-coarse grid	Form SB-medium grid	Form SB-fine grid
(knots)	(m/s)		RT (kN)	RT (kN)	RT (kN)
5.5	2.829	0.154	8.857	8.662	8.612
7.5	3.858	0.210	18.246	17.398	17.117
9.5	4.887	0.266	33.187	32.518	32.408
11.5	5.916	0.322	64.107	62.906	62.657
13.5	6.944	0.378	119.126	117.100	116.632

CFD: Computational Fluid Dynamics; SB: Special Bulb Form; RT: Total Resistance.

Resistance by Total Resistance, and then subtracting the result from 1. Thus, the effective power values account for the power losses caused by the Holtrop method's inability to fully calculate wave resistance at higher speeds.

From the graphs, it can be observed that the CFD results for Form WB and Form EB closely match the Holtrop results. However, for Forms SBE and SB, the Holtrop results fall below the CFD results after a speed of 11 knots. This is due to the wave rising above the bulbous bow at 11 knots, causing the bulbous bow to submerge and creating additional frictional and pressure resistance. The Holtrop method in the Maxsurf Resistance program is unable to account for this effect. Considering all these calculations, the total resistance values obtained from the CFD are within acceptable ranges.

The comparison graphs for the frictional resistance coefficient (C_F), the pressure resistance coefficient (C_P) and the total resistance coefficient (C_T), are shown in Figures 20, 21, and 22, respectively. To equalize the displacement values of the ships, it was necessary to adjust their draft values. Changing the draft values altered the waterlines (L_{WL}) at which the ships float, and consequently, the Froude numbers (Fn) for the same speed values also changed. As a result, different Fn values were obtained for the same speed values. The CF, CP, and CT values were plotted in the graphs as functions of Fn. The points on the curves in the graphs represent the speeds of 5.5, 7.5, 9.5, 11.5, and 13.5 knots in order from the origin outward.

As can be seen in Figure 20, as the Froude number increases, the C_F values decrease for all forms, indicating the typical behavior of frictional resistance. This is expected because frictional resistance diminishes with higher speeds relative to the boundary layer effects. Form WB has the highest C_F across most Fn values, indicating that the bulb-less form generates higher frictional resistance due to the absence of a streamlined bulbous bow to smooth water flow. Form SB and Form SBE exhibit similar trends, but lower C_F values compared to Form WB. This suggests that the addition of a bulbous bow reduces frictional resistance. Between these two, Form SB generally performs better, showing the lowest C_F values at most Fn values. Form EB shows moderate performance compared to the others, with C_F values slightly higher than Form SBE but generally lower than Form WB and sometimes Form SB. Form SB demonstrates the best performance in terms of frictional resistance reduction across most Fn values, followed closely by Form SBE. There are points where the lines intersect, indicating that at specific Fn values, the relative performance of the forms changes. This suggests that the efficiency of the bulbous bow design may vary depending on the operational speed (represented by Fn). In summary, Form WB consistently exhibits the highest frictional resistance, making it the least efficient. The addition of bulbous bows (SB, SBE, EB) improves hydrodynamic performance, with Form SBE being the most effective in reducing frictional resistance, especially at higher Fn values. The results emphasize the importance of bulbous bow design in minimizing resistance and improving efficiency, particularly for higher-speed ranges.

As can be seen in Figure 21, across all forms, C_P increases as Fn rises. This is expected, as higher Fn values correspond to increased wave-making resistance, which is a significant component of pressure resistance. Form WB exhibits relatively higher C_P values compared to other forms at most Fn values, especially at higher Froude numbers. This indicates that the absence of a bulbous bow

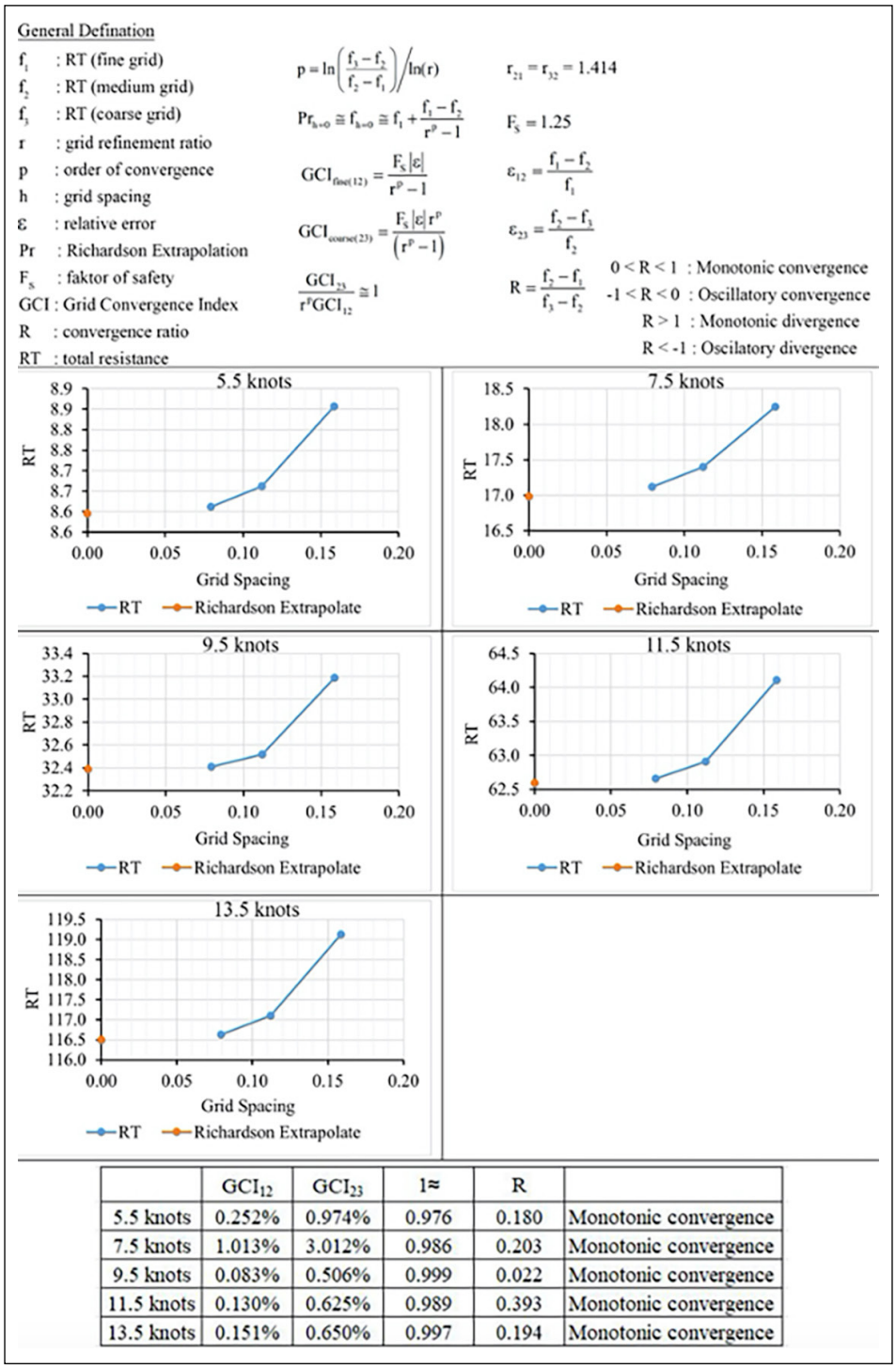

	GCI_{12}	GCI_{23}	1≈	R	
5.5 knots	0.252%	0.974%	0.976	0.180	Monotonic convergence
7.5 knots	1.013%	3.012%	0.986	0.203	Monotonic convergence
9.5 knots	0.083%	0.506%	0.999	0.022	Monotonic convergence
11.5 knots	0.130%	0.625%	0.989	0.393	Monotonic convergence
13.5 knots	0.151%	0.650%	0.997	0.194	Monotonic convergence

Figure 15. Grid convergence index (GCI) calculations and graphs.

leads to increased wave-making resistance due to less efficient flow dynamics at the bow. Form SB consistently shows lower C_P values than Form WB. This suggests that the addition of a bulbous bow significantly reduces wave-making resistance by altering the wave system and improving flow conditions at the bow. Form SBE exhibits the lowest C_P values for a wide range of Fn values, particularly in the mid-to-high Fn range. This indicates that the special elliptical bulbous bow design is the most effective at reducing wave-making resistance among the forms. Form EB shows moderate C_P values, lower than Form WB but higher than Form SB and SBE at most Fn values. This suggests that the elliptical bulbous bow is effective but not as optimized as the special elliptical bulbous bow (SBE). At higher Fn values, the differences in C_P become more pronounced, with Form SBE consistently outperforming the other forms. Form WB's C_P increases sharply at higher Fn, highlighting the inefficiency of the bulb-less form in reducing wave-making resistance. At lower Fn values, the C_P differences between the forms are minimal, indicating that bulbous bow design has a lesser impact at lower speeds. In summary, Form SBE is the

Table 6. Results of CFD resistance analysis for form WB

Velocity		Fn	Total resistance	Pressure resistance	Shear resistance	ITTC 1957 (friction correlation)	Effective power (RT*V)
[knots]	[m/s]		[kN]	[kN]	[kN]	[kN]	[kW]
5.5	2.829	0.160	7.842	3.962	3.880	3.784	22.185
7.5	3.858	0.218	16.764	9.806	6.958	6.728	64.676
9.5	4.887	0.277	33.154	22.580	10.574	10.436	162.024
11.5	5.916	0.335	66.694	51.360	15.334	14.890	394.562
13.5	6.944	0.393	118.560	97.340	21.220	20.060	823.281

CFD: Computational Fluid Dynamics; WB: Without Bulb Form; ITTC: The International Towing Tank Conference; RT*V: Total Resistance*Speed.

Table 7. Results of CFD resistance analysis for form SB

Velocity		Fn	Total resistance	Pressure resistance	Shear resistance	ITTC 1957 (friction correlation)	Effective power (RT*V)
[knots]	[m/s]		[kN]	[kN]	[kN]	[kN]	[kW]
5.5	2.829	0.154	8.662	4.670	3.992	3.840	24.505
7.5	3.858	0.210	17.398	10.176	7.222	6.828	67.121
9.5	4.887	0.266	32.518	21.280	11.238	10.594	158.915
11.5	5.916	0.322	62.906	47.160	15.746	15.116	372.152
13.5	6.944	0.378	117.100	95.260	21.840	20.380	813.142

Table 8. Results of CFD resistance analysis for form SBE

Velocity		Fn	Total resistance	Pressure resistance	Shear resistance	ITTC 1957 (friction correlation)	Effective power (RT*V)
[knots]	[m/s]		[kN]	[kN]	[kN]	[kN]	[kW]
5.5	2.829	0.154	8.442	4.424	4.018	3.848	23.882
7.5	3.858	0.209	16.368	9.098	7.270	6.842	63.148
9.5	4.887	0.265	31.852	20.720	11.132	10.618	155.661
11.5	5.916	0.321	64.916	48.820	16.096	15.150	384.043
13.5	6.944	0.377	116.320	94.560	21.760	20.420	807.726

Table 9. Results of CFD resistance analysis for form EB

Velocity		Fn	Total resistance	Pressure resistance	Shear resistance	ITTC 1957 (friction correlation)	Effective power (RT*V)
[knots]	[m/s]		[kN]	[kN]	[kN]	[kN]	[kW]
5.5	2.829	0.160	9.886	5.900	3.986	3.982	27.980
7.5	3.858	0.218	17.816	10.648	7.168	7.076	68.740
9.5	4.887	0.276	32.684	22.180	10.504	10.978	159.700
11.5	5.916	0.335	68.278	52.100	16.178	15.662	404.000
13.5	6.944	0.393	122.840	100.460	22.380	21.100	853.200

most efficient in reducing pressure resistance, particularly at higher Fn values. Form SB is Effective, but slightly less efficient than SBE. Form EB is moderate performance; better than WB but not as optimized as SBE or SB. Form WB is the least efficient, showing the highest C_P values, especially at higher speeds. This graph highlights the effectiveness of bulbous bow designs, especially the special elliptical bulbous bow (SBE), in minimizing wave-making resistance and improving overall hydrodynamic efficiency at higher operational speeds.

As can be seen in Figure 22, across all forms, the C_T increases as the Fn rises. This is expected because, at higher speeds, wave-making resistance and viscous resistance become more significant, contributing to the overall resistance. Form WB consistently shows higher C_T values compared to the other forms, particularly at higher Fn values. This suggests that the absence of a bulbous bow results in higher total resistance, likely due to increased wave-making resistance. Form SB exhibits lower C_T values compared to Form WB. This indicates that the bulbous bow effectively

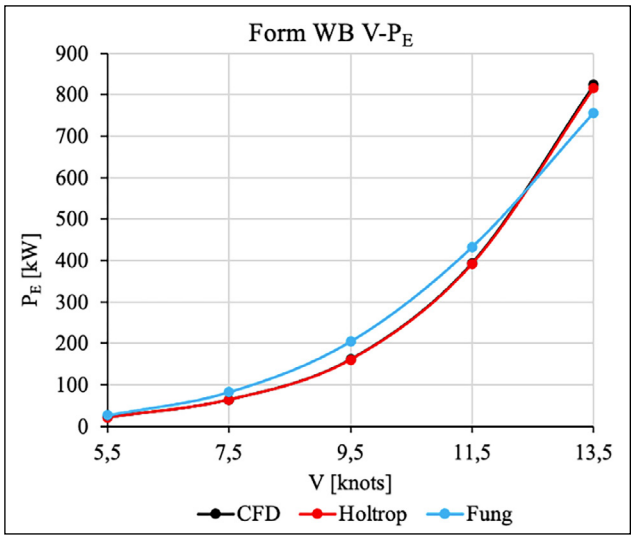

Figure 16. CFD, Holtrop, and Fung effective power curves for Form WB.

CFD: Computational Fluid Dynamics; WB: Without Bulb Form.

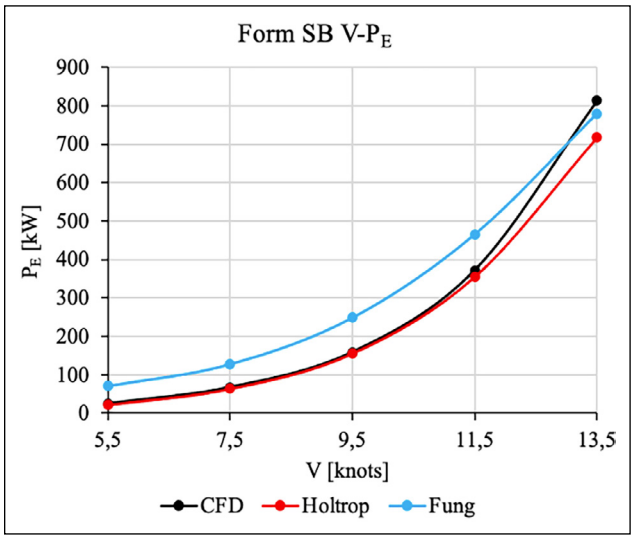

Figure 17. CFD, Holtrop, and Fung effective power curves for Form SB.

SB: Special Bulb Form.

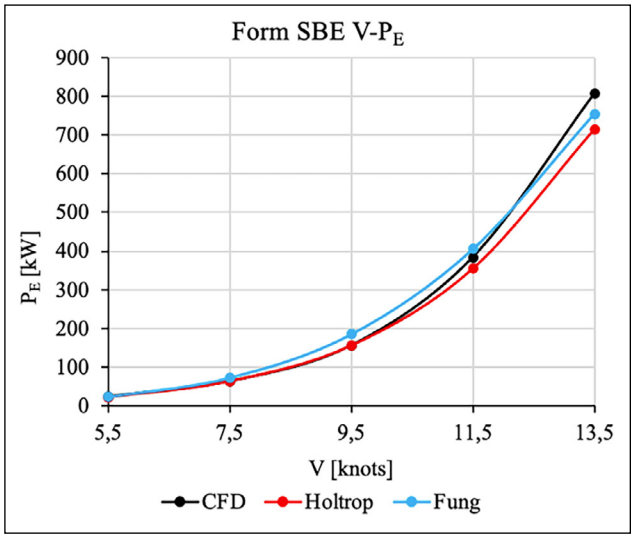

Figure 18. CFD, Holtrop, and Fung effective power curves for Form SBE.

SBE: Special Elliptical Bulb Form.

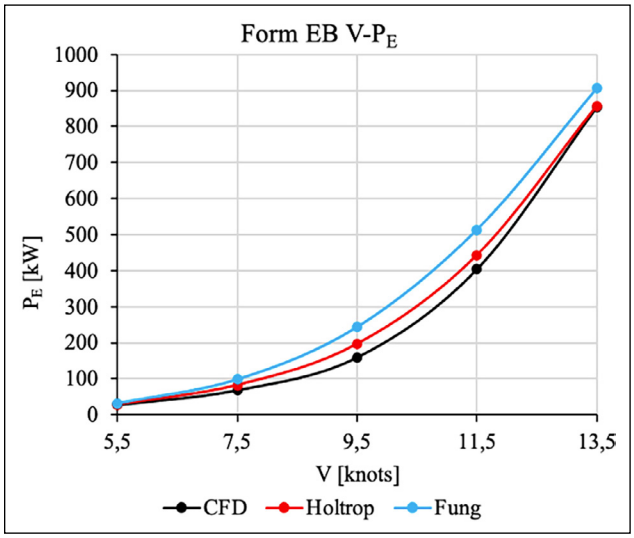

Figure 19. CFD, Holtrop, and Fung effective power curves for Form EB.

EB: Elliptical Bulb Form.

reduces total resistance by improving flow dynamics and reducing wave formation. Form SBE demonstrates the lowest C_T values across most Fn ranges. This suggests that the special elliptical bulbous bow is the most efficient design in minimizing total resistance. Form EB generally shows higher C_T values than Forms SB and SBE, indicating that while the elliptical bulbous bow design is effective, it is not as optimized as the special elliptical design (SBE). At higher Fn values, the difference in C_T values between the forms becomes more pronounced, with Form SBE maintaining the lowest total resistance. At lower Fn values, the differences between the forms are minimal, suggesting that bulbous bow designs have a more significant impact at higher speeds. The efficiency of the bulbous bow designs is clearly evident, with Form SBE consistently outperforming the other forms, followed by Form SB. In summary, Form SBE is the most efficient in reducing total resistance, especially at higher Fn values. Form SB performs well but slightly less effective than SBE. Form EB is moderately effective; better than WB but not as efficient as SBE or SB. Form WB is the least efficient, with consistently the highest C_T values. This graph highlights the importance of optimized bulbous bow designs, particularly at higher speeds, in reducing total resistance and improving the hydrodynamic performance of the vessel.

Figure 23 illustrates the percentage difference in resistance compared to Form WB across a range of Fn 0.150-0.400 for three different forms: Form SB, Form SBE, and Form EB. The y-axis represents the percentage difference in C_T, where positive values indicate an increase and negative values indicate a decrease in C_T relative to the baseline form. The x-axis represents the Froude number (Fn), which correlates with the vessel's speed.

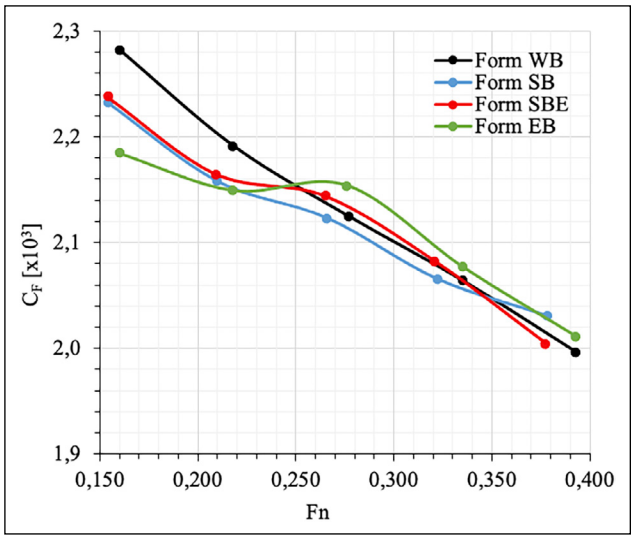

Figure 20. Comparison graph of the coefficients of frictional resistance for the forms.

WB: Without Bulb Form; SB: Special Bulb Form; SBE: Special Elliptical Bulb Form; EB: Elliptical Bulb Form.

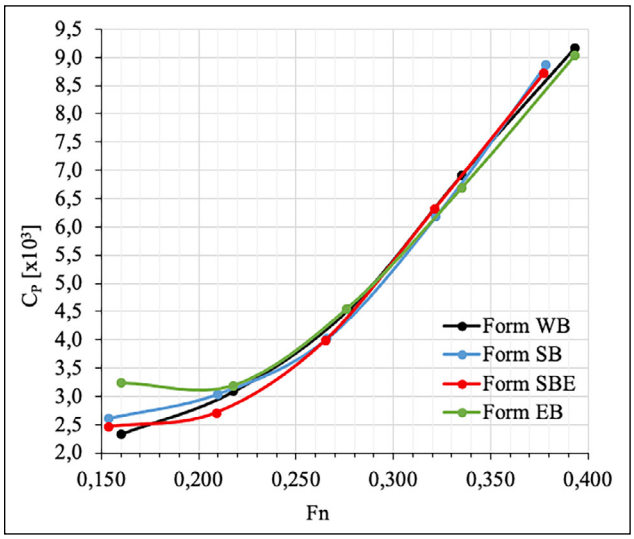

Figure 21. Comparison graph of the coefficients of pressure resistance for the forms.

WB: Without Bulb Form; SB: Special Bulb Form; SBE: Special Elliptical Bulb Form; EB: Elliptical Bulb Form.

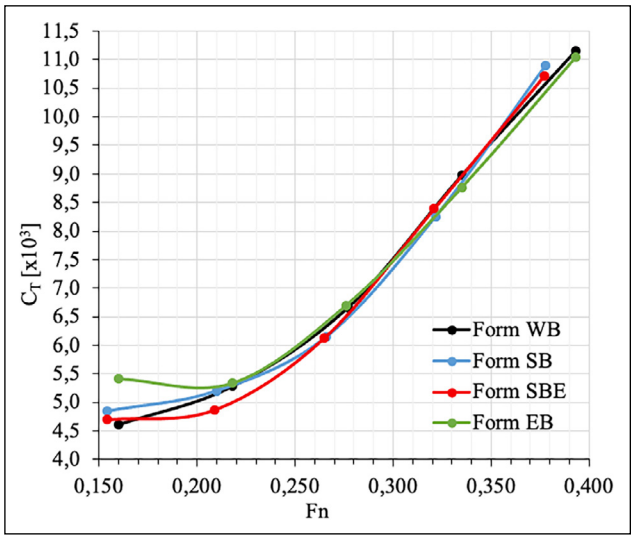

Figure 22. Comparison graph of the coefficients of total resistance for the forms.

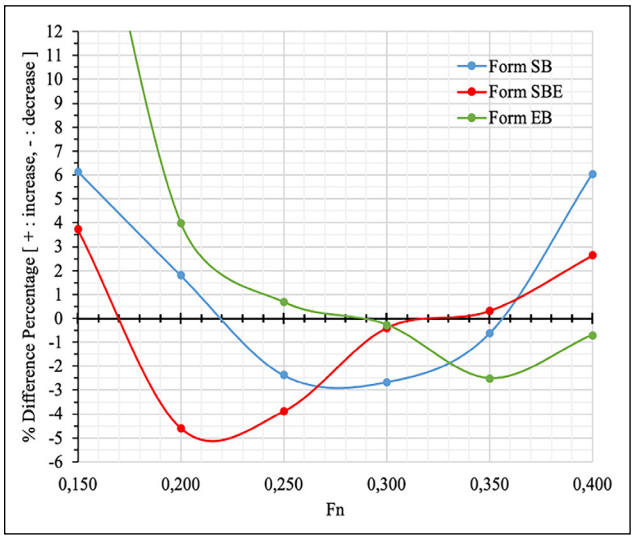

Figure 23. The percentage changes in C_T values of Forms SB, SBE, and EB compared to Form WB.

When analyzing the changes in C_T of Form SB compared to Form WB, the following conclusions are reached: At lower Fn values, Form SB initially exhibits a slight increase in resistance compared to Form WB. As Fn increases (around 0.2–0.3), the resistance begins to decrease, reaching a negative peak (indicating a reduction in resistance) at around Fn=0.25. At higher Fn values (Fn>0.35), resistance increases sharply, making this form less efficient at higher speeds.

When analyzing the changes in C_T of Form SBE compared to Form WB, the following conclusions are reached: Form SBE shows the largest resistance reduction at mid-range Fn values, peaking around Fn=0.215 with a percentage decrease of approximately -5%. It maintains a consistent reduction in resistance across most Fn values, demonstrating good performance. At higher Fn values (Fn>0.35), resistance begins to slightly increase, though the increase is less pronounced compared to Form SB.

When analyzing the changes in CT of Form EB compared to Form WB, the following conclusions are reached: At lower Fn values, Form EB shows a significant increase in resistance, likely due to suboptimal performance of the elliptical bulbous bow at low speeds. As Fn increases, the resistance stabilizes and becomes comparable to the baseline form at around Fn=0.3. Form EB shows the largest resistance reduction at Fn 0.30 values, peaking around Fn=0.35 with a percentage decrease of approximately -2.5%. At higher Fn values, the resistance begins to increase again, though less sharply than Form SB.

Form SBE demonstrates the best performance in reducing resistance, particularly in the mid-Fn range (0.2–0.3), where it consistently achieves the largest percentage decrease. This makes it the most efficient design for moderate-speed operations. In contrast, Forms SB and EB perform less efficiently at higher Fn

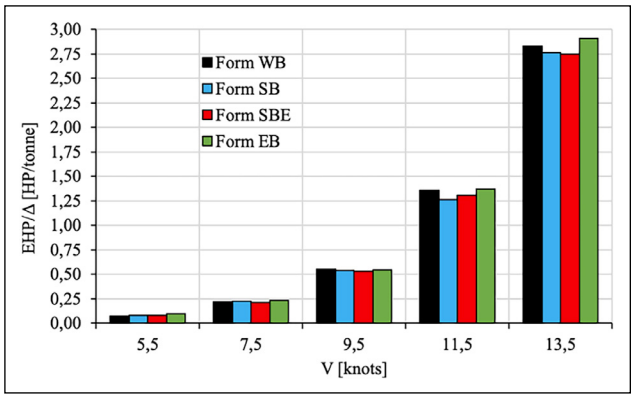

Figure 24. Values of the EHP/Δ (effective power/displacement tonnage) ratio for the speeds.

WB: Without Bulb Form; SB: Special Bulb Form; SBE: Special Elliptical Bulb Form; EB: Elliptical Bulb Form; EHP: Effective Horsepower.

values, as their resistance percentages increase relative to the baseline. Additionally, Form EB shows the poorest performance at low Fn values, likely due to its design being less suited to slower speeds.

Form SBE proves to be the most efficient design for reducing resistance, particularly in the mid-range Fn values, making it highly suitable for moderate speeds. Form SB demonstrates moderate performance but becomes less effective at higher speeds, while Form EB struggles at lower speeds, stabilizing in the mid-Fn range before showing a slight increase in resistance at higher Fn values. This analysis underscores the importance of tailoring bulbous bow designs to the vessel's operational speed range to achieve optimal hydrodynamic performance.

In Figure 24, the EHP/Δ (effective power per displacement ton) ratios of the forms are compared based on their velocities. The effective power per ton was calculated for each speed. At 5.5 knots, Form EB exhibited the worst performance, while the other forms performed almost identically. At 7.5 knots, Form SBE achieved the best performance, whereas Form SB performed the worst. At 9.5 knots, Form SBE emerged as the optimal form, while Form WB showed the poorest performance. At 11.5 knots, Form SB delivered the best performance, with Form EB being the least efficient. Finally, at 13.5 knots, Form SBE again demonstrated the best performance, while Form EB showed the worst. Overall, Form SBE consistently demonstrated the best performance, except at speeds of 5.5 and 11.5 knots.

7. CONCLUSION

This study investigated the hydrodynamic performance of various bow forms, including bulbous bow designs, on a typical Black Sea fishing vessel using Computational Fluid Dynamics (CFD) analyses. The primary objective was to evaluate the effectiveness of different bulbous bow shapes in reducing total resistance across a range of operational speeds. Four forms were analyzed: the baseline bulb-less form (Form WB), the conventional bulbous bow form (Form SB), the special elliptical bulbous bow form (Form SBE), and the elliptical bulbous bow form (Form EB).

The results revealed that the bulbous bow designs significantly influence the total resistance of the vessel, with the special elliptical bulbous bow (Form SBE) consistently demonstrating the best overall performance. Form SBE exhibited the lowest effective power per displacement tonnage (EHP/Δ) and reduced wave heights at higher speeds, particularly in the critical speed range of 9.5 to 13.5 knots, where wave-making resistance becomes dominant. The conventional bulbous bow form (Form SB) also performed well but was less efficient than Form SBE at higher speeds. The elliptical bulbous bow form (Form EB) showed moderate performance, especially at lower speeds, while the bulb-less form (Form WB) had the highest resistance values across all speed ranges.

A key observation was the relationship between speed and the effectiveness of the bulbous bow designs. At lower speeds, frictional resistance dominated, reducing the impact of bulbous bows. However, at higher speeds, where wave-making resistance is significant, the optimized bulbous bow designs effectively reduced total resistance and smoothed wave patterns along the hull.

This study underscores the importance of tailored bulbous bow designs for specific vessel types and operational profiles. For Black Sea fishing vessels, the special elliptical bulbous bow (Form SBE) is recommended as the optimal solution for minimizing resistance and enhancing efficiency. Future research could focus on validating these results through experimental towing tank tests and exploring the performance of these designs under varying sea conditions.

ACKNOWLEDGEMENTS

The authors gratefully acknowledge the high-speed computing laboratory of Naval Architecture and Marine Engineering Department, Karadeniz Technical University.

DATA AVAILABILITY STATEMENT

The published publication includes all graphics and data collected or developed during the study.

CONFLICT OF INTEREST

The author declared no potential conflicts of interest with respect to the research, authorship, and/or publication of this article.

ETHICS

There are no ethical issues with the publication of this manuscript.

USE OF AI FOR WRITING ASSISTANCE

No AI technologies utilized.

FINANCIAL DISCLOSURE

The authors declared that this study has received no financial support.

REFERENCES

Abramowski, T., & Sugalski, K. (2017). Energy saving procedures for fishing vessels by means of numerical optimization of hull resistance. *Zeszyty Naukowe Akademii Morskiej w Szczecinie, 49*(121), 19–27.

Atlar, M. (1977). *Investigation the effect of scale and bulbous bow on the fishing boats* [Unpublished master thesis]. Istanbul Technical University. [Turkish]

Baba, E. (1969). A new component of viscous resistance of ships. *Transactions of the Society of Naval Architects of Japan, 125*, 69–81. [CrossRef]

Başaran Gemi. *Eminoğulları 3*. https://www.basarangemi.com.tr/ships/balik-avci/eminogullari-3 Accessed on Nov 01, 2024.

Başaran Gemi. *Habibin Yavuz*, https://www.basarangemi.com.tr/ships/balik-avci/habibin-yavuz Accessed on Nov 01, 2024.

Başaran Gemi. (2024). Hakkımızda, başaran gemi sanayi. https://www.basarangemi.com.tr/pages/hakkimizda Accesed on Nov 01, 2024.

Bahatmaka, A., & Kim, D. J. (2019). Numerical approach for the traditional fishing vessel analysis of resistance by CFD. *Journal of Engineering Science and Technology, 14*(1), 207–217.

Bragg, M. (1930). Results of experiments upon bulbous bows. *Transactions SNAME, 38*, 13–43.

CD-Adapco. (2014). User Guide, Star-CCM+ Version 9.04, CD-Adapco.

Díaz-Ojeda, H. R., Pérez-Arribas, F., & Turnock, S. R. (2023). The influence of dihedral bulbous bows on the resistance of small fishing vessels: A numerical study. *Ocean Engineering, 281*, Article 114661. [CrossRef]

Díaz Ojeda, H. R., Oyuela, S., Sosa, R., Otero, A. D., & Pérez Arribas, F. (2024). Fishing vessel bulbous bow hydrodynamics-a numerical reverse design approach. *Journal of Marine Science and Engineering, 12*(3), Article 436. [CrossRef]

Dinçer, A. C. (1992). *A design study of Turkish Black Sea fishing vessels [Master thesis]*. University of Glasgow. Available from ProQuest Dissertations & Theses Global database. (UMI No. 11011427).

Ergün Gemi. (2024). *Kurumsal tarihçe*. https://ergungemi.com.tr/hakkimizda/ Accessed on Nov 01, 2024.

Ferguson, A. M. (1967). Hull and bulbous bow interaction. *Transactions RINA, 112*(4), 421–441.

Inui, T., Takaehi, T., & Kumano, M. (1960). Wave profile measurement on the wave making characteristics of the bulbous bow. Society of Naval Architects of Japan (Translation from the University of Michigan), 16–35. [CrossRef]

Inui, T. (1962). Wave making resistance of ships. *Transactions SNAME, 70*, 283–313.

Iqbal, M., Budiarto, U., Hidayat, K. Z., Hernanta, H. H., & Trimulyono, A. (2021). The influence of foil-shaped center bulb geometry into catamaran fishing vessels resistance. *In IOP Conference Series: Materials Science and Engineering, 1034*(1), IOP Publishing.

ITTC. (2021). *ITTC-Recommended Procedures and Guidelines: Uncertainty analysis in CFD verification and validation methodology and procedures*. Eff. Date 2021, Revision 04.

Kafalı, K., Şaylan, O., & Salcı, A. (1979). *Developing of hull forms of fishing boats suitable for Turkish waters*. The Scientific & Technological Research Council of Turkey, Project No. G-416. [Turkish]

Kim, D.J., Iqbal, M., Bahatmaka, A., & Prabowo, A. R. (2018). *Bulbous bow applications on a catamaran fishing vessel for improving performance.* In: MATEC Web of Conferences, 159, (1-6), EDP Sciences. [CrossRef]

Kracht, A. M. (1978). Design of bulbous bows. *Transactions SNAME, 86*, 197–217.

Li, C., Wang, Y., Chen, J. (2016). *Study on the shape parameters of bulbous bow of tuna longline fishing vessel*. 5th International Conference on Energy and Environmental Protection (ICEEP 2016), 17-18 September 2013, (250–255). Shenzhen. [CrossRef]

Muntjewerf, J. J. (1967). Methodical series experiments on cylindrical bows. *Transactions RINA, 112*(2), 199–223.

Oyuela, S., Ojeda, H. R. D., Arribas, F. P., Otero, A. D., & Sosa, R. (2024). Investigating fishing vessel hydrodynamics by using EFD and CFD tools, with focus on total ship resistance and its components. *Journal of Marine Science and Engineering, 12*(4), Article 622. [CrossRef]

Özdemir, Y., H. (2007). *Investigation of the flow surrounding the ship by using computational fluid dynamics* [Master thesis]. Yıldız Technical University. Council of Higher Education Thesis Center (Accession No. 213256). [Turkish]

Raju, M.S.P., Sivabalan, P., Thamby, T., & Saravanan, B. (2020). Effect of bulbous bow on resistance of a tuna longliner. *International Journal of Advanced Research in Engineering and Technology, 11*(2), 136–145.

Roache, P., J. (1994). Perspective: a method for uniform reporting of grid refinement studies. *Journal of Fluids Engineering, 116*(3), 405–413. [CrossRef]

Richardson, L. F. (1927). The deferred approach to the limit. *Transactions of the Royal Society of London, Series A, 226*, 299–361. [CrossRef]

Samuel, S., Iqbal, M., Utama, I.K.A.P. (2015). An investigation into the resistance components of converting a traditional monohull fishing vessel into catamaran form. Int*ernational Journal of Technology, 6*(3), 432–441. [CrossRef]

Saral, D. (2016). *A systematic investigation of the effects of various bulbous bows on resistance of fishing boats* [Master thesis]. Karadeniz Technical University. Council of Higher Education Thesis Center (Accession No. 430371). [Turkish]

Saral, D. (2023). *Form optimization of the Black Sea type fishing vessels* [Doctorial Thesis]. Karadeniz Technical University. Council of Higher Education Thesis Center (Accession No. 791295). [Turkish]

Saral, D., Aydın, M. & Köse, E. (2018). A systematic investigation of the effects of various bulbous bows on resistance of fishing boats. *Brodogradnja, 69*(2), 93–117. [CrossRef]

Saral, D. & Köse, E. (2020). Resistance analyses of a traditional Black Sea type fishing ship with CFD in calm water. *Turkish Journal of Maritime and Marine Sciences, 6*(2), 207–223.

Saral, D., & Köse, E. (2024). Academic studies on fishing vessels in Turkey. *Ocean Engineering, 308*, Article 118295. [CrossRef]

Setyawan, D., Utama, I. K., Murdijanto, M., Sugiarso, A., & Jamaluddin, A. (2010). Development of catamaran fishing vessel. *IPTEK The Journal for Technology and Science, 21*(4), 167–173. [CrossRef]

Sharma, R., & Sha, O. P. (2005). Practical hydrodynamic design of bulbous bows for ships. *Naval Engineers Journal, 117*(1), 57–75. [CrossRef]

Shearer, J. R., & Steele, B. N. (1970). Some aspects of the resistance of full form ships. *Transactions RINA, 112*(4), 69–83.

Shih, T. H., Liou, W. W., Shabbir, A., Yang, Z., & Zhu, J. (1995). A new k–ε Eddy-viscosity model for high Reynolds number turbulent flows-model development and validation. *Computers Fluids, 24*(3), 227–238. [CrossRef]

Siemens. (2021). *User Guide, Simcenter STAR-CCM+ Hull Performance Workflow 2021.2.*

Söylemez, M. (1983). *Application of bulb to fishing boats* [Undergraduate Graduation Project]. Istanbul Technical University. [Turkish]

Szelangiewicz, T., Abramowski, T., Żelazny, K., & Sugalski, K. (2021). Reduction of resistance, fuel consumption and GHG emission of a small fishing vessel by adding a bulbous bow. *Energies, 14*(7), Article 1837. [CrossRef]

Taylor, D. W. (1923). Marine Engineering and Shipping Age (pp. 540–548). Aldrich Publishing Company.

Tran, T. G., Van Huynh, C., & Kim, H. C. (2021). Optimal design method of bulbous bow for fishing vessels. *International Journal of Naval Architecture and Ocean Engineering, 13*, 858–876. [CrossRef]

Weinblum, G. (1935). Die theorie der wulstschiffe. Der Gesellshaft fur Angevandte Mathematik, 135-156.

Wigley, W. C. S. (1936). The theory of bulbous bow and its practical application. *Transactions NECIES, 52*, 65–88.

Yim, B. (1963). On ships with zero and small wave resistance. Paper presented at the in Proceedings of International Seminar on Theoretical Wave Resistance, Michigan, USA, 163–193. [CrossRef]

Yim, B. (1965). Analyses of spherical bulbs on a ship bow. Inc. *Technical Report 117*, 28–39.

Yim, B. (1974). A simple design theory and method for bulbous bows of ships. *Journal of Ship Research, 18* (3), 141–152. [CrossRef]

Yim, B. (1980). Simple calculation of sheltering effect on ship-wave resistance and bulbous bow design, *Journal of Ship Research, 24* (4), 232–243. [CrossRef]

Seatific, Vol. 4, Issue. 2, pp. 77–87, December 2024

Seatific Journal
https://seatific.yildiz.edu.tr
DOI: https://doi.org/10.14744/seatific.2024.0009

Review Article

Reliability analysis of the Porto Velho Pier - Rio Grande/RS through limit equilibrium and finite element method

Luiza Antiqueira da SILVA NETA*, Diego de Freitas FAGUNDES, Antônio Marcos de Lima ALVES

Department of Engineering, Federal University of Rio Grande, Rio Grande, Brasil

ARTICLE INFO

Article history
Received: October 30, 2024
Revised: December 13, 2024
Accepted: December 24, 2024

Key words:
Finite element method; Porto Velho pier in the city of Rio Grande - RS, seawall; stability analysis; reliability analysis; limit equilibrium method

ABSTRACT

This study analyzes the global stability of the Porto Velho pier, a structure in the port complex of the city of Rio Grande - RS, Brazil. This structure is a gravity pier with a length of 640 m which has been showing excessive displacements in a 150 m stretch. Limit Equilibrium and Finite Element tools associated with the Monte Carlo and FOSM Methods were applied. Four scenarios will be analyzed that represent the evolution of the erosion of the base of the pier structure, in which it can be concluded that as the loss of soil and rockfill of the base occurs, it presents a reduction in the safety factor and according to the FEM results in its rupture. In addition, the FEM analysis shows that the strength criterion of the pier's protective rockfill has a significant influence on the stability of the pier, since when it is considered to be linearly elastic, the structure behaves very similarly to that found by the LEM, while when the Mohr Coulomb criterion is adopted, the structure behaves in a way that is more representative of what is observed in situ.

Cite this article as: Silva Neta LA, Fagundes DF, Alves AML. Reliability analysis of the Porto Velho Pier - Rio Grande/RS through limit equilibrium and finite element method. Seatific 2024;4:2:77–87.

1. INTRODUCTION

In traditional deterministic analyzes of slope stability, uncertainties related to the problem are commonly neglected. A better understanding of these uncertainties, whether intrinsic or epistemic, has become an object of great interest in geotechnical research in the last two decades through the use of reliability analyzes to assess the probability of slope failure (Dyson and Tolooiyan 2019, Hostettler et al. 2019, Li et al. 2019).

According to Vanmarcke (1977), there are many uncertainties involved in slope engineering, especially with regard to the spatial variability of geotechnical properties and the uncertainties associated with deterministic calculations to estimate the safety margin of slope stability. The assessment of slope stability is affected as the variability of the soil affects the analysis systematically or randomly. Thus, geotechnical variability is complex, resulting from various sources of uncertainty, such as the mechanical and physical properties of soils and rocks, which are naturally dispersed, plus inaccuracies in transformation models and uncertainties related to human error (Phoon and Kulhawy 1999, Yang et al. 2020, Ansari et al. 2021).

System failure occurs when the slope slides along a critical surface. Thus, slope reliability analysis is defined as a system reliability analysis problem in which the overall failure probability (or system failure probability, Pf) of a slope, considering several potential sliding surfaces, is of interest and is greater than the failure probability of any individual potential sliding surface as a result of system effects (Diltlevsen 1979, Cho 2013, Zeng et al. 2015, Metya et al. 2017).

*Corresponding author.
*E-mail address: antiqueiraneta@gmail.com

Several authors have been studying the use of reliability analysis. Haldar (2019) presents an overview of foundation design methodologies highlighting methodologies such as FORM (First Order Reliability Method) and the Monte Carlo method. The author highlights the importance of foundation designs based on reliability, then considering the variability and spatial correlation of the soil, leading to rational design decisions.

Beloni et al. (2017) analyzed the geotechnical reliability of the pile foundation of a port pier located in the city of Rio Grande, RS. In their study, the probabilistic distribution of the bearing capacity was assessed using Bayesian theory concepts. The authors also emphasized the importance of reliability studies for accurately evaluating the safety of any engineering project.

In 2000, the Porto Velho pier, in Rio Grande/RS (Fig. 1), began to show excessive displacements towards the channel and the formation of cracks in the sidewalk, possibly related to the rupture of the structure (Fig. 2). The objective of this work is, therefore, to analyze the stability of the Porto Velho pier through a reliability analysis, as well as to infer the evolution of the safety factor as an erosion process occurs at the base of the pier structure. The stability analysis will consist of using two approaches, the limit equilibrium method (LEM) and the finite element method (FEM). From these, a reliability analysis will be carried out using the Monte Carlo method (MMC) and the first order first moment method (FOSM). This study will enable the understanding of the development of port structures' stability, thus providing a basis for decision-making regarding future mitigation projects for the pathological manifestations observed along the structure. Furthermore, the study may also contribute to future investigations on stability analysis, using reliability methods in gravity-type port structures.

2. MATERIALS AND METHODS

2.1. Deterministic method

The most common techniques for slope stability analysis are deterministic. These techniques assume the constancy of the variables used in the calculation model. This methodology usually uses the Limit Equilibrium Method (LEM) to determine the minimum safety factor for the slope failure surface (Ortigão and Sayão, 2004). According to Cho (2010), slope stability problems are commonly analyzed using the LEM. The failing soil mass is divided into a number of vertical layers (slices) to calculate the factor of safety, which is defined as the ratio of the shear strength stresses to the mobilized shear stresses, so the static equilibrium between the slices and the mass as a whole are used to solve the stability problem. However, all slice methods are statically indeterminate and, as a result, require assumptions to solve the problem. Furthermore, LEM does not consider the stress-strain behavior of the materials involved in the analysis.

Another technique for slope stability analysis is the Finite Element Method (FEM). According to Zaman et al. (2000) the FEM represents a powerful alternative approach to slope stability analysis. This method is accurate, versatile and requires fewer a priori assumptions, especially regarding the failure mechanism. In this method, the changing stress-strain condition in the soil is considered, thus focusing mainly on the failure mechanism during a slope failure (Duncan, 2014).

According to Griffiths and Lane (1999), in this method the shear strength parameters of the soil c' and tan ϕ' are reduced by a Strength Reduction Factor (SRF) until failure occurs (Equation 1). In this study, PLAXIS 2D (2016) software was used for stability analysis. It is understood that the value of the safety factor is the same as the value of the SFR at the time of failure.

$$\mathrm{SRF} = \frac{\tan(\emptyset')}{\tan(\emptyset'_{reduced})} = \frac{C'}{C'_{reduced}} \quad (1)$$

2.2. Probabilistic method

Probabilistic procedures for slope stability analysis vary in their assumptions, limitations, ability to deal with complex problems and mathematical complexity. Most of them, however, fall into one of two categories: approximate methods (First Order Second Moment Method, Point Estimation Method) and Monte Carlo Simulation (El-Ramly, 2002).

According to Da Re et al. (2001), reliability analysis provides a systematic method for evaluating the combined influences of uncertainties in the parameters that affect the factor of safety. Thus, probabilistic analysis evaluates the stability conditions of slopes, taking into account the errors associated with the nature of the problem and the variability of the characteristics of the slope and its soil. Through this analysis, the safety of a slope is characterized by the value of the safety factor (FS) based on average values corrected for probabilistic parameters, or by the value of the reliability index (β), which implicitly involves the behavior of a function of random parameters, which defines the state of safety of a slope.

Thus, the reliability index describes the stability of the slope by the number of standard deviations separating the average factor of safety from its failure value, which is defined as 1. The reliability index can also be defined as a way of normalizing the factor of safety in relation to its uncertainty. Equation 2 shows the calculation for determining the reliability index (Abbaszadeh et al. 2011).

$$\beta = \frac{E[FS] - 1}{\sigma[FS]} \quad (2)$$

Where β represents the reliability index, E[FS] the expected value of the safety factor and σ[FS] the standard deviation of the factor of safety. Table 1 illustrates the relationship between the reliability index and the probability of failure, assuming a normal distribution for the safety factor.

The variability of the parameters is given as a function of the coefficient of variation (COV). Duncan et al. (2014) defines the COV as the ratio between the standard deviation (σ) and the arithmetic mean (μ) of a sample, so this parameter designates the dispersion of the data in relation to the mean, and its result is expressed as a percentage (Eq. 3).

$$COV = \frac{\sigma}{\mu} * 100 \quad (3)$$

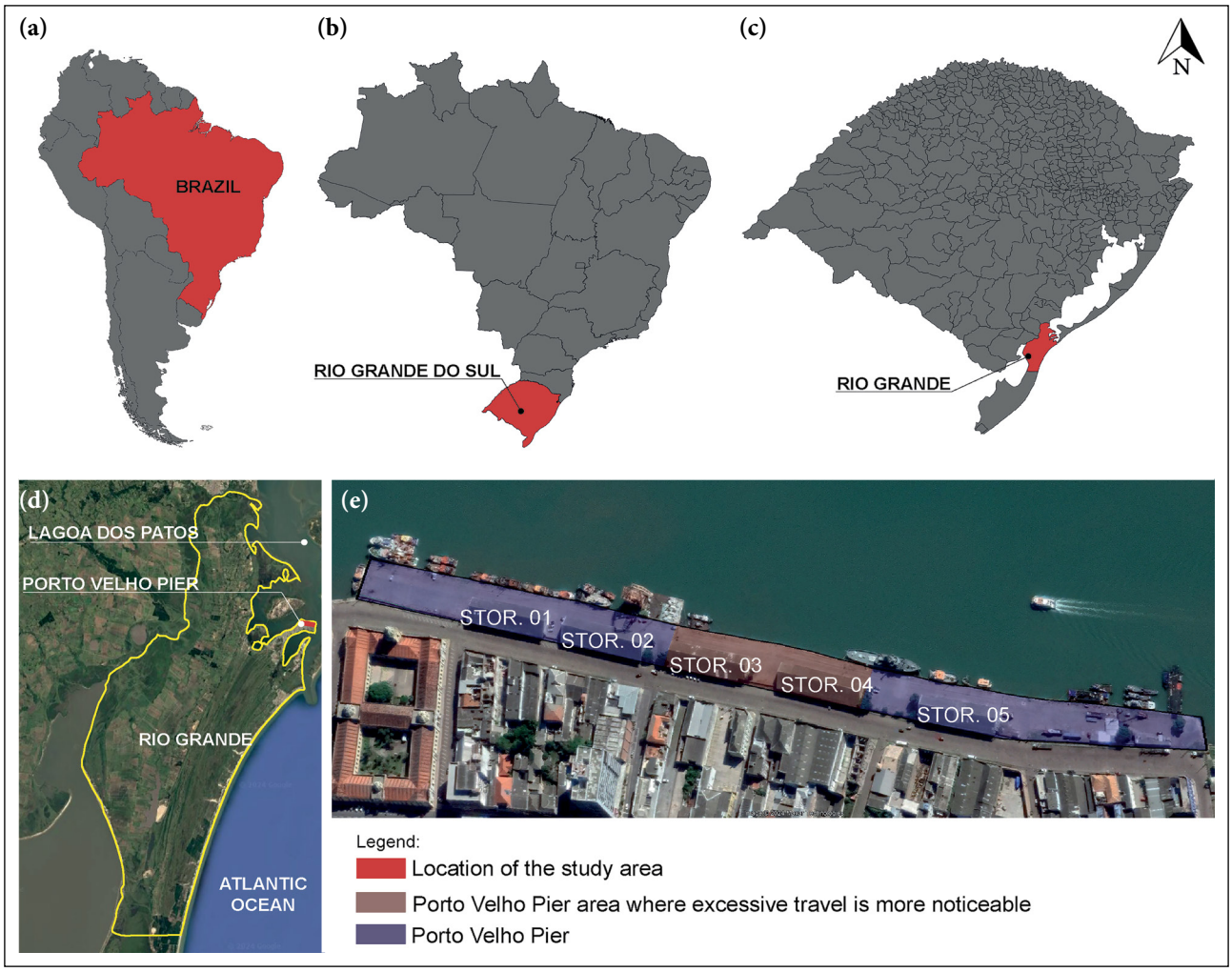

Figure 1. (a) Continental, state and municipal identification of the studied location; (b) Location of the Porto Velho Pier in the municipality of Rio Grande; (c) Identification of the study area.

In the Monte Carlo Method (MMC), the stability of the structure is calculated by generating a large number of random data for the input variables (such as friction angle and cohesion), since the probability distribution of these variables is known. As the data is generated, stability is analyzed using deterministic methods, which also makes it possible to determine the measures of central tendency corresponding to the factor of safety, as well as the corresponding probability of failure (Cho, 2010).

There are two important aspects to MMC. The first refers to the search for the critical surface for each set of randomly generated input data values, which involves significant computational effort, making it impractical. The way commonly used to resolve this difficulty is to take as the critical rupture surface the one obtained by the deterministic method, which is therefore independent of the values of the probabilistic analysis input data set (El Ramly, 2001).

According to Li et al. (2013) the probability of system failure (P_{fs}) is frequently calculated using a large, but finite, number of potential sliding surfaces. Let S_1, S_2, ..., S_{Ns} denote N_s potential slip surfaces that are considered in the limit equilibrium analysis of slope stability. Then, the slope can be considered as a series system consisting of N_s components (i.e. S_1, S_2, ..., S_{Ns}). System failure occurs when any component (i.e. S_1, S_2, ..., S_{Ns}) fails. The probability of system failure (P_{fs}) can be calculated using Equation 4.

$$P_{f,s} = \frac{1}{N_t} * \sum_{k=1}^{Nt} I(FS_{mim} < 1) \quad (4)$$

Where N_t is the total number of simulations generated during the MCS; FS_{min} is the minimum safety factor value among the safety factor values for the N_s potential slip surfaces for a given set of random samples of uncertain parameters X (i.e., c_u, c and $\varnothing$) involved in the slope stability analysis; and $I\{.\}$ is the function indicator. For a given random sample $I(FS_{min}<1)$ is taken as a value of 1 when $FS_{min}<1$ occurs. Otherwise, it is equal to zero.

The slip surface with FS_{min} (i.e. critical slip surface) needs to be located between potential slip surfaces for each sample generated during MCS, and its correspondent is calculated using a deterministic slope stability analysis method, such as limit equilibrium methods (Duncan et al. 2014).

The First-Order, Second Moment (FOSM) method is based on truncating the Taylor Series expansion function. According to Griffith (2007), this method provides analytical

Figure 2. (a) Displacement of the pier structure blocks. (b) Height variation along the pavement and pier crown blocks. (c) Displacement of the gravity wall towards the navigation channel. (d) Area where displacements are most intense.

approximations for the mean and standard deviation of a parameter of interest, as a function of the mean and standard deviation of the various input factors, and their correlations.

Thus, the calculation is based on the variation in the FS caused by a small oscillation in the independent variables. The number of analyses required for this procedure is equal to n+1, where n is the number of independent values. Equation 5 shows this process.

$$V[FS] = \sum_{i=0}^{n} \left(\frac{\delta FS_{ii}}{\delta X_{ii}}\right)^2 * V[X_i] \quad (5)$$

Where $V[FS]$ equals the variance of the FS, δFS_{ii} corresponds to the variance of the FS when the study variables are varied by δX_i and $V[X_i]$ means the variance of each of the variables (X_i).

2.3. Stability analysis using SLIDE 6.0 Software

The SLIDE 6.0 software uses LEM for global stability analysis, which can be either deterministic or probabilistic. The probabilistic analysis is carried out by applying the Monte Carlo method, so in order to optimize the computational demand, the software allows this analysis to be carried out in two ways, the Global Minimum and the Overall Slope.

In the Global Minimum type analysis, parameter variability is applied only to the critical rupture surface, while the Overall Slope analysis considers parameter variation for all rupture surfaces. This study will therefore focus on analyzing the Overall Slope analysis only.

Stability analysis using the FOSM method was carried out using SLIDE 6.0 and Excel software. First, deterministic analyses were carried out for each of the parameter variations required by the method and then the equations were used in Excel. Based on this methodology, it is possible to identify which parameters have the greatest influence on the safety factor.

2.4. Stability analysis using PLAXIS 2D software

The analysis was carried out using PLAXIS 2D software, where, and the Safety Factors for each of the scenarios studied were calculated using the Finite Element Method. To do this,

Table 1. Expected performance level according to reliability index values and probability of failure

Expected performance level	Reliability index (β)	Probability of failure (Pf)
High	5.0	0.0000003
Good	4.0	0.00003
Above average	3.0	0.001
Below average	2.5	0.006
Poor	2.0	0.023
Unsatisfactory	1.5	0.07
Dangerous	1.0	0.16

Source: Adapted from U.S. Army Corps Engineers (1995).

a mesh study was first carried out. The main objective of this study is to identify the most optimized analysis model, i.e. the model that requires the least possible computational effort in order to provide the most assertive results possible.

To generate the finite element mesh, it is necessary to divide the domain into several parts. For two-dimensional analysis, several triangles are generated to represent the simulation domain. In the general properties of PLAXIS 2D, the number of nodes to be analyzed per element triangle is defined. Where there is the option of using an analysis with 6 or 15 nodes per element, in this study the use of 15 nodes was adopted.

Subsequently, the analysis began, in which it was identified that the fine and very fine meshes are the ones with the most assertive results. Table 2 shows the results of the mesh analysis. It can be seen that although the very coarse mesh does not show convergence on the safety factor, the difference between the result obtained by the very coarse mesh and the very fine mesh is less than 1%. Based on this analysis, it was decided to carry out all the analyses with the very fine mesh.

Therefore, the modeling steps consisted of importing the cross section of the pier, as well as its geotechnical profile. Subsequently, the geotechnical parameters involved in the analysis were defined, as well as the boundary conditions, such as the water table level, for example. After defining the input data and generating the mesh. The construction stages of the model were defined, where phase 1 consisted of determining the initial stress field in the soil through the "k0 procedure". The phase consists of the insertion of the pier structure, as well as the backfilling of the back area. In phase 3, the service and mooring loads are inserted, in this step the analysis of scenarios 1 and 2 is carried out. Subsequently, in phases 4 and 5, respectively, the analysis of the structure begins as a function of the erosive process at the base of the wall. Thus, characterizing scenarios 3 and 4 respectively.

3. GEOTECHNICAL CONDITIONS AND SCENARIOS ANALYZED

Through a historical search of the Port of Rio Grande's technical archives, in addition to the project for the structure of the Porto Velho Pier, 12 SPT test tests were found, all of them of the Standard Penetration Test (SPT) type. Figure 3 shows the location of each of the tests. As mooring bollards 13 is the place where the pathological manifestations are most intense, it can be seen that this is also the place where there are the greatest number of tests. An analysis of the SPT test reports shows that they are very similar. When analyzing the SP1, SP1A and SP1B tests, it can be seen that they all have a layer of approximately 3m of sand where the SPT test is interrupted, once it reaches an impenetrable layer, because at these points where the test was carried out there is the rockfill structure at the end of the pier. Already the SP1C test goes into deeper layers, in this report it is possible to identify the other soil layers of the site, Figure 4 shows the result of the SP1B sounding report, which is similar to the SP1 and SP1A reports, and SP1C. Based on these tests, the geotechnical profile of the site was defined.

Table 2. FEM mesh analysis

Mesh type	Number of elements	FS
Very thick	5351	1.658
Thick	6665	1.656
Average	7787	1.649
Thin	10279	1.644
Very fine	14057	1.644

FEM: Finite element method; FS: Safety factor.

By applying empirical equations that correlate the NSPT number with its properties, the average geotechnical parameters of the soil that makes up the Pier structure were defined. The rockfill parameters were the same as those used in the studies by Meirelles (2008).

Therefore, for this study, a high variability of the geotechnical parameters will be considered, since previous studies have already analyzed how the COV influences the stability of the structure, where it was possible to observe that higher COVs present a greater probability of failure and lower reliability rates. Therefore, the standard deviations of each of the geotechnical parameters were calculated based on the definition of the coefficient of variation (Eq. 3). Table 3 illustrates the values adopted for each of the parameters according to the analyses carried out. It was possible to define the layout of the structure by reviewing the history of the works and the quay project. By overlaying this information with the results of the SPT tests, the cross-section of the Porto Velho pier was defined.

According to Lacasse and Nadim (1998), most geological processes follow a normal or lognormal probabilistic distribution. A normal distribution was adopted for the random variables, in this case, the soil resistance parameters (undrained resistance and friction angle) as well as the specific weight. The other parameters were treated as deterministic, as in Johari (2019) (Table 4).

Thus, an analysis of four scenarios is proposed, in which scenario 1 represents the original undamaged structure, considering only the variability of the soil and its respective parameters, and the rockfill protection soil is characterized

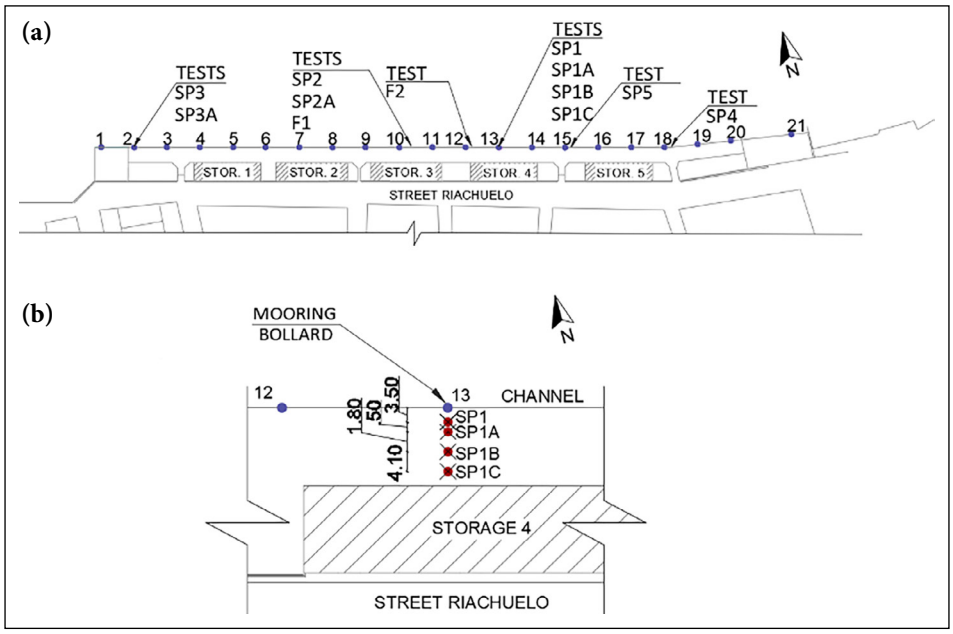

Figure 3. Geotechnical investigation (a) locations of the SPT test along the pier; (b) Identification of boreholes in front of mooring bollard 13.

SPT: Standard Penetration Test.

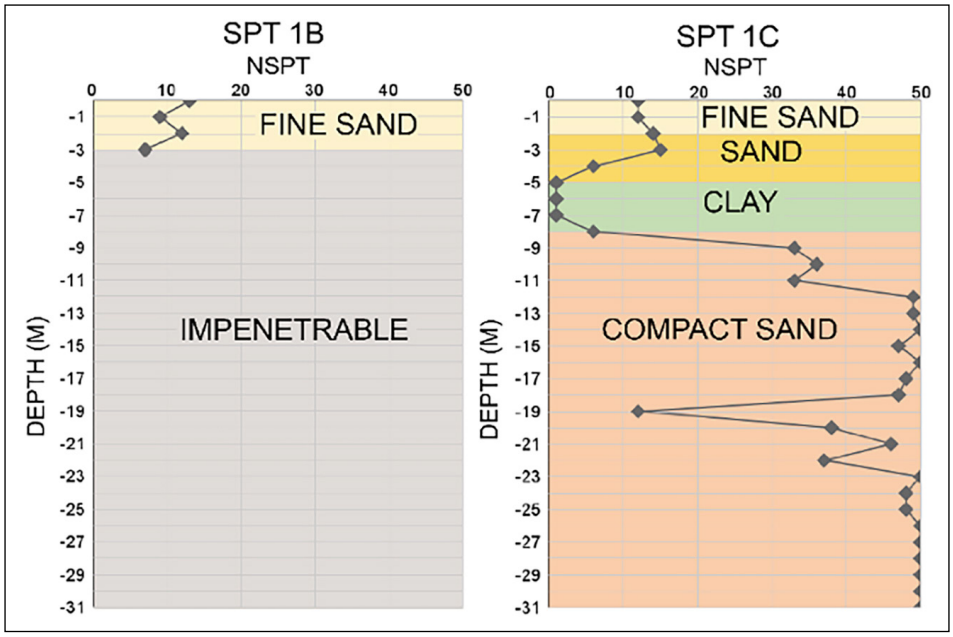

Figure 4. Results of the soil profile of the tests SP1B and SP1C, carried out in front of mooring bollards 13.

as compact sand. In order to understand how the rockfill protection soil influences the stability of the structure, it was considered that this soil is clay, so this new scenario was assigned as scenario 2.

As observed in a diving survey carried out by SUPRG (2016), there was erosion at the base of the rockfill protecting the wall, so this situation was defined as scenario 3 for this study. Finally, scenario 4 is represented as an evolution of scenario 3, in which erosion of part of the quay's protective rockfill is observed. Figure 5 illustrates the section of the quay for the different scenarios analyzed.

After defining the soil parameters, the structure was modeled using SLIDE 6.0 and PLAXIS 2D software (Fig. 6). In the PLAXIS 2D software, the continuum was discretized into a mesh with 1726 ground elements 1726, 14286 nodes, the average size of the elements 2,139 m, maximum element size 4.694m and minimum element size 0.0448m. The dimensions of the structure were defined based on old projects found in the SUPRG technical collection. It is important to highlight that the dimensions of the structure remained the same for both the LEM and FEM analyses.

Table 3. Geotechnical parameters for the LEM

Monte Carlo soil					FOSM		
	Parameters	Average	COV (%)	Standard deviation	Relative minimum	Relative maximum	Average +10% variation
Soil 1: Fine sand	γ (kN/m³)	19	10	1.9	13.3	24.7	20.9
	∅ (°)	35	15	5.25	19.25	50.75	38.5
Soil 2: Sand	γ (kN/m³)	18	10	1.8	12.6	23.4	19.8
	∅ (°)	29	15	4.35	15.95	42.05	31.9
Soil 3: Clay	γ (kN/m³)	15	10	1.5	10.5	19.5	16.5
	Su (kPa)	25	30	7.5	2.5	47.5	27.5
Soil 4: Compact sand	γ (kN/m³)	20	10	2	14	26	22
	∅ (°)	35	15	5.25	19.25	50.75	38.5
Soil 5: Filter (sand)	γ (kN/m³)	18	10	1.8	12.6	23.4	19.8
	∅ (°)	29	15	4.35	15.95	42.05	31.9
Rockfill	γ (kN/m³)	30					
	∅ (°)	45					

LEM: Limit equilibrium method; FOSM: First order first moment method; COV: Coefficient of variation.

Table 4. Geotechnical parameters for the FEM

Material	Average parameter values				
	Specific weight (kN/m³)	Angle of friction (°)	Non-drained resistance (Kpa)	Modulus of elasticity (kPa)	Poisson's coefficient
Soil 1: Fine sand	19	35	-	2.00E+04	0.3
Soil 2: Sand	18	29	-	1.50E+04	0.3
Soil 3: Clay	15	-	25	7000	0.4
Soil 4: Compact sand	20	35	-	5.00E+04	0.35
Soil 5: Filter (unidentified material)	18	29	-	1.50E+04	0.3
Rockfill	30	45		1.56E+05	0.3

FEM: Finite element method.

4. RESULTS AND DISCUSSIONS

4.1. Probabilistic analysis

Table 5 shows the evolution of the safety factor for each of the scenarios analyzed. It can be seen that scenario 1 had a safety factor greater than 2, very low failure probabilities and high reliability indices, and the same can be seen for scenario 2. As the analyses move on to scenarios 3 and 4, it can be seen that the safety factor values are lower than 2 and higher than 1.8, with a low probability of failure and a reliability index close to 3, which according to Table 1, characterizes an above-average reliability index. Thus, it can be seen that the safety factor decreases by 20% when the base of the rockfill is lost. It can also be seen that the value of the safety factor according to the probabilistic analysis is higher than the values found in the deterministic analysis, because the probabilistic analysis takes into account the variability of the materials.

In order to understand how soil variability influences the safety factors found by the FEM, a probabilistic analysis was carried out. It is important to emphasize that this analysis was based on the safety factors calculated using the Mohr-Coulomb rockfill resistance criterion.

4.2. Finite element method

It should be noted that throughout the analysis, it was noticed that the values of the safety factors found were lower than the values of the safety factors found by the Limit Equilibrium Method. In order to understand the reason for this difference, a series of changes were made to the input parameters in order to identify which properties would significantly affect the safety factor:

- Insertion of soil-structure interaction interfaces;
- Exponential increase in modulus of elasticity;
- Updating the mesh at each new analysis stage;
- Removal of distributed and point loads;
- Change in the rockfill resistance criterion from Mohr Coulomb to Linear Elastic;

In view of all these changes, the only one that had a significant impact was the change in the rupture criterion. Table 6 shows a comparison of the safety factor values found considering the rockfill failure criterion as Mohr-Coulomb and Linear Elastic for the FEM. The table also shows the results of the deterministic LEM analysis. Figure 7 shows the failure surfaces of Scenarios 1, 2,3

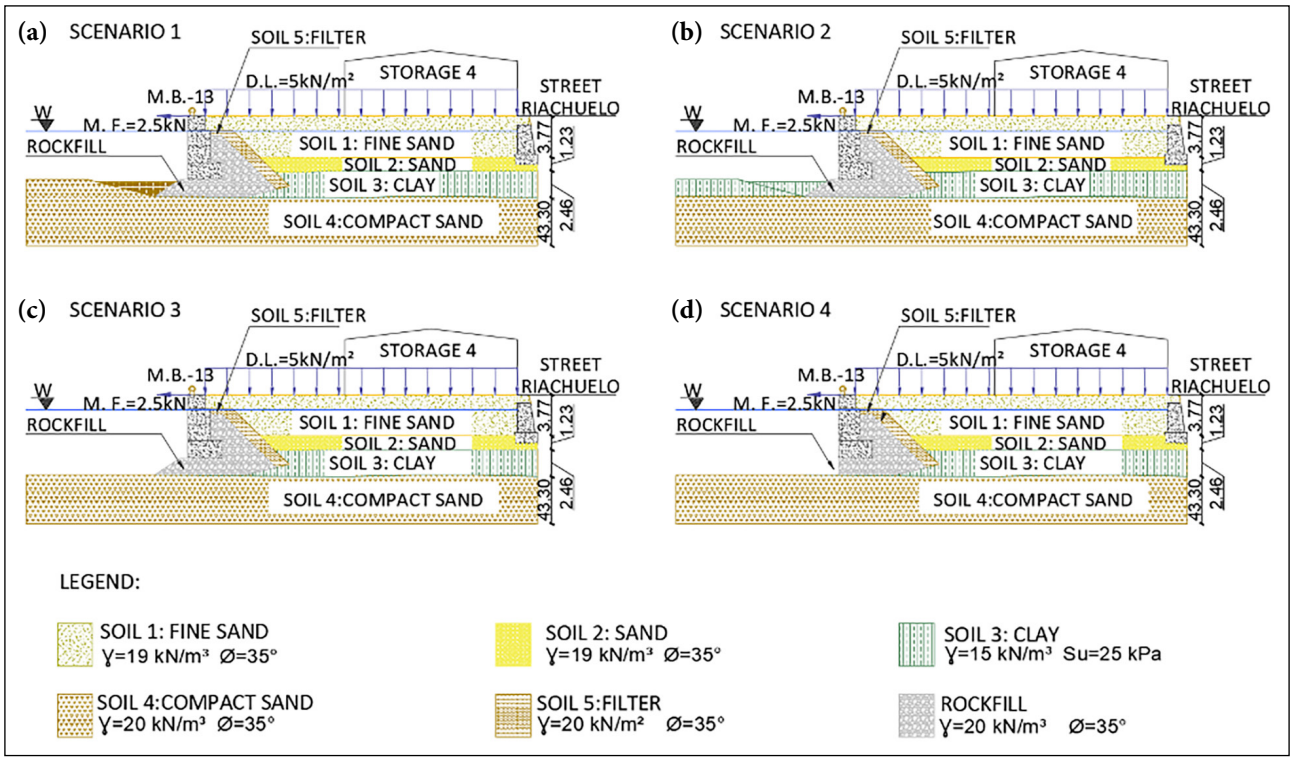

Figure 5. (a) Scenario 1: Sandy soil at the base of the rockfill protection. (b) Scenario 2: Clayey soil at the rockfill protection base. (c) Scenario 3: Intermediate erosion process with loss of soil protecting the rockfill. (d) Scenario 4: Critical stage where erosion of the rockfill at the base of the structure occurs.

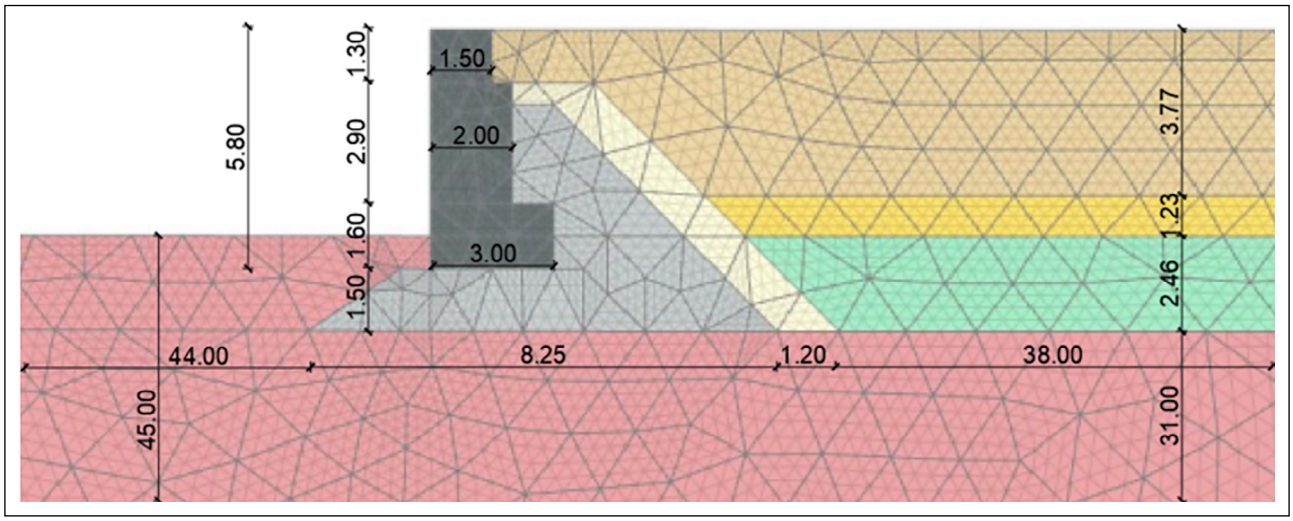

Figure 6. Dimensions of the PLAXIS 2D software model, the continuum was discretized into 1726 triangular elements with 15 nodes.

and 4 using the Limit Equilibrium Method and the Finite Element Method, respectively.

Based on these results, it can be understood that LEM is based on the premise that the safety factor is defined on the basis of the balance between the stresses and the stresses developed during the analysis. The FEM, on the other hand, considers the integration between the elements of the structure, so that they respond directly to the stress-strain relationship. Therefore, by adopting a linear elastic strength criterion for the rockfill, it is possible to see that the system behaves in a very similar way to that found in the FEM analysis, since the linear elastic strength criterion gives the rockfill a very high rigidity, similar to what is reproduced in the SLIDE software, where the FEM analysis is carried out, in which the modulus of deformation of the materials is not taken into account, as well as the interaction between them.

This analysis can be seen by comparing the results of the safety factors between the LEM and the FEM (Linear Elastic). It can be seen that the values are very close, and Figure 7 shows the rupture zones of the structure. It can be seen that the critical rupture surface of the LEM is very close to the plasticization zone of the FEM using the Linear Elastic model.

Table 5. Stability analysis results for LEM

Method	Scenario 01			Scenario 02			Scenario 03			Scenario 04		
	$\overline{FS}$	P_f	β	$\overline{FS}$	P_f	β	$\overline{FS}$	P_f	β	$\overline{FS}$	P_f	β
DET	2.204	-	-	2.289	-	-	1.845	-	-	1.778		
MMC	2.46	1.00E-05	4.261	2.365	2.00E-05	4.046	1.985	4.00E-04	3.345	1.93	5.00E-04	3.3
FOSM	2.348	9.00E-06	4.281	2.289	2.00E-06	4.567	1.915	3.00E-05	4.029	1.849	2.00E-04	3.54

LEM: Limit equilibrium method; DET: Deterministic; MMC: Monte Carlo method; FOSM: First order first moment method.

Table 6. Comparison of the results of safety factors for LEM and FEM

Scenarios	FEM		LEM
	Mohr coulomb	Linear elastic	Morgenstern & price
1	1.646	2.903	2.204
2	1.604	2.647	2.289
3	1.071	2.005	1.84
4	-	1.538	1.778

LEM: Limit equilibrium method; FEM: Finite element method.

By adopting the Mohr-Coulomb strength criterion for the rockfill, there is a significant reduction in the safety factor. This is because in this analysis, the rockfill has a more realistic resistance criterion, so that the load related to the mooring effort causes a stress-strain relationship that has a direct impact on the value of the safety factor, which does not occur in the LEM analysis.

It is therefore understood that the PLAXIS 2D software satisfactorily reproduces the stability analysis of the structure so that when similar analysis criteria are inferred,

Table 7. Results of the FOSM method for the FEM

Scenario	Analysis method	$\overline{FS}$	P_f	β
1	Phi/c-reduction	1,646	8E-05	4,175
2		1,604	6E-06	4,392
3		1,071	7E-05	3,799

FEM: Finite element method; FOSM: First order first moment method.

the results found are very close to those calculated using the SLIDE software. However, it should be noted that the analysis methodologies are very different, so that when a more realistic failure criterion is applied to the structure, the analysis results in safety factors that are lower than those calculated by LEM. This is because the FEM considers a wider range of parameters in its analysis. In addition, this method also takes into account the horizontal forces acting on the structure, which LEM does not.

In order to understand how the variability of the soil influences the safety factors found by the FEM, a probabilistic analysis was carried out. It is important to emphasize that this analysis was based on the safety factors calculated using the Mohr-Coulomb rockfill resistance criterion.

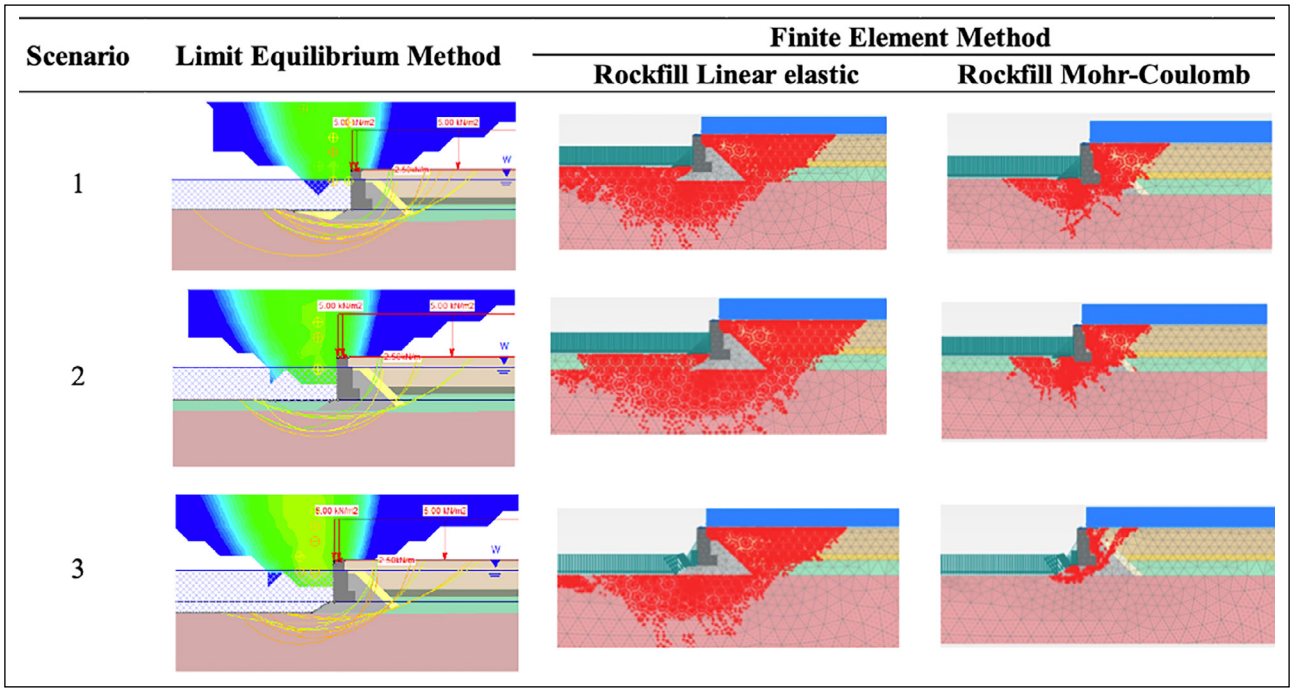

Figure 7. Comparison of the rupture surfaces of the LEM and FEM.

LEM: Limit equilibrium method; FEM: Finite element method.

Table 7 shows the results of the FOSM analysis. It shows that the factor of safety is lower than the factor of safety found in the FOSM method for the LEM. However, for both analyses it is possible to see that as the variability of the geotechnical parameters is applied, there is a reduction in the reliability index. When relating the results of Figure 7 to the results of the FOSM analysis for the LEM, it can be seen that the reliability index is very similar to that found by the LEM.

It is important to highlight that even though the FEM results in lower safety factors than those found by the LEM, the structure's reliability index continues to present an above-average level of performance. Therefore, it is understood that as erosion of the base of the structure occurs, its reliability reduces.

6. CONCLUSION

From this study it is possible to understand how the stability of the Porto Velho pier is influenced by the variability of the geotechnical parameters, as well as the probability of failure of each of the scenarios analyzed. In addition, it was possible to see the evolution of the safety factor as the loss of the quay base structure occurs.

By applying the probability analyses for the Limit Equilibrium Method, it was possible to notice a convergence between the results found for the Monte Carlo and FOSM methods.

The Finite Element Method analysis showed that adopting the rockfill strength criterion as Linear Elastic resulted in a plasticization area very similar to the areas of the critical rupture surfaces found in the Limit Equilibrium Method, as well as having very close safety factor values. However, by adopting the rockfill resistance criterion as being Mohr Coulomb, the safety factors showed much lower values than those calculated by the Limit Equilibrium Method. With regard to Scenario 4, the FEM identified the rupture of the structure at this stage.

In view of the above, it can be seen that the variability of the parameters directly influences the probability of failure of the structure as well as its reliability index. Furthermore, it can be understood that the stability of the Porto Velho pier is influenced both by the loss of the protective soil at the base of the rockfill and by the erosion of the rockfill base itself.

This research showed that for the configuration of the Porto Velho pier section, the Finite Element Method presented more assertive results when compared to the results inferred by the Limit Equilibrium Method. This is because the FEM takes into account the interaction between the elements as well as their stiffness. Through the analyses carried out and the results presented, it was identified that the rockfill strength criterion has a major influence on the safety factor.

In addition, the FEM identified the rupture of the quay structure from the moment the base of the rockfill was lost. This conformation is also observed in the existing structure of the Porto Velho pier. Therefore, it is assumed that the deformations found at the site stem from the loss of the rockfill base.

ACKNOWLEDGEMENTS

The Federal University of Rio Grande and the Port of Rio Grande for sharing their technical assets to enable this research to be carried out.

DATA AVAILABILITY STATEMENT

The published publication includes all graphics and data collected or developed during the study.

CONFLICT OF INTEREST

The author declared no potential conflicts of interest with respect to the research, authorship, and/or publication of this article.

ETHICS

There are no ethical issues with the publication of this manuscript.

USE OF AI FOR WRITING ASSISTANCE

No AI technologies utilized.

FINANCIAL DISCLOSURE

The authors declared that this study has received no financial support.

REFERENCES

Abbaszadeh, M., Shahriar, K., Sharifzadeh, M., & Heydari, M. (2011). Uncertainty and reliability analysis applied to slope stability: A case study from Sungun copper mine. *Geotechnical and Geological Engineering, 29*(5), 581–596. [CrossRef]

Ansari, T., Kainthola, A., Singh, K. H., Singh, T. N., & Sazid, M. (2021). *Geotechnical and micro-structural characteristics of phyllite-derived soil: Implications for slope stability*. Lesser Himalaya, Uttarakhand, India. Catena, 196, 104906. [CrossRef]

Beloni, A. V., Alves, A. M. L., & Real, M. V. (2017). Análise de confiabilidade das estacas do cais do Porto Novo de Rio Grande (Brasil) empregando metodologia bayesiana. *Geotecnia, 141*, 19–39. [CrossRef]

Cho, S. E. (2013). First-order reliability analysis of slope considering multiple failure modes. *Engineering Geology, 154*, 98–105. [CrossRef]

Cho, S. E. (2010). Probabilistic assessment of slope stability that considers the spatial variability of soil properties. *Journal of Geotechnical and Geoenvironmental Engineering, 136*(7), 975–984. [CrossRef]

Christian, J., Ladd, C., & Baecher, G. (1994). Reliability applied to slope stability analysis. *Journal of Geotechnical Engineering, 120*(12), 2180–2207. [CrossRef]

Corps of Engineers. (1997). *Engineering and design introduction to probability and reliability methods for use in geotechnical engineering*. Engineering Technical Letter No. 1110-2-547. Department of the Army, U.S., Washington, DC.

Da Re, G., Germaine, J. T., & Ladd, C. C. (2001). *Physical mechanisms controlling the pre-failure stress-strain*

behavior of frozen sand. Massachusetts Institute of Technology, Department of Civil and Environmental Engineering.

Ditlevsen, O. (1979). Narrow reliability bounds for structural systems. *Journal of Structural Mechanics, 7*(4), 453–472. [CrossRef]

Duncan, J. M., & Wright, S. G. (2014). *Soil strength and slope stability*. Wiley.

Dyson, A. P., & Tolooiyan, A. (2019). Probabilistic investigation of RFEM topologies for slope stability analysis. *Computers and Geotechnics, 114*, Article 103129. [CrossRef]

El-Ramly, H. (2001). *Probabilistic analyses of landslide hazards and risks: Bridging theory and practice* [Doctorial thesis]. University of Alberta, Canada.

Griffiths, D. V., & Lane, P. A. (1999). Slope stability analysis by finite elements. *Geotechnique, 49*(3), 387–403. [CrossRef]

Griffiths, D. V., & Fenton, G. A. (2007). Probabilistic methods in geotechnical engineering. In *International Center for Mechanical Sciences* (pp. 71–112). Springer. [CrossRef]

Haldar, S. (2019). Reliability-based design of pile foundations. In K. Ilamparuthi & G. R. Robinson (Eds.), *Geotechnical design and practice* (pp. 225–236). Springer. [CrossRef]

Hostettler, S., Jöhr, A., Montes, C., & D'Acunzi, A. (2019). Community-based landslide risk reduction: A review of a Red Cross soil bioengineering for resilience program in Honduras. *Landslides, 16*(9), 1779–1791. [CrossRef]

Jiang, S., Huang, J., Griffiths, D. V., & Deng, Z. (2022). Advances in reliability and risk analyses of slopes in spatially variable soils: A state-of-the-art review. *Computers and Geotechnics, 141*, Article 104498. [CrossRef]

Johari, A., & Mousavi, S. (2019). An analytical probabilistic analysis of slopes based on limit equilibrium methods. *Bulletin of Engineering Geology and the Environment, 78*, 4333–4347. [CrossRef]

Lacasse, S., & Nadim, F. (1998). *Risk and reliability in geotechnical engineering*. Proceedings of the 4th International Conference on Case Histories in Geotechnical Engineering, 1172–1192.

Li, D. Q., Wang, L., Cao, Z. J., & Qi, X. H. (2019). Reliability analysis of unsaturated slope stability considering SWCC model selection and parameter uncertainties. *Engineering Geology, 260*, Article 105207. [CrossRef]

Li, L., Wang, Y., Cao, Z., & Chu, X. (2013). Risk de-aggregation and system reliability analysis of slope stability using representative slip surfaces. *Computers and Geotechnics, 53*, 95–105. [CrossRef]

Meirelles, M. C. (2008). *Determination of the rockfill shear strength of the Machadinho HPP through large-scale direct shear tests* [Master thesis]. Federal University of Santa Catarina.

Metya, S., Mukhopadhyay, T., Adhikari, S., & Bhattacharya, G. (2017). System reliability analysis of soil slopes with general slip surfaces using multivariate adaptive regression splines. *Computers and Geotechnics, 87*, 212–228. [CrossRef]

Ortigão, J. A. R., & Sayão, A. S. F. J. (2004). *Handbook of slope stabilization*. Springer-Verlag.

Phoon, K. K., & Kulhawy, F. H. (1999). Characterization of geotechnical variability. *Canadian Geotechnical Journal, 36*(4) [CrossRef]

Plaxis 2D. (2016). *Plaxisbv*. Delft, Netherlands.

Queiroz, I. M. (2016). Comparison between deterministic and probabilistic stability analysis, featuring a consequent risk assessment. In: S. Aversa, L. Cascini, L. Picarelli, & C. Scaiva (Eds.), *Landslides and engineered slopes. Experience, theory and practice*. CRC Press.

SUPRG Technical Collection. (2016). *Inspection report on pathological manifestations along the Porto Velho Quay structure*.

Vanmarcke, E. H. (1977). Probabilistic modeling of soil profiles. *Journal of Geotechnical Engineering, 103*(11), 1227–1246. [CrossRef]

Yang, J., Dai, J., Yao, C., Jiang, S., Zhou, C., & Jiang, Q. (2020). Estimation of rock mass properties in excavation damage zones of rock slopes based on the Hoek-Brown criterion and acoustic testing. *International Journal of Rock Mechanics and Mining Sciences, 126*, Article 104192. [CrossRef]

Zaman, M., Booker, J. R., & Gioda, G. (2000). *Modeling in geomechanics*. John Wiley & Sons.

Zeng, P., Jimenez, R., & Jurado-Piña, R. (2015). System reliability analysis of layered soil slopes using fully specified slip surfaces and genetic algorithms. *Engineering Geology, 193*, 106–117. [CrossRef]

Seatific, Vol. 4, Issue. 2, pp. 88–99, December 2024

Seatific Journal
https://seatific.yildiz.edu.tr
DOI: https://doi.org/10.14744/seatific.2024.0005

Seatific

Review Article

Wrong use of SMCP in marine communication: A review study

Fahimeh FARJAMI*

Department of Translation and Interpretation, Nişantaşı University Faculty of Economics, Administrative and Social Sciences, İstanbul, Türkiye

ARTICLE INFO

Article history
Received: April 18, 2024
Revised: September 9, 2024
Accepted: September 21, 2024

Key words:
Standard marine communication phrase; maritime english; misuse of SMCP; english for maritime

ABSTRACT

The Standard Marine Communication Phrases (SMCP) are largely used on commerce ships to ensure safe navigation and to standardize communication between ships and between ships and shorelines. Therefore, it is crucial to raise training standards among important players in the sector: institutions for maritime education and training. This review study uses a theoretical and comprehensive systematic methodology and gathers data through analyzing SMCP previous papers in the context of onboard and external communication. The main objective of this research is to examine the improper usage of the SMCP, and marine safety to determine the needs and prospects for future study. According to this analysis of the literature, intercultural collaboration, communication and a seafarer's language proficiency are the most significant factors that affect maritime safety on an individual level. Additionally, SMCP use for external communication is 9% optional, 26% recommended, and 65% required. There are ways that English is used in crew radio communication, particularly for onboard communication. 41% of respondents selected recommended, 48% selected mandatory, and 11% selected optional. This paper serves as a thorough literature source pinpointing major issues in the use of SMCP to be touched in future studies.

Cite this article as: Farjami F. Wrong use of SMCP in marine communication: A review study. Seatific 2024;4:2:88–99.

1. INTRODUCTION

Persistent communication issues have been linked to several maritime accidents that resulted in the loss of people, property, and goods (James et al., 2018). The safety of seafarers, cargoes, and ships is of the utmost importance to the shipping industry because marine transportation is one of the most important and dangerous sectors of the global economy (Sarkodie et al., 2018). The term "Maritime English" refers to a dialect of English that is used in the maritime sector and has a vocabulary significantly distinct from General English. It may be treated as English for some purposes (Sar and Aprizawati, 2019). The maritime sector uses English as its primary language. The Standard Marine Communication Phrases (SMCP) are largely used on board commercial ships for safe navigation and standardizing communication between ships as well as among ships and shorelines. There are numerous seafarers from various countries that speak various languages throughout the globe, who are in need to have training of Maritime English (Demydenko, 2013; Vidhiasi and Syihabuddin, 2022). To cope with the demands of the modern global economic and political system as well as technical advancements, seafarers must possess a high degree of training. Due to the requirement for seafarers to be globally minded, they must be proficient in English to communicate effectively for both personal and professional reasons while at sea. Therefore, it is crucial to raise training standards among key

***Corresponding author.**
*E-mail address: fahimeh.farjami@nisantasi.edu.tr

players in the sector, including Maritime Educational and Training institutes (METs) and global merchant shipping corporations. A practical option is to review and integrate the SMCP training requirements for cadet navigation officers (Rosedi et al., 2015).

The International Maritime Organization (IMO) developed the Standard Marine Communication Phrases (SMCP), a set of core English terms that have acquired general acceptability for use at sea (Sukomardojo, 2022). According to John et al. (2017), the SMCP has terms which encompass the verbal shore-to-ship (and vice versa) and boat communications sectors that are crucial for safety. It is impossible to overstate the significance of marine transport to the global economy given that more than 90% of all international trade is carried out by sea. As a result, the prosperity of the marine industry is crucial to the interdependence of national economies around the world (Anurag et al., 2014). In contrast to other forms of transportation, maritime transportation has proven to be the most economical method of moving containerized cargo, petroleum products, food supplies, manufactured goods, bulk items, and other goods over vast distances. Maritime boats can be generically categorized as tankers, general cargo ships, bulk carriers, passenger ships, containerships, and fishing vessels, according to an IMO document (Boris, 2004).

Despite the significant advancements in E-navigation and the use of related infrastructures, ships of all sizes, even the smallest coastal vessels, from gigantic ocean-going vessels, have limited internet connectivity (Sari and Aprizawati, 2019). As a result, when a ship departs from a port or from a coast, it is unable to connect to large data portals. In 68th session, the Maritime Safety Committee (MSC) at the IMO asserted that numerous issues, including alcohol abuse, inadequate technical knowledge or language skills, fatigue, low morale, injury, staffing levels, work environment, and company management, could affect seafarers' ability to perform their jobs and, as a result, contribute to accidents. Later, under the following definition, the phrase "inadequate language skills" was defined in depth and added to the list of human element common terms: a lack of the basic linguistic abilities essential for communication and doing tasks. To understand all shipboard commands, instructions, procedures, labels, warnings, and rules, one must be completely or partially able to speak, read, or comprehend the primary language and/or additional needed languages (Seor & Park, 2020). The foundational communicative abilities of the SMCP are based on a basic comprehension of the English language. With its specific terminology, English has long been a widely used language in all industries, from maritime law to shipyard management, maritime transportation to ship management, and maritime education to ship management (John et al., 2017). Ships, port authorities, and pilots must use marine English accurately for the safety of navigation. The reasons why SMCP is misused in marine communication are thoroughly examined in this paper.

1.1. International Regulations and Guidelines Established by Maritime English Education Standards

English is the official language on a global scale and is used in varying sectors. English for Marine, which appears to be taught and learned in the marine business, is one of them. Maritime English is a specific form of English spoken by people working in the shipping and marine industries as well as by mariners (Dirgeyasa, 2018). The number of marine casualties (MC) is significantly influenced by human error (HE), according to studies from the U.S. Coast Guard and development center. Human mistake is the reason for between 75 and 96 percent of marine casualties. Therefore, International Maritime Organization (IMO) has developed the Maritime English Model Course 3.17, which establishes guidelines for teaching Maritime English to marine college students. Every country's educational system is based on this model coursework, which is regarded to be the syllabus. SMCP, along with the Maritime English Model Course 3.17, is well recognized for its importance to Maritime English (ME) education. If the IMO model curriculum or course is the prospectus utilized by the course developers and lecturers, the SMCP is more like study guides; it outlines a variety of communication skill sets that are employed onboard vessels (Seor and Park, 2020).

In industrial revolution, the entire world has been changing dramatically. Since then, radio wave technology has given the maritime shipping industry the advantage of adopting this type of communication. The ability to communicate effectively depends on both parties using the same language; on commerce ships, this language is typically English (Ziarati et al. 2012). With more advanced technology and global human resources operating in different places around the world, the marine industry has expanded more quickly recently than it did in the 1920s and 1930s. The marine system is a social system, as demonstrated by Papastergiou et al. in 2021. Technology, the environment, and organizational variables all interact with people. Although there is a weak link between the way organizational, environmental, or technical elements determine the role that human mistake plays in marine accidents, human mistake or error is a factor in 84 to 88% of tanker accidents, 79% of towing vessel groundings, 89–96% of collisions, and 75% of fires and explosions, according to United States Coast Guard (USCG) studies. HE that is classified as being under this category includes decisions that were made incorrectly, actions that were carried out improperly, and lack of proper communication (Ahmed, 2013).

USCG studies have been conducted in the country to examine the most prevalent HE in the maritime industry. The results indicate that there are many regions in which the industry can improve performance and safety by applying human factor principles (Barsan et al., 2012). Many regulations and conventions have referred to maritime English as a crucial element. "IMO has obviously set out the English Language Competence Requirements as for Working Language," claims Velikova (2009). According to the latter document, Officers of the navigational watch

are required to have a satisfactory understanding of both written and spoken English to comprehend charts, maritime publications, meteorological information, and messages pertaining to the vessel's safety and operation, as well as the requirement to communicate with other vessels, Vessel Traffic Service (VTS) stations, multinational seafarers crew, and to use the IMO SMCP. (Bleor and Sampson, 2009; Ding and Liang,2005; Velikova, 2009).

At the twenty-seventh session, it was established in 1973 by the Maritime Safety Committee (MSC) that English should be the standard language of instruction for navigation. At its sixty-eighth session in 1997, the IMO Maritime Safety Committee approved the new SMCP, which was developed by the IMO Sub-Committee on Safety of Navigation. In November 2001, the IMO Assembly adopted the SMCP as resolution A.918 (22). The capability to comprehend and use of the SMCP is required for authorization of the navigational watch officers who manages the vessels of 500 gross tonnage or more under the International Convention on Standards of Training, watchkeeping and Certification for Seafarers (STCW), 1978 and its amendments. SMCP should be used, together with written and spoken English (John et al., 2017; Trenkner, 2005). Table 1 indicates the IMO Assembly adopted the SMCP as resolution in 2010.

2. LITERATURE REVIEW

Previous studies about the SMCP had been the subject of research. Mujiyanto et al. (2023) discussed some research on SMCP-related onboard vessel communication. He contends that it is impossible to teach SMCP by means of conventional language instruction. Commonly, an unlimited number of new structures will be created using the components of language and the rules of grammar. He also warns about the limited ability of marine college students to remember the extensive marine vocabulary in SMCP.

Takagi, (2015) has conducted additional research in this area. He reported about a workshop that was designed to teach SMCP-based marine communication using computer dialogue systems, sometimes known as Chabot. The exercise that will be presented at the workshop will focus on the SMCP's mandatory component when used for Very High Frequency (VHF) communication. Participants are given the task of coming up with an effective communication plan during a simulated phone call to learn relevant information about a navigational disaster. In preliminary research on the SMCP conducted by Rosedi (2015), 110 navigation cadets from the leading maritime training academy in Malaysia named ALAM were involved. His research had the intended effect of assisting concerned parties in further enhancing SMCP training to adhere to the standards established by the STCW Codes.

According to evaluation of Frolova (2020) that most cadets find it difficult to become proficient in SMCP, even though using SMCP is one of the primary prerequisites for seafarers. He advised using SMCP as a strategy to reinforce both vocabulary and grammatical understanding in the

Table 1. Showing the IMO Assembly adopted the SMCP as resolution (IMO, 2010)

Competence	Knowledge, understanding and proficiency	Methods for demonstrating competence	Criteria for evaluating competence
Use the IMO Standard Marine Communication Phrases and use English in written and oral form	Adequate knowledge of English language to enable the officers to use charts and nautical publications to understand meteorological information and messages concerning ship's safety and operations to communicate with other ships, coasts stations and VTS centers and to perform the officer's duties along with the multilingual crew including ability to use and understand the IMO Standard Marine Communication Phrases	Examination and assessment of investigation obtained from practical instructions	English language nautical publication and messages relevant to safety of the ship are correctly interpreted and drafted. Communications are clear and understood.

IMO: International Maritime Organization; SMCP: Standard Marine Communication Phrases; VTS: Vessel Traffic Service

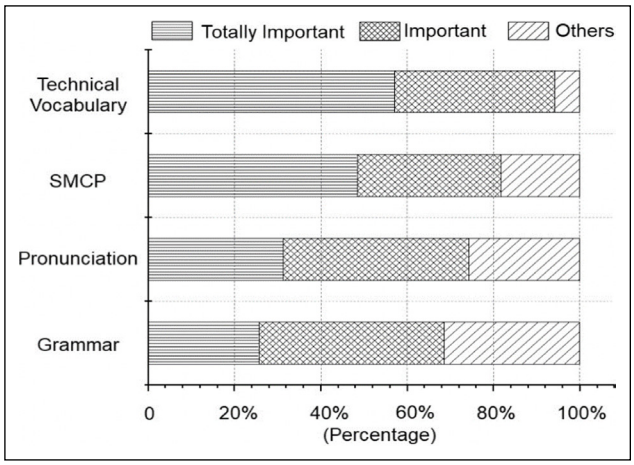

Figure 1. Showing the important elements for communication onboard (Seor and Park, 2020).

SMCP: Standard Marine Communication Phrases.

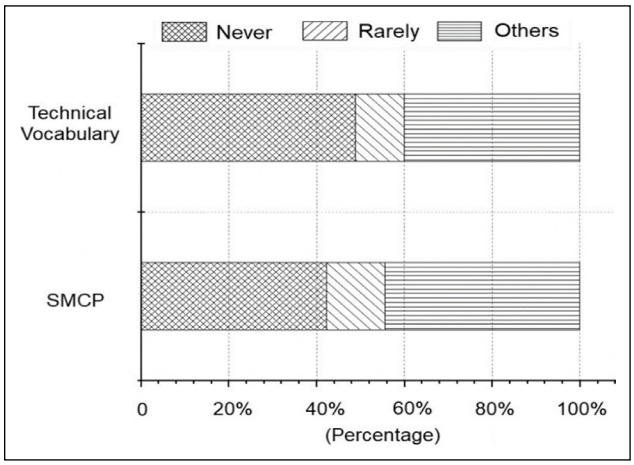

Figure 2. Showing the past 5 years Education experience of seafarers (Seor and Park, 2020).

SMCP: Standard Marine Communication Phrases.

marine English course. For instance, he suggested using SMCP to attach grammatical patterns. It is not sufficient to concentrate solely on the appropriate application of SMCP patterns because SMCP encompass and provide instructions on both routine and emergency on-board operations. Every seafarer must be proficient in the usage of SMCP to be prepared for the challenges that the modern, global shipping business faces (Schriever, 2018; Valle, 2011). Researchers have decided to analyze the detailed syllabus of the IMO Model course 3.17 "Maritime English" (IMO Model Course 3.17. (International Maritime Organization (IMO, 2010) due to the various situations that necessitate the use of SMCP (shore-to-ship, from ship-to-ship, and on-board communications), it is essential to identify the suitable topics and skills which can be used for incorporating SMCP into Maritime English courses.

Additionally, SMCP and maritime technical terminology education is required. Vangehuchten, (2010) carried out study to determine how well English is utilized in the workplace and what more development is required for improved communication onboard. 127 members of the maritime workforce, including seagoing navigation officers and engineers, participated in the study. The SMCP is thought to be relevant by 81% of respondents, and nearly 93 percent of members considered that technical Maritime English vocabulary is necessary. Figure 1 shows the important elements for communication onboard (Seor and Park, 2020).

Furthermore, according to the same study, 90% as well as 100% of respondents, respectively, claimed that technical ME vocabulary and the SMCP are significant for hiring and promoting. But as shown in Figure 2, 54% and 60% of respondents, respectively, said they had only occasionally or never received such instruction when asked if they had received any kind of instruction in SMCP and technological ME vocabulary over the previous five years, which emphasizes the significance of studying and analyzing content developed in English for specific purposes. Figure 2 portrays the past 5 years Education experience of seafarers (Seor and Park, 2020).

Education in SMCP and technical terminology used on board ships is necessary, according to Improving Onboard English Communication in the Republic of Korea (Hoel and Mason, 2018; Korea Institute of Maritime and Fisheries Technology, 2018). With this, we could acknowledge that the maritime sector needs and requires two components, SMCP and technical terms associated educations.

Pyne and Koester, (2005) highlighted several instances of poor communication in their study. These instances are stated as issues with the crew and the pilot's diverse cultures and languages, the crew and passengers aboard, passenger ships as well as problems with VHF connections with other vessels and problems with external communication. They argued that it is possible to decrease most occurrences that are specifically related to poor communication. They concluded that significant percentage of accidents occur when the level of English comprehension is unsatisfactory. Other aspects that need to be addressed include communication protocols, employee selection, and the design of maritime technology and equipment, including communication channels.

According to Pyne & Koester (2005), crew communication is a key contributing element in marine accidents. Misunderstandings are possible when crew members speak the same language. Miscommunication becomes far more likely when English language learners and potential cultural factors are included. English is crucial in social settings, according to Sampson and Zhao (2003), which will result in a more uniform workforce with an improved safety culture.

According to Cole and Trenkner (2009), "there is a practical and globally recognized assessment measuring tool, namely a yardstick that determines the Maritime English communication performance particularly set out in the STCW Convention Operational, Management Levels along with the SOLAS Convention." The Standard Marine Communication Phrases (SMCP) and the Maritime English model course 3.17 have both been adopted by the IMO and made available to MET institutes as a guide, respectively.

Table 2. Selected publications by year and the Journal/study design

No	Author's name	Publication year	Journal/study design
1	Acar and Varsami	2021	International Journal on Marine Navigation and Safety of Sea Transportation
2	Mates & Barbu	2015	Retrospective study
3	Haryani et al.	2022	Qualitative Research approach
4	Sarkodie et al.	2018	International Journal in Africa
5	Valle	2011	International Journal of English Studies
6	Boström	2020	Quantitative Research
7	Ahmed	2013	Literature Review
8	John et al.	2017	Quantitative research
9	James et al.	2018	WMU Journal of Maritime Affairs
10	Frolova	2020	Review

This yardstick, shown in Table 2, is what the author believes to be the most accurate and useful tool for evaluating how well seafarers at operational and managerial levels communicate in English in accordance with the standards of the STCW and SOLAS Conventions.

Ships using international transportation logistics carried out by more than 80% of global trade, according to data collected by the International Marine Organization (Haralambides, 2019; Jacks and Pendakur, 2010; and Rodrigue, 2010). According to the United Nations Conference on Trade and Development (UNCTAD), seaborne trade developed by 2.7% in 2018, which was less than the 3.0% annually average growth rate. The UN Conference on Trade has forecast a 3.4% annual average growth rate for 2019–2024 (Michail, 2020). Even though the shipping sector is constantly growing, human factors are major contributors to maritime accident. The negligence of humans is accountable for between 75–96% of marine casualties (Berg, 2013). The main factor that requires attention in maritime accidents is human error. According to USCG research, human error is a factor in 89 to 96% of collisions, 79% of grounded towing vessels, 84 to 88% of tanker incidents, and 75% of explosions and fires (Rothblum, 2000). On trade ships, 80% of the crew communicates through multiple languages and from various ethnic backgrounds (Hetherington et al., 2006; Valle, 2010).

The main human errors that have been linked to ship collisions (Sotiralis et al., 2016; Ung, 2019; Weng et al., 2019; Yıldırım et al., 2019) include oversight mistakes (not keeping the proper lookout, failing to take early actions). Ineffective communications are typically caused by ambiguities, misinterpretations, inappropriate technology, and a lack of closed-loop communication to provide feedback on messages (Boström, 2020). For a long time, only very high frequency of radio (VHF) had been accessible for communication and its improper use is a major cause of casualties (León, 2000; MCA, 2016).

According to the report of United Nations Conference on Trade and Development (UNCTAD), Asia will supply most of the world's seafaring labor in 2021, with Indonesia, Philippines, China, Russia and India, making up the top five suppliers of seafarers. None of these nations speak English as their mother tongue. The Standard Marine Communication Phrases (SMCP) was created to help crew members who are multilingual and non-native speakers communicate while on board ships (Trenkner, 2005).

3. METHODOLOGY AND SEARCHING STRATEGY

This study has theoretical and comprehensive systematic design. A literature review and qualitative research methods were deemed necessary for the study to be as successful as possible. The selection was impacted by some of the previous research and publications.

3.1. Searching terms

In this section difficulties in maintaining efficient communication as well as the requirements and difficulties associated with SMCP use will be reviewed. The focus of this study is on proceedings and journal articles that have been written about the improper usage of SMCP in marine communication. The number of databases that could be used was unlimited. To find articles written in English, the following keywords were used: Maritime English OR Marine Communication, SMCP and marine system. However, it should be noted that the phrase Standard Marine Communication Phrase, or SMCP, also well-known to maritime workers with employment involving sailing onboard ships, whether they are ocean-going or domestic.

3.2. Data collection

Numerous systematic evaluations involve using search engines and specific websites' content for analysis. Search engines like Google Scholar, PubMed, and Science-Direct were used to find the approved, peer-reviewed content, which includes reviews. Additionally, a secondary review of all the publications' links was accomplished and contacted renowned academics. Figure 3 illustrates the study selection process:

As indicated in the above flowchart diagram, 288 different studies were produced using this methodology. The various databases used slightly different in-depth search techniques. Studies that did not include data on marine communication (n=199), studies that were not about SMCP (n=33), studies that used evaluations of specific areas of research as their main source of data on maritime English (n=12), and studies that had no connection to English in

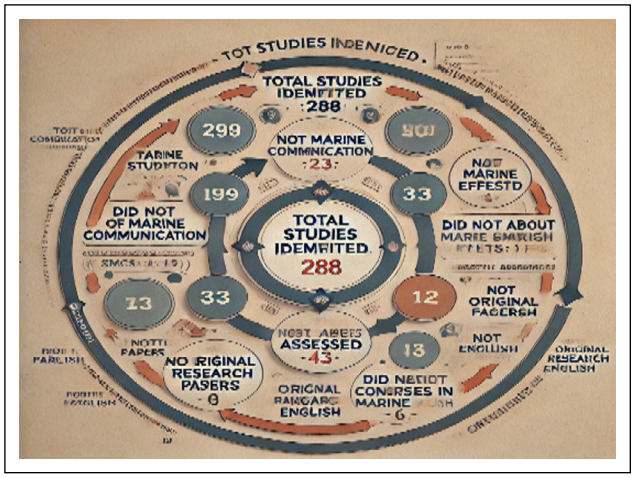

Figure 3. Showing the study selection process.

Marine (n=1) were all eliminated from consideration. The full papers for the other abstracts (n=43) were obtained and assessed. Studies that did not address lack of marine English (n=1), did not address SMCP effects (n=4), did not address original research papers (n=3), and studies that did not address courses maritime English (n=6) were excluded.

3.3. Inclusion or exclusion criteria

To ensure the research's high quality, broad applicability, and accuracy, inclusion and exclusion criteria must be established. These are helpful in narrowing down the study articles that appear in search results and helping to collect precise information that is crucial to the investigation's goals. Articles that did not specifically address the improper usage of SMCP in marine communication, were eliminated from the narrative and theme analysis synthesis. The data did not include any English-language articles that might have contained discrepancies, mistakes, or misrepresentations.

3.4. Method of analysis

The remaining 29 study articles go into SMCP's wrong use in maritime communication. Most of this research (n=10) use various disease-specific descriptive approaches to evaluate the lack of marine English in the maritime environment. By categorizing and organizing acceptable data using qualitative content analysis, it was possible to determine the Marine's lack of proficiency in maritime English.

4. RESULT

By examining relevant literature, this research attempted to highlight issues related to the lack of marine English in the marine environment. It is more challenging for seafarers to learn effective communication skills due to practical problems with intercultural communication and educational institutions. It also highlights issues with the curriculum's design, the learners' prior knowledge, the teachers' lack of experience, and the course materials (James et al., 2018; Ahmed, 2013; John et al., 2017; Acar and Varsami, 2021). Table 2 shows the selected publications by year and the Journal/study design.

Table 3 is an indication of selected publications' objectives and conclusions.

5. DISCUSSION

The SMCP was approved by 22nd Assembly of the IMO in November 2001. The Standard Marine Communication Phrasebook (SMCP) provides sailors with instructions for communicating on board ships with one another or with shore on international (oceangoing) or local lines. The jargon and predetermined statements or phrases in the SMCP book have become the norm for sailors in communicating with internal and external vessels, while the crew is composed of people of various linguistic and national backgrounds.

Numerous previous studies suggested that inadequate communication played a role in maritime accidents. The cause of this communication issue is the absence of a common language among maritime professionals. Human factors account for 80% of marine accidents, with poor communication accounting for a third of these (Ahmed, 2013).

Information is transmitted from one crew to another on a different board vessel during communication on the bridge, which uses the radio as the main tool. The captain, second officer, or third officer typically conducts the communication in the bridge room. Additionally, in the marine environment, verbal routine communication and external distress information are discussed. To prevent misunderstandings and ambiguity in meaning, the form of the language should be standardized with SMCP. The regular operations of the crew are carried out on ships via onboard communication. Only the internal crew, including those working in the deck, engines, galley, and radio departments, can communicate among different grades, roles, and job sectors. Usually, walkie talkies are used for communicating messages.

On the other hand, external communication differs slightly from onboard communication in the previous sentence. All departments of the ship's crew use this communication to carry out their daily tasks. Communication takes place from one ship to another ship, a ship to land, and in both directions. Typically, radio or walkie-talkies are used to transmit communications, particularly distress calls for help in the event of a disaster (accident or incident at sea).

There have been numerous maritime mishaps that have resulted in the loss of people, commodities, and property, and which have been partially caused by recurrent communication errors or wrong use of standard marine communication phrases. The safety of seafarers, cargoes, and vessels is of the utmost importance to the shipping industry as maritime transportation is one of the most important and dangerous sectors of the global economy. English for Specific Purposes is an acknowledged approach to satisfying the needs of the worldwide industry, while English is accepted as a common communication language in the marine industry. Seafarers are expected to complete the marine English learning phase.

Table 3. Selected publications' objectives and conclusions

No	Objective	Conclusion
1	To determine the primary causes of frequent communication issues at sea.	This systematic review showed many accidents taking place due to miscommunication or wrong use of standard marine communication phrases.
2	To evaluate the problems associated with communication failure.	Results revealed that lack of communication on board due to different international languages are more likely to cause accidents.
3	To highlight the language recommendations of radio communication in English from a maritime perspective.	To prevent miscommunication and avoid maritime accidents and incidents, English language users and skilled communicators need to know how to convey their messages accurately.
4	To determine how formation is used in marine communication and navigation in the maritime environment.	People aboard a ship or vessel can travel safely and securely thanks to technology for marine communication and navigation.
5	To evaluate the significance of a common coded language, such as the Standard Maritime Communication Phrases (SMCP), and to learn more about instances in which misunderstandings played a factor.	The investigation's findings demonstrate the widespread acceptance of English as a universal language, identify numerous language groups that are seen to be difficult to connect with using maritime English, and uncover some indications of linguistic hostility. It also shows how underutilized the SMCP is and how frequent misunderstandings brought on by linguistic and cultural differences.
6	To showcase correct or incorrect implementation of SMCP	Due to the high rate of human error that results from poor communication and poor assessments made while navigating in pilot seas, it may be concluded that bridge crew coordination might be enhanced. On tugboats, however, crew error is greater than 50%. This growth appears to be a result of the challenges presented by navigating through narrow waterways.
7	To improve maritime communication based on Maritime English by providing instruction in a variety of efficient methods.	The absence of an effective and up-to-date regulatory framework is one of the primary barriers to develop a standard for Maritime English communication skills training.
8	To highlight the distinctive structural features of maritime English for its use in discourse that takes place outside of a nautical environment. To improve the effectiveness of team communication in Maritime English.	Benchmarking can improve the effectiveness of team communication in Maritime English. It is also concluded that fatal accidents in shipping can be prevented by improving education and training in bridge team communication.
9	To analyze the potential for enhanced marine communication with real-world training.	Maritime English has modified, or developed words and phrases from other languages, which is only used in the IMI being classified as a particular form of English.
10	To evaluate the needs and challenges of SMCP use by seafarers	The findings of papers under evaluation demonstrated that the major purpose of learning SMCP in a maritime English course is to simulate a ship's setting in the classroom and to provide some realistic examples of maritime on-board communication in foreign crews.

Table 4. Showing the part A and part B of SMCP (IMO, 2002) (SMCP Book, 1995)

Part A: IMO standard marine communication phrases	**Part B: IMO standard marine communication phrases**
External communication phrase	**On-board communication phrases**
A1/1: Distress traffic	**B1/1: Handling over the watch**
A1/1.1 Distress communication: Fire, explosion, flooding, collision, grounding, sinking, disabled and adrift, equipped/attack/ piracy, list-danger of capsizing Unplanned distress, an adrift ship, and someone overboard.	B1/1 Brief description of position, motion, and draught.
A1/1.2 Search and Rescue Communication (SAR); SAR Communication, Acknowledge and/or relaying SAR messages, carrying out or organizing SAR operations, and wrapping up SAR operations	B1/1.2 a description of the neighborhood traffic scenario.
A1/1.3 Requesting for medical help.	Briefing on radio communication (B1/1.4).
A1/2 Traffic in an emergency: technical malfunction, ice damage, and cargo.	B1/1.5 Providing an overview of the weather.
A1/3 Safety Communications: Winds, storms, tropical storms, sea state, limited visibility, ice, navigational warnings and other hydrological and meteorological situations.	B1/1.6 Briefing on bridge organization and standing orders.
	B1/1.7 Special navigational event briefing.
	B1/1.8 Temperature, pressure, and soundings briefing.
	B1/1.9 Briefing on main engine's operating.
	B1/1.13 Taking control and managing the watch.

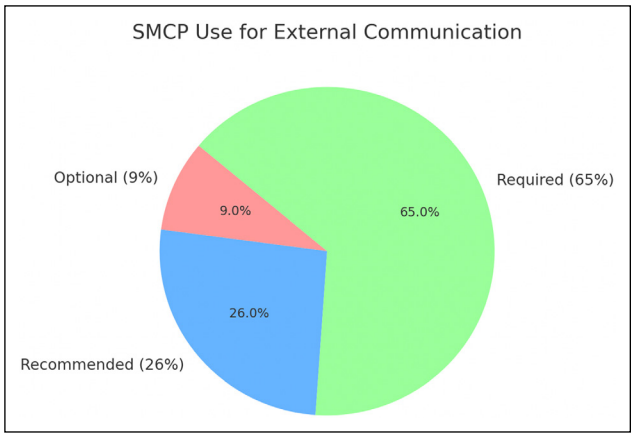

Figure 4. The Usage of SMCP for the External Communication (Mujiyanto et al., 2023).

SMCP: Standard Marine Communication Phrases.

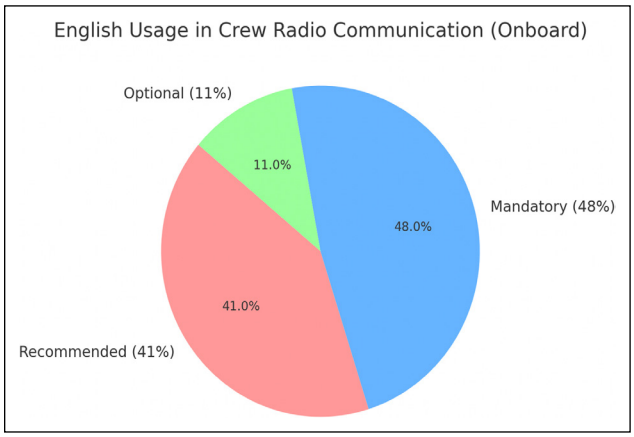

Figure 5. The usage of SMCP for on-board communication (Mujiyanto et al., 2023).

SMCP: Standard Marine Communication Phrases.

5.1. The less awareness of using Standard Marine Communication Phrases (SMCP)

According to the respondents' responses in a previous interview, most of them claimed that they utilized the Standard Marine Communication Phrase (SMCP) infrequently while working on the bridge while at sea (Şihmantepe et al., 2019). Since the crew was entirely made up of Indonesian seafarers, they were unwilling to speak the language because there was no incentive or penalty for following the rule or disobeying it. In addition, memorizing every term in the SMCP book and its standard phrase becomes a significant burden for them. As a result, the researcher offers a table that divides the IMO Standard Marine Communication Phrase (SMCP) into parts A and B, which serves as a representative from the hefty book. The information can be in the form of a subject matter:

International sailors must be able to understand Standard Marine Communication Phrases (SMCP) to serve on ships in places like Europe, America, or Australia. Poor coastal technical knowledge causes many tragic events that harm the ecosystem and the victims (Ahmed, 2018), including fires on the ship named “MS Scandinavian Star”, originally named MS Massalia, that killed 158 people and sank the empress' "tanker sea" to the coast and marine environment in Wales (England) (Yurzhenko, 2019). The investigation into the accident concluded that the crew's insufficient knowledge of the English language had a substantial impact on their ability to communicate with the passengers. The ability of the passengers to leave is hampered by this. The "sea empress" cases, which at first only lost 2500 tons of crude oil, are reduceable. China's true "de yue" empress" caused 71.800 tons more oil to explode into the sea than what was required for mariners due to incorrect communication by a cook on a tugboat (Davy and Noh, 2010). Table 4 shows the split of Standard Maritime Phrases into Part A and Part B (IMO, 2002) (SMCP Book, 1995).

As seen in the table above, the IMO SMCP book's material is split into two halves, designated as part A and part B. In-depth discussion of external communication terms such as "distress communication," "search and rescue (SAR), "request for medical assistance," "urgent traffic," "safety communication," "meteorological and hydrological conditions," and "navigational warnings involving environmental protection communications" is provided in part A of the International Maritime Organization's Standard Marine Communication Phrases (Park and Choe, 2015) which transfer from vessel traffic service (VTS) to another vessel traffic service. Part B of IMO Standard Marine Communication Phrases also focuses on onboard communication, including operational ship handling, handling over the watch, safety onboard, operational safety, damage control, SAR onboard activities, cargo handling, cargo care, and passenger care (Wójcik et al., 2016).

5.2. The essential of using SMCP for internal and external communication

In the workplace, especially onboard ships or on land, communication between internal and external interests becomes essential. English is utilized since it is a universally recognized official and legal language. Achieving effective radio communication becomes the top objective to prevent maritime mishaps and disasters. Based on the results of the surveys, it is possible to determine the type of SMCP on actual ships. Based on the reviewed papers, it was discovered that there were differences in the percentages of onboard and external communication settings that used SMCP as optional, recommended, and obligatory. The information about the use of SMCP in external communication is shown in Figure 4 below (Mujiyanto et al., 2023).

According to the diagram, using SMCP for external communication is 9% optional, 26% recommended, and 65% required. As a result, because a seafarer's work is associated with foreign crew and vessels, English must be spoken whenever there is radio transmission on board a ship. Plotting the navigational route and performing berthing and un-berthing, anchorage, docking, bunkering, etc. are all part of the task at hand. The information about the use of SMCP for on-board communication is shown in Figure 5 below (Mujiyanto et al., 2023).

The graph above demonstrates the variations in English usage in crew radio communication, particularly for onboard communication. 41% of respondents selected recommended, 48% selected mandatory, and 11% selected optional. In comparison to the data on external communication above, this percentage is very different. In other words, each vessel has a unique set of call signs, a Maritime Mobile Service Identity (MMSI) number unique to that vessel, and a seaworthy document.

5.3. Language barriers and cultural differences

Additionally, these communication problems are brought on by linguistic and cultural limitations. In addition to "human obstacles," there are regional variations in the English language and word meanings (Sukomardojo, 2022). Most of these expressions have to do with berthing and emergencies. The mariners can improve their foundational English skills by learning these expressions. Therefore, these words and phrases used at work and in practical sectors must be familiar to mariners. The truth is that seafarers require a common vocabulary for usage in the workplace (John, Brooks and Schriever, 2017; Haryani et al., 2022). Seafaring is a profession connected to a global maritime career. As a matter of fact, international and multicultural crews are a staple of contemporary nautical and shipping activities. To bridge amicable gaps and reduce disputes at work through efficient communication, the Marine and shipping industries require professionals with intercultural communicative competence (ICC) (Ahmed, 2013; Acar and Varsami, 2021).

For a safe evacuation, the seamen must be able to communicate with the terrified passengers. The seafarers will not be aware of the areas where they should not discard non-biodegradable items, oil, or plastic if the IMO convention on reducing marine pollution is not translated into all languages (Sarkodie et al., 2018). Top management should maintain constant communication with lower-level seafarers and employees, holding regular meetings to discuss English maritime communication and closely monitoring any problems that arise (Haryani et al., 2022).

5.4. Education system and status

The ME has not been fully incorporated into school and technical education due to flaws in the system. Various institutes produce different ME levels and attitudes. Additionally, trainees are trained by personnel who are lacking in practical experience. Because of this, Maritime English communication in daily life receives little widespread societal attention (Sarkodie et al., 2018).

In the past, ME had little success in getting the public's attention, and families also have little impact on interpersonal interactions. MEC receives little media coverage as a result (Ahmed, 2013). People are less concerned about MEC in their surroundings due to these considerations (in school and at home). People are, however, very focused on money because of their heavy familial responsibilities and the social pressure to maintain high standards of life (Haryani et al., 2022). Marine workers earn fairly high salaries; thus, they are hesitant to take responsibility for things like maritime mishaps brought on by poor communication out of fear of losing their employment in the event of carelessness (John, Brooks and Schriever, 2017). Finally, most Iraqis Iraqis avoid talking in English because they feel embarrassed when they make mistakes in other languages (Acar and Varsami, 2021).

6. CONCLUSION

Several important findings in the use of SMCP are underscored through this literature analysis in this research. The study indicates that application of SMCP in real setting is inconsistent and sometimes inadequate despite the establishment of SMCP as a standardized communication tool by the International Maritime Organization (IMO). The gaps in SMCP usage and training are found and analyzed. The findings reinforce the significant need for improved training programs that are in line with the realities of modern maritime operations. Current study offers precious guidance for policymakers, educators, and industry stakeholders by revealing practical solutions to promote SMCP adherence. Moreover, the study adds a new dimension to the research by insisting on the intersection of language proficiency, intercultural communication, and maritime safety. There is an emphasis on holistic approach of maritime education to address technical and human factors.

The insights provided in the current study can affect future training programs and education policies by identifying the key factors that contribute to the improper use of SMCP. The challenges identified in the literature are directly addressed by expressing the significance of practical, simulation-based training and the urgent need for intercultural communication. The present study extends the goal of improving maritime safety by advancing communication practices. It provides a clear path for future studies to better the communication standards in the maritime industry by highlighting the areas where there is a lack of SMCP use. The recommendations in this study can serve as a basis for further research and development in this area, ultimately contributing to safer and more efficient maritime operations.

6.1. Misuse and non-compliance with SMCP

Misuse and non-compliance with SMCP among seafarers, especially in onboard communication was indicated in the literature review. The survey results showed that while a majority of respondents (48%) recognize the mandatory nature of SMCP, a substantial portion (41%) view its use as recommended, and a small percentage (11%) consider it optional. Varying understanding and application cause a gap in training and enforcement, which could lead to serious implications for maritime safety.

There are numerous reasons beyond misuse of SMCP such as insufficient training, lack of awareness, and the impact of intercultural communication barriers. The literature review supports these findings, with multiple studies showcasing human error, communication breakdowns, and cultural differences as major contributors to maritime accidents. For

instance, the work of Mujiyanto et al. (2023) indicates the challenges of teaching SMCP through conventional language instruction, which may not properly prepare seafarers for the complex communication scenarios they encounter at sea.

6.2. Implications for maritime training institutions

Maritime Educational and Training (MET) institutions are committed to ensure that seafarers are well-prepared to use SMCP properly. Findings of this literature study warn MET institutions to reevaluate their current training curricula and take more practical, hands-on training opportunities into consideration. Collaborations with shipping companies to provide real-life training experiences and feedback mechanisms could be an effective way to bridge the gap between classroom learning and real-world practice.

Additionally, these institutions must draw their attention to cultural diversity of trainees and revise the modules to lessen the intercultural communication challenges. This can aid seafarers to easier develop and apply the skills required to navigate the complexities of multilingual and multicultural environments at sea.

6.3. Recommendations for future studies

Developing and testing innovative training methodologies that go beyond traditional classroom instruction must be the core focus of future studies. More importantly, expanding and evaluating the integration of simulation-based training, as highlighted in the conclusion, is extremely crucial. The effectiveness of virtual reality (VR) and augmented reality (AR) environments in enhancing SMCP competency among seafarers is another critical area for future researchers. These technologies offer immersive, realistic training scenarios that can better prepare trainees for real-world communication challenges.

Based on the findings of the current study, investigating the influence of intercultural communication training on the effective use of SMCP can be another future research challenge. Multinational maritime industry can improve the effectiveness of their programs by considering how cultural factors influence communication. Lastly, comparative studies across different regions and maritime institutions could bring about insights leading to best practices for SMCP education.

NOTE

The author initiated this review study while holding the position of Assistant Professor at Piri Reis University, Istanbul. The study is completed under the author's current affiliation with Istanbul Nişantaşı University.

DATA AVAILABILITY STATEMENT

The published publication includes all graphics and data collected or developed during the study.

CONFLICT OF INTEREST

The author declared no potential conflicts of interest with respect to the research, authorship, and/or publication of this article.

ETHICS

There are no ethical issues with the publication of this manuscript.

USE OF AI FOR WRITING ASSISTANCE

No AI technologies utilized.

FINANCIAL DISCLOSURE

The authors declared that this study has received no financial support.

REFERENCES

Acar, U. and Varsami, C. (2021). Practical Communication Approach in Maritime English. TransNav. *International Journal on Marine Navigation and Safety of Sea Transportation, 15*(3), 601–604. [CrossRef]

Ahmed, H. J. (2013). *The impact of maritime English communication training for non-native English language speakers concerning the competency of seafarers: Iraqi maritime sector case study* [Dissertation]. World Maritime University.

Anurag, C., A. Gaurav, and J. Meghna (2014). A review on applications of smart class and e-learning. *International Journal of Scientific Engineering and Research, 2*, 79–80. [CrossRef]

Ahmmed, R. (2018). The Difficulties of Maritime Communication and the Roles of English Teachers. https://www.researchgate.net/publication/327890958_The_Difficulties_of_Maritime_Communication_ nd_the_Roles_of_English_Teachers.

Apostol-Mates, R., & Barbu, A. (2015). *Is maritime english the key in solving communication problems within multinational crews?*. In International Conference Knowledge-based Organization (Vol. 21, No. 2, pp. 541–544). [CrossRef]

Barsan, E., Surugiu, F. and Dragomir, C. (2012). Factors of human resources competitiveness in maritime transport. *International Journal on Marine Navigation and Safety of Sea Transportation, 6*(1), pp.89-92.

Berg, H. P. (2013). Human factors and safety culture in maritime safety. *International Journal on Marine Navigation and Safety Culture in Maritime Safety, 107*, 107–115. [CrossRef]

Bin Mohd Rosedi, S. R., Sap, M. A. B. M., & Oommen, C. P. G. (2015). *Aligning occupational, national and global standards in maritime english competency: a preliminary study on standard marine communication phrases (smcp)*. International Maritime English Conference 2015 (IMEC 27)At: Johor Bharu, Johor Darul Takzim, Malaysia.

Bloor, M. and Sampson, H. (2009). Regulatory enforcement of labour standards in an outsourcing globalized industry: the case of the shipping industry. *Work, Employment and Society, 23*(4), 711–726. [CrossRef]

Bocanegra-Valle, A. (2010). *Global markets, global challenges: The position of maritime English in today's shipping industry*. English in the European context: The EHEA challenge, 151–174.

Boris, P. (2004). *A databank of maritime english resources*, 16th International Maritime English Conference, 26–27.

Boström, M. (2020). Mind the Gap! A quantitative comparison between ship-to-ship communication and intended communication protocol. *Safety Science, 123*, Article 104567. [CrossRef]

Chauvin, C., Lardjane, S., Morel, G., Clostermann, J. P. and Langard, B. (2013). Human and organizational factors in maritime accidents: Analysis of collisions at sea using the HFACS. *Accident Analysis & Prevention, 59*, 26–37. [CrossRef]

Cole, C., & Trenkner, P. (2008). *The yardstick for maritime English STCW assessment purposes*. In Proceedings of IMLA 16th Conference (pp. 163–173).

Demydenko, N. (2012). Teaching maritime English: A linguistic approach. *Journal of Shipping and Ocean Engineering, 2*(4), Article 249.

Ding, J., & Liang, G. (2005). The choices of employing seafarers for the national shipowners in Taiwan: an empirical study. *Maritime Policy & Management 32*(2), 123–137. [CrossRef]

Dirgeyasa, I. W. (2018). The need analysis of maritime english learning materials for nautical students of maritime academy in indonesia based on STCW'2010 curriculum. *English Language Teaching, 11*(9), Article 41. [CrossRef]

Davy, J. G., & Noh, C.-K. (2010). A basic study on maritime english education and the need for raising the instructor profile. *Journal of Navigation and Port Research, 34*(7), 533–538. [CrossRef]

Frolova, O. O. (2020). Integrating standard marine communication phrases into maritime english Course. *Pedagogy of the Formation of a Creative Person in Higher and Secondary Schools, 2*(68), 212–215. [CrossRef]

Haralambides, H. E. (2019). Gigantism in container shipping, ports and global logistics: a time-lapse into the future. *Maritime Economics & Logistics, 21*(1), 1–60. [CrossRef]

Haryani, H., Mujiyanto, J., Hartono, R., & Yuliasri, I. (2022). *English communication skill used by indonesian seafarer on radio communication*. In English Language and Literature International Conference (ELLiC) Proceedings (Vol. 5, pp. 627–634).

Hoel, T., & Mason, J. (2018). Standards for smart education–towards a development framework. *Smart Learning Environments, 5*, 1–25. [CrossRef]

Hetherington, C., Flin, R., & Mearns, K. (2006). Safety in shipping: The human element. *Journal of Safety Research, 37*(4), 401–411. [CrossRef]

International Maritime Organization. (2010). *IMO Model Course 3.17. Maritime English*. International Maritime Organization (IMO), Article 138.

International Maritime Organization. (2010). *ISM Code*. International Maritime Organization.

Jacks, D. S., & Pendakur, K. (2010). Global trade and the maritime transport revolution. *The Review of Economics and Statistics, 92*(4), 745–755. [CrossRef]

John, P., Brooks, B., & Schriever, U. (2017). Profiling maritime communication by non-native speakers: A quantitative comparison between the baseline and standard marine communication phraseology. *English for Specific Purposes, 47*, 1–14. [CrossRef]

Losey-León, M. A. (2000). *Facing new changes in the maritime English curriculum: tasks' design towards the acquisition of the standard marine communication phrases*. 2nd International Congress on Maritime Technological Innovations and Research, Cádiz, Spain.

MCA. (2016). Navigation: Watchkeeping Safety–Use of VHF Radio and AIS. Maritime and Coastguard Agency. https://www. gov.uk/government/publications/mgn-324-mf-navigation-watchkeeping-safety-use-of-vhf-radio

Michail, N. A. (2020). World economic growth and seaborne trade volume: quantifying the relationship. *Transportation Research Interdisciplinary Perspectives, 4*, Article 100108. [CrossRef]

Miles, M. B., & Huberman, A. M. (1994). *Qualitative data analysis: An expanded sourcebook*. Sage Publication.

Mujiyanto, J., Hartono, R., & Yuliasri, I. (2023). The essential of using standard marine communication phrases in avoiding accidents at sea for indonesian seafarers. *International Journal of Education, Vocational and Social Science, 2*(02), 51–67.

James, A. J., Schriever, U. G., Jahangiri, S., & Girgin, S. C. (2018). Improving maritime English competence as the cornerstone of safety at sea: a focus on teaching practices to improve maritime communication. *WMU Journal of Maritime Affairs, 17*(2), 293–310. [CrossRef]

Kovacevic, S. (2014). Maritime English Language Restrictedness. *European Journal of Social Sciences Education and Research, 2*(1), Article 89. [CrossRef]

Papastergiou, S., Kalogeraki, E. M., Polemi, N., & Douligeris, C. (2021). *Challenges and issues in risk assessment in modern maritime systems. Advances in Core Computer Science-Based Technologies*. Papers in Honor of Professor Nikolaos Alexandris, 129–156. [CrossRef]

Park, J. S., & Choe, S. H. (2015). *Workshop: IMEC and computer dialogue teaching approach in VHF communication*. In Proceedings of the Korean Institute of Navigation and Port Research Conference (pp. 233-236). Korean Institute of Navigation and Port Research.

Pyne, R., & Koester, T. (2005). Methods and means for analysis of crew communication in the maritime domain. *Archives of Transport, 17*(3-4), 193–208.

Rodrigue, J. P. (2010). *Maritime transportation: drivers for the shipping and port industries* (No. Forum Paper 2). ITF.

Rosedi, S. R. B. H. M., bin Dahari, C. M., & bin Mohd Said, K. (2015). The need to incorporate inaesthetic learning as one of primary methods in maritime English/ communication classes. *Asian TEFL International Conference, 4*, 181–202.

Rothblum, A. (2000). *Human Error and Marine Safety, US Coast Guard research& Development Center*. In Maritime Human Factors Conference.

Sampson, H., & Zhao, M. (2003). Multilingual crews: communication and the operation of ships. *World Englishes, 22*(1), 31–43. [CrossRef]

Seor, J. K., & Park, Y. S. (2020). A study on the educational efficacy of a maritime English learning and testing platform. *Journal of the Korean Society of Marine Environment & Safety, 26*(4), 374–381. [CrossRef]

Sotiralis, P., Ventikos, N.P., Hamann, R., Golyshev, P. and Teixeira, A. P. (2016). Incorporation of human factors into ship collision risk models focusing on human centred design aspects. *Reliability Engineering & System Safety, 156*, 210–227. [CrossRef]

Sari, D. P., & Aprizawati, A. (2019). The effect of standard marine communication phrases application through english for maritime ability. *Inovish Journal, 4*(2), 119–130. [CrossRef]

Şihmantepe, A., Beşikçi, E. B., & Özsever, E. (2019). Efficiency of IMO SMCP for safe navigation at sea: needs and challenges. *Young Scientist, 71*(2), Article 25.

Sarkodie, P. A., Zhang, Z. K., Benuwa, B. B., Ghansah, B., & Ansah, E. (2018). A survey of advanced marine communication and navigation technologies: Developments and strategies. *International Journal of Engineering Research in Africa, 34*, 102–115. [CrossRef]

Sukomardojo, T. (2022). The using of media games to improve smcp (standard marine communication phrases) vocabulary in maritime English. *International Journal of Entrepreneurship and Business Development, 5*(6), 1056–1064. [CrossRef]

Takagi, N., & Björkroth, P. (2015). *Using Computer Dialogue Systems for Providing a Student-Centred Teaching Approach in SMCP-Based Maritime Communication (workshop)*. Hochschule Flensburg University of Applied Sciences.

Trenkner, P. (2005). *The IMO Standard Marine Communication Phrases–refreshing memories to refresh motivation*. In Proceedings of the IMLA 17th International Maritime English Conference (pp. 1–17).

Ung, S. T. (2019). Evaluation of human error contribution to oil tanker collision using fault tree analysis and modified fuzzy Bayesian Network based CREAM. *Ocean Engineering, 179*, 159–172. [CrossRef]

Vangehuchten, L. (2010). *Communication for maritime purposes: a research project focusing on linguistic and intercultural features*. In Proceedings of the 22nd International Maritime English Conference (pp. 122–140).

Velikova, G. V. (2009). *Maritime English testing current state of affairs*. Vaptsarov Naval Academy Proceedings.

Vidhiasi, D. M., & Syihabuddin, S. (2022.) Maritime English: Teaching English for Maritime Sciences or Teaching Maritime Sciences in English?. *Saintara: Jurnal Ilmiah Ilmu-Ilmu Maritim, 6*(1), 71–77. [CrossRef]

Valle, A. B. (2011). The language of seafaring: Standardized conventions and discursive features in speech communications. *International Journal of English Studies, 11*(1), 35–53. [CrossRef]

Weng, J., Yang, D., Chai, T., & Fu S. (2019). Investigation of occurrence likelihood of human errors in shipping operations. *Ocean Engineering, 182*, 28–37. [CrossRef]

Wójcik, A., Hatłas, P., & Pietrzykowski, Z. (2016). Modeling communication processes in maritime transport using computing with words. *Archives of Transport System Telematics, 9*(4), 47–51.

Yıldırım, U., Başar, E., & Uğurlu, Ö. (2019). Assessment of collisions and grounding accidents with human factors analysis and classification system (HFACS) and statistical methods. *Safety Science, 119*, 412–425. [CrossRef]

Yurzhenko, A. Y. (2019). An e-course based on the LMS moodle to teach "Maritime English for professional purpose", *Information Technologies and Learning Tools, 71*(3), Article 92. [CrossRef]

Ziarati, M., Ziarati, R., Bigland, O. & Acar, U. (2012). *Communication and practical training applied in nautical studies*. Coventry: Coventry University Technology Park.